COMENIUS UNIVERSITY, BRATISLAVA

FACULTY OF MATHEMATICS, PHYSICS AND INFORMATICS

Spectral Techniques for Economic Time Series

DISSERTATION THESIS

1688f35e-4a28-4223-a35f-0e25eb955301

2012 **Ivana Bátorová**

COMENIUS UNIVERSITY, BRATISLAVA
FACULTY OF MATHEMATICS, PHYSICS AND INFORMATICS

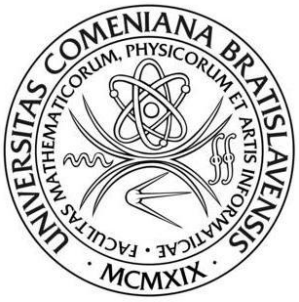

Spectral Techniques for Economic Time Series

DISSERTATION THESIS

9.1.9 Applied Mathematics
Department of Applied Mathematics and Statistics
doc. Ing. Jarko Fidrmuc, Dr.

Bratislava, 2012

Mgr. Ivana Bátorová

UNIVERZITA KOMENSKÉHO, BRATISLAVA
FAKULTA MATEMATIKY, FYZIKY A INFORMATIKY

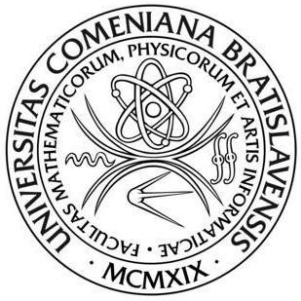

Aplikácia metód spektrálnej analýzy v ekonometrii

DIZERTAČNÁ PRÁCA

9.1.9 Aplikovaná matematika
Katedra aplikovanej matematiky a štatistiky
doc. Ing. Jarko Fidrmuc, Dr.

Bratislava, 2012

Mgr. Ivana Bátorová

Department of Applied Mathematics and Statistics
Faculty of Mathematics, Physics and Informatics
Comenius University
Mlynská dolina
842 48 Bratislava
Slovakia

Dissertation Thesis in Applied Mathematics

Comenius University in Bratislava
Faculty of Mathematics, Physics and Informatics

THESIS ASSIGMENT

Name and Surname:	Mgr. Ivana Bátorová
Study programme:	Applied Mathematics (Single degree study, Ph.D. III. deg., full time form)
Field of Study:	9.1.9. applied mathematics
Type of Thesis:	Dissertation thesis
Language of Thesis:	English
Secondary language:	Slovak

Title: Spectral Techniques for Economic Time Series

Aim: Analysis and applications of Spectral Techniques for Economic Time Series.

Tutor: doc. Ing. Jarko Fidrmuc, Dr.
Departments: FMFI.KAMŠ - Department of Applied Mathematics and Statistics

Electronic version available:
bez obmedzenia

Assigned: 21.10.2010

Approved: 22.10.2010 prof. RNDr. Marek Fila, DrSc.
Guarantor Of Study Programme

.....
Student

.....
Tutor

Univerzita Komenského v Bratislave
Fakulta matematiky, fyziky a informatiky

95204597

ZADANIE ZÁVEREČNEJ PRÁCE

Meno a priezvisko študenta: Mgr. Ivana Bátorová
Študijný program: aplikovaná matematika (Jednoodborové štúdium, doktorandské III. st., denná forma)
Študijný odbor: 9.1.9. aplikovaná matematika
Typ záverečnej práce: dizertačná
Jazyk záverečnej práce: anglický
Sekundárny jazyk: slovenský

Názov: Spectral Techniques for Economic Time Series

Cieľ: Analysis and applications of Spectral Techniques for Economic Time Series.

Školiteľ: doc. Ing. Jarko Fidrmuc, Dr.
Katedra: FMFI.KAMŠ - Katedra aplikovanej matematiky a štatistiky

Spôsob sprístupnenia elektronickej verzie práce:
bez obmedzenia

Dátum zadania: 21.10.2010

Dátum schválenia: 22.10.2010

prof. RNDr. Marek Fila, DrSc.
garant študijného programu

.....
študent

.....
školiteľ práce

I declare this dissertation thesis was written on my own, with the only help provided by my supervisor and the referred-to literature.

Bratislava, 2012 .....

Mgr. Ivana Bátorová

Acknowledgment

I would like to express my deep sense of gratitude to doc. Ing. Jarko Fidrmuc, Dr. for his invaluable help and guidance during the elaboration of this thesis. I am grateful to him for having given me the support and confidence.

I would like to express my thanks to colleagues Katka Danišková and Dáška Bartošová for their help, support and friendship.

And also I would like to express special thanks to my family, especially my parents, my sister and her family, for their support during my study.

Abstract

The properties of time series are typically analyzed in the time domain, although the same information may be effectively obtained from frequency domain approach, i.e. spectral analysis. These two methods are not mutually exclusive. Any stationary process has both a time domain and a frequency domain representation. For some properties the time domain approach is more suitable, for another one the frequency domain suits more. In this thesis we focus our attention on the frequency domain approach and try to introduce various tools of the spectral analysis.

Keywords: population spectrum • cross-spectral analysis • dynamic correlation • cohesion

Abstrakt

Vlastnosti ekonomických časových radov sa zvyčajne popisujú ako premenné závislé od času. Hovoríme o ich časovej štruktúre. Tie isté vlastnosti ekonomických radov sa však dajú efektívne popísať aj v závislosti od frekvencie, kedy hovoríme o frekvenčnej štruktúre časových radov. Analýza časových radov pomocou frekvencií je predmetom skúmania spektrálnej analýzy. Vyššie spomenuté reprezentácie sa navzájom nevylučujú, každý časový rad je možné popísať pomocou oboch metód. Avšak niektoré vlastnosti sú jednoduchšie popisateľné pomocou spektrálnej analýzy. V tejto práci predstavujeme čitateľovi spektrálnu a krížovú spektrálnu analýzu, ich nástroje ale aj praktické použitie pre štúdium ekonomických javov.

Kľúčové slová: populačné spektrum • krížová spektrálna analýza • dynamická korelácia • kohézia

Contents

List of Tables

List of Figures

1

Introduction

The fluctuations of aggregate output and especially the development of business cycles belong to the traditional arrears of economic research. Its importance was further increased by the recent developments. The financial crisis showed that despite a variety of econometric methods used for the analysis of economic development, we still do not know much about the determinants of business cycles.

The financial crisis underlined the inter-dependence of business cycles in the world economy. In particular, the financial crisis started with a crisis of mortgage market and Lehman collapse in the USA in 2008. Both issues were highly specific to the US financial developments, but economic and financial integration supported the transmission of negative shocks to other countries. Eventually, it seems that the European economies, including the euro area and by this also inevitably the Slovak economy, may be affected by the financial crisis even harder than the USA, the origin of the shock.

The interdependence of the international business cycles represents the main research topic of presented thesis. It does not address the financial crisis directly, because it broke out only in the later part of our research. It is also highly questionable whether we can already draw at least preliminary conclusions from the development of the financial crisis, which is not yet completed. This issue is left to further research. Nevertheless, the thesis describes the importance of interdependence of business cycles already in the period before the financial crisis. It shows that countries tend to follow some common developments which are related to economic and financial integration.

Moreover, the thesis analyze the effects of globalization on world's business cycles. Already before the financial crisis China has become an important player in the world economy. It was integrated deeply with other countries through intensive trade and financial links. Despite of this, China has kept a highly distinct pattern of economic fluctuations. This contributed to the emergence of China as the most important growing market during the financial crisis.

This thesis reviews different spectral techniques used for the analysis of economic time series. Its main part presents of classical spectral analysis and its bivariate extension, cross-spectral analysis. Although this part is based on previous literature, it presents a unique framework for spectral analysis which is missing in the literature.

My first application of the spectral analysis was included already in my master thesis ([9]) where I used the concept of dynamic correlation, cohesion and cross-cohesion to assess the degree of synchronization of the CEECs business cycle with the euro area. This was a starting point of my research in this area, which includes also international partners. I would like to mention especially my supervisor Jarko Fidrmuc, who was affiliated during the work on my thesis at the University of Munich and more recently at the Zeppelin University in Friedrichshafen, Germany. In June 2007 we attend the Workshop on Integration of Russia and China into the World Economy in Helsinki, Finland. As a result, we started a long-term co-operation with Iikka Korhonen, Bank of Finland. In our paper [10], which was published as BOFIT Discussion Paper[1] in 2008, we use the concept of dynamic correlation to illustrate the impact of China and globalizations on business cycles in the developed OECD countries. These research results were presented at numerous international conferences including e.g. CESifo Economic Studies Conference on Measuring Economic Integration 2011 in Munich, Germany or Annual Meeting of the Austrian Economic Association 2008 in Vienna, Austria . Then we provided more details on our results also by the cohesion analysis in [11], which was a result of Infer workshop in January 2008 in Brussels. While these analyses were analyzing fluctuations of gross domestic product of examined countries, in paper [12] we try to analyse the problem from another side. We use the stock prices of examined countries and calculate the dynamic correlation for these high frequency data. We presented this paper at the CEPR conference at the Hungarian National Bank

[1] A revised version of this paper is currently resubmitted for a publication at the CESifo Economic Studies.

in 2008.

The spectral analysis was initially used in economics already in the 1960s. Clive Granger, a later Nobel Prize laureate, belonged to authors paving the road for its application in business cycle research. Despite of this, the spectral analysis is only seldom used in research. For example, there are only few standard reference sources in this area. The best reference includes the Hamilton's Time Series Analysis [35] where he clearly describes the one-dimensional and multi-dimensional spectral analysis. However, this textbook does not discuss some more recent spectral methods including especially dynamic correlations and cohesion. In many other publications, however, the spectral analysis is mentioned only briefly (Green, [33]). Therefore, we include into dissertation a chapter that describes the concept of univariate and multivariate spectral analysis and theoretical foundations faced with the examples which became the basis for further investigation of Monte Carlo simulations.

The next parts of the thesis are organized as follows. In the second chapter we present the main topic of the thesis in a more detail. Chapter 3 offers a brief review of literature on spectral techniques applied in economics. Chapter 4 provides a review of the classical spectral analysis. It defines the population spectrum, sample periodogram and also describes the methods for the estimation of the spectrum. The cross-spectral analysis is described in the chapter 5. It is an extension of classical spectral analysis to the simultaneous analysis of two time series. While classical spectral analysis allows to detect the movements inside the time series, cross-spectral analysis determine the relationship between two time series. In chapter 6 and 7 we derive the autocovariance-generating function and the population spectrum for selected AR, MA and ARMA models generally and demonstrate the results on some examples. We present Monte Carlo analysis to detect which described method for spectrum estimation is more precise. The main results of analysis are introduced in chapter 8. In chapter 9 we apply the concept of cross-spectral analysis to China and OECD countries. Finally, the conclusions in the chapter 10 summarize the main results of the thesis.

2

Aims of the Thesis

The main topic of this thesis is the frequency domain approach for business cycle analysis. Spectral analysis has a large tradition in various scientific area. Despite of this, there are only few applications of spectral analysis in economics although the first contribution to this topic were done by Clive Granger a later laureate of the Nobel Prize in economics. A possible reason may be the difficulty to derive the policy interpretations. Moreover, the methods of spectral analysis are not built in the standard broadly used software. We are trying to fill this gap in the literature especially in the following areas:

- **Theoretical foundation of classical spectral analysis:** We describe the classical spectral analysis and introduce main idea of this method. Thesis introduces terms like spectrum, periodogram and describes the method for the spectrum estimation.
- **Theoretical foundation of classical cross-spectral analysis:** We introduce the cross-spectral analysis and terms related to this method, like a dynamic correlation, cohesion and cross-cohesion.
- **Presentation of population spectrum for standard random processes:** We derive the autocovariance-generating function and theoretical population spectrum for selected autoregressive processes, moving average and ARMA processes and demonstrate theoretical results.

- **Application of Monte Carlo techniques:** We employ Monte Carlo simulations for various processes to analyze which method for spectrum estimation is more precise and more robust. As the usual criterion of the method's quality and precision, we use the mean squared error (MSE) of the estimator, which should achieve lowest values for preferred method of estimation.

- **Application of spectral analysis to business cycles: Dynamic correlation analysis:** We apply cross-spectral analysis (dynamic correlation and cohesion) to illustrate the impact of China and globalizations on business cycles in the developed OECD countries.

3

Spectral Techniques and their Applications in Economics

Spectral analysis has been primary developed and used especially in scientific fields such as engineering, digital signal processing, geophysics, oceanography, atmospheric science, astronomy, and meteorology.

Allen *et al.* in [2] state that spectral analysis is motivated by the observation that the most regular, and hence predictable, behavior of a time series is to be periodic. This approach then proceeds to determine the periodic components embedded in the time series by computing the associated periods, amplitudes, and phases.

While the spectral analysis, provided a description of the main oscillatory components of time series, it has not been developed primarily for the economic purposes. Nowadays it is highly attractive also for applied economic inquiries such as identifying trend of economic time series, analyzing the business cycles, seasonalities and low-frequency components, analyzing the co-movements among series and the study of international business cycles.

The first application of spectral analysis in the study of macroeconomic time series dates from the middle 1960s. This process of expansion was motivated by the requirement of a more insightful knowledge of the series structure and was supported by the contemporaneous progress in spectral computation. Nerlove in [67], as the first, used the frequency domain approach in the problem of seasonal adjustment procedures.

Two publications ([30] and [31]) written by Clive Granger, who was awarded the Nobel Memorial Prize in Economic Science in 2003, proved extremely influential in the adoption of spectral analysis as a new method. Granger, as the first, used also the cross-spectral techniques in his paper from 1969 ([32]). In the following years, the range of applications of spectral analysis were extended to the study of the other econometric issues.

While analysis in time dimension is a standard tool of business cycle analysis, the application of spectral analysis may introduce new and more robust insights. Statistical filters, especially the Hodrick-Prescott filter, may generate artificial cycles (see Harvey and Jaerger, [39]). Moreover, the Hodrick-Prescott filter suffers from an end-point bias. The band-pass filter, which is recommended in the more recent literature, results in a loss of observation at the beginning and ending of the time series. By contrast, first differences are available for the whole sample at the same quality, but they include all frequencies.

The application of proper spectral method can enhance the comprehension of the structure and cyclical behaviour of the series in different time scale without the end-point bias or loss of observations therefore the issue of analyzing the business cycle is the most frequent object of spectral tools. The spectral analysis may provide a solution to several of caveats of standard business cycle analysis. As an example, Owens and Sarte examines in [70] whether the diffusion indexes, for which they estimate the power spectra, can be tied to the business cycle. Also Pollock in [74] argues that a clear understanding of the business cycle can be achieved only in the light of its spectral analysis. Poměnková and Maršálek in their papers ([62], [63] and [64]) inquire the structure and the nature of the cyclical behavior of economic growth cycle in Czech Republic using the spectral analysis. They compare the obtained results with another economic studies and with the results of time domain analysis. Their analysis proves that the frequency domain provides a deeper insight into the structure and the cyclical behavior of time series in different time scales. The time domain methods are not sufficient because they do not reveal the existence of nested cycles.

A various spectral techniques are also used for studying the international business cycles. A'Hearn and Woitek ([1]) investigate national and international business cycles in the late 19th century. Hughes-Hallett and Richter ([44] and [45]) use the spectral approach to analyse the business cycle of European emerging countries. They apply this method to answer the question, if there is an emerging European business cycle,

and how well have existing and candidate countries converged at different cycles and different periods of time? Poměnková and Kapounek ([51]) focus on the business cycles development of Czech and Slovak economies using frequency approach. Following the results which identify different waves with different periods in the same business cycle they argues that a common stabilization macroeconomic policy for both countries is not efficient. Baxter and King ([7]) focus on isolating business-cycle fluctuations in economic time series, defined as cycle in the data between specified frequency bands.

All another interesting economic topics, unexplained within time domain approach, have found some answers within the frequency domain econometric framework. For example, Wang in [82] proposes the frequency domain approach to measure the persistence in economic time series. Iacobucci in her paper [46] shows how cross-spectral analysis and filtering can be used to find correlation between unemployment and inflation in USA (i.e. the Phillips curve) in some specific frequency bands, even if it does not appear in raw data. The issue of identifying the trend-cycle component from an economic time series is discussed in the paper [41] from Higo and Nakada. Atesoglu and Vilasuso in [6] employ the spectral techniques to determine the relationship between real export growth and real output growth in the United States across different frequency bands. They reveal significant, positive relationship between long-run frequency components.

Croux with several coauthors used the spectral techniques, especially dynamic correlation and cohesion, to reveal the relations between time series which are unknown in time domain approach. Croux *et al.* in [15] first discussed the measure of dynamic correlation which can be used as a measure of comovement of two time series. This paper also proposes a measure of dynamic comovement between more than two time series, called cohesion and illustrates these new indeces of comovement on empirical example. Croux *et al.* adopt the concept of dynamic correlation and cohesion in [16] to detect whether European Union can be treated as single market. Moreover Croux *et al.* apply the spectral approach for Granger-causality tests. In [17] they propose a new testing procedure for the Pierce spectral Granger causality measure and then apply this methodology in the context of the predictive value of the European production expectation surveys.

Also Bátorová in [9] use the concept of dynamic correlation, cohesion and cross-cohesion to assess the degree of synchronization of the CEECs business cycle with the euro area as one of two applied approaches. Wozniak and Parzen in [71] also ob-

serve the relationship between euro area and new member state using the coherence. Bátorová, Fidrmuc and Korhonen ([10], [11] and [12]) apply the concept of cross-spectral analysis to detect how much influence China has on business cycles in the developed OECD countries.

Spectral tools are very attractive not only for macroeconomic inquiries but also for financial applications. For instance, they are applied in order to evaluate security prices, especially prices of derivative securities. Mario, for example, used spectral methods for computing the value of double barrier options ([60]) or for computing the value of European call options ([61]).

4

Classical Spectral Analysis

This chapter introduces a base terminology of classical spectral analysis. More detailed discussion of spectral analysis are provided by Fuller ([28]), Harvey ([38]), Hamilton ([35]), Chatfield ([14]), Hatanaka ([40]) and others.

4.1 Introduction

A time series, $\{Y_t\}_{t=-\infty}^{\infty}$, is the collection of observations indexed by the date of each observation. Its properties are generally analyzed in the *time domain* representation. It means, that the value of the variable Y_t at the date t is presented in the following form

$$Y_t = \mu + \sum_{j=0}^{\infty} \psi_j \varepsilon_{t-j},$$

where $\{\varepsilon_t\}_{t=-\infty}^{\infty}$ represents a sequence of innovations and μ is the mean of Y_t.

Also dynamical properties of economic time series are typically inquires in the time domain. However, information about dynamics of time series obtained from time domain analysis could be effectively supplemented by *frequency domain* approach, i.e. *spectral analysis*.

Spectral analysis is concerned with exploration of cyclical patterns of data and its main purpose is to decompose the original series into an infinite sum of periodic functions, each having a different *frequency* ω ranging between 0 and π. This fundamental

of the spectral analysis is captured in *spectral representation theorem* which states that any covariance-stationarity process $\{Y_t\}_{t=-\infty}^{\infty}$ can be expressed as

$$Y_t = \mu + \int_0^{\pi} \alpha(\omega).\cos(\omega t)d\omega + \int_0^{\pi} \beta(\omega).\sin(\omega t)d\omega, \tag{4.1}$$

where each frequency ω corresponds to a unique time horizon $\mathbf{T}$, such $\mathbf{T} = 2\pi/\omega$, and weights $\alpha(\omega)$ and $\beta(\omega)$ are random variables with zero mean. It means that the process Y_t is periodic function with frequency ω or with period $\mathbf{T}$.

4.1.1 Illustrative Example

The underlying intuition of the spectral analysis for two simulated processes is illustrated in figure 4.1. Both series have been simulated over 120 months $\sim$ 10 years and they are formed by three components of different frequencies.

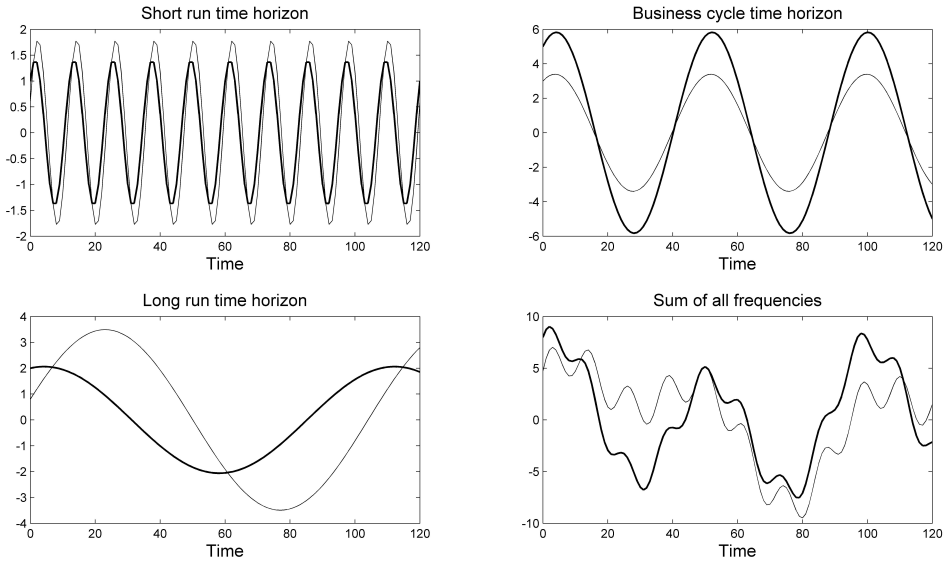

Figure 4.1: The decomposition of two time series into their components.

The first plot represents high frequency components which correspond to the short-run time horizon. The second one illustrates the medium frequency components corresponding to the business cycle time horizon and the components in the low frequencies

corresponding to the long-run time horizon are presented in the third plot. The sum of these components creates a final time series illustrated in the last plot of the figure.

All three time series are constructed according to spectral representation theorem (4.1). We assume that one unit of time is month. The time series illustrated short-run time horizon were constructed with the frequency $\omega = \pi/6$ which corresponds to the period $\mathbf{T} = 2\pi/(\pi/6)$ = 12 months $\sim$ 1 year. In contrast, long-run time series were created with the frequency $\omega = \pi/54$, corresponds to the period $\mathbf{T} = 2\pi/(\pi/54)$ = 108 months $\sim$ 9 years. And time series representing business cycle horizon were constructed with frequency $\omega = \pi/24$ which corresponds to the period $\mathbf{T} = 2\pi/(\pi/24)$ = 48 months $\sim$ 4 years. In reality, a time series are composed of an infinite sum of such components, which can be isolated through the spectral analysis.

4.2 The Autocovariance-Generating Function

Let $\{Y_t\}_{t=-\infty}^{\infty}$ define a covariance-stationary process with mean $E(Y_t) = \mu$ and with the sequence of autocovariances $\{\gamma_j\}_{j=-\infty}^{\infty}$, where jth autocovariance is defined as

$$\gamma_j = E(Y_t - \mu)(Y_{t-j} - \mu).$$

If the sequence of autocovariances is absolutely summable[1], then *autocovariance-generating function* for a time series Y_t is defined as

$$g_Y(z) = \sum_{j=-\infty}^{\infty} \gamma_j z^j, \tag{4.2}$$

where its argument (z) is a complex scalar. Thus, the autocovariance-generating function is defined like a sum of jth autocovariance multiplied by z raised to the jth power over all possible values of j.

Of a particular interest as an argument for the autocovariance-generating function is z represented by

$$z = \cos(\omega) - i.\sin(\omega) = e^{-i\omega},$$

where i is a complex unit and ω is a real number. Then the autocovariance-generating function for a time series Y_t can be rewritten as

$$g_Y(e^{-i\omega}) = \sum_{j=-\infty}^{\infty} \gamma_j e^{-i\omega j}, \tag{4.3}$$

The construction of the autocovariance-generating function for various processes is described in Appendix 6.

[1] A sequence of numbers $\{\gamma_j\}_{j=0}^{\infty}$ is absolutely summable, if it satisfies $\sum_{j=0}^{\infty} |\gamma_j| < \infty$.

4.3 The Population Spectrum

If the autocovariance-generating function defined in (4.2) is evaluated at $z = e^{-i\omega}$ and divided by 2π, we obtain a formula of the *population spectrum* or *spectral density function* of Y:

$$s_Y(\omega) = \frac{1}{2\pi} g_Y(e^{-i\omega}) = \frac{1}{2\pi} \sum_{j=-\infty}^{\infty} \gamma_j e^{-i\omega j}. \tag{4.4}$$

It is clear that the population spectrum is a function of ω. Therefore population spectrum $s_Y(\omega)$ of a time series process Y_t with the set of autocovariances $\{\gamma_j\}_{j=-\infty}^{\infty}$ can be computed at any value of ω.

The following facts can be combined to simplify the population spectrum:

- Symmetry of autocovariances: $\gamma_j = \gamma_{-j}$.
- DeMoivre's theorem: $e^{-i\omega j} = \cos(\omega j) - i.\sin(\omega j)$. One consequence of this theorem is an equation: $e^{i\omega j} + e^{-i\omega j} = 2\cos(\omega j)$.
- Trigonometry results: $\cos(0) = 1$, $\cos(\pi) = 0$, $\sin(0) = 0$, $\sin(\pi) = 1$.
- Symmetries of $\sin$ and $\cos$ functions: $\cos(-\omega) = \cos(\omega)$, $\sin(-\omega) = -\sin(\omega)$.

Following the relations above, spectrum defined in (4.4) simplifies to

$$s_Y(\omega) = \frac{1}{2\pi}\left\{\gamma_0 + 2\sum_{j=1}^{\infty} \gamma_j \cos(\omega j)\right\} \qquad \omega \in [0, \pi]. \tag{4.5}$$

Thus, if the sequence of autocovariances $\{\gamma_j\}_{j=-\infty}^{\infty}$ is known, the value for the population spectrum $s_Y(\omega)$ is obtained from (4.4) or (4.5). The opposite is also true. If the spectrum is known for all ω from $[0, \pi]$, the jth autocovariance γ_j for any given j is calculated from

$$\gamma_j = \int_{-\pi}^{\pi} s_Y(\omega) e^{i\omega j} d\omega \tag{4.6}$$

or equivalently from

$$\gamma_j = \int_{-\pi}^{\pi} s_Y(\omega) \cos(\omega j) d\omega. \tag{4.7}$$

This means that the population spectrum and the sequence of autocovariances contain the same information.

4.3.1 Properties of Population Spectrum

The population spectrum is defined according to the expression (4.5). From this expression and from the properties of cosine function (symmetry around 0 and periodicity with the period 2π) implies the following properties of the population spectrum $s_Y(\omega)$:

- Population spectrum is strictly real-valued, continuous function of ω.
- The population spectrum is a periodic function of ω: $s_Y(\omega + 2k\pi) = s_Y(\omega)$ for any integer k. It means, if we know the value of the population spectrum for all ω between 0 and π, we can infer the value of $s_Y(\omega)$ for any ω.
- The spectrum is symmetric around $\omega = 0 : s_Y(-\omega) = s_Y(\omega)$.

4.3.2 Interpretation of the Population Spectrum

If the j in (4.7) is set to zero, the following result is obtained:

$$\int_{-\pi}^{\pi} s_Y(\omega)d\omega = \gamma_0. \tag{4.8}$$

It means that the total variance γ_0 of Y_t, can be viewed as the sum of the spectral densities over all possible frequencies. More precisely, the area under the population spectrum between $[-\pi, \pi]$ gives γ_0, the variance of Y_t. To use the symmetry of population spectrum, this equation can be rewritten to the form:

$$2\int_{0}^{\pi} s_Y(\omega)d\omega = \gamma_0.$$

More generally, consider integration over only some of the frequencies:

$$\int_{-\omega_1}^{\omega_1} s_Y(\omega)d\omega = 2\int_{0}^{\omega_1} s_Y(\omega)d\omega \qquad 0 < \omega_1 \leq \pi. \tag{4.9}$$

The result would be a positive number that can be interpreted as the portion of the total variance of time series Y_t that is associated with frequencies less than or equal to ω_1.

4.4 The Sample Periodogram

The population spectrum for the covariance-stationary process Y_t is defined in (4.5). Let $y_1, y_2, \ldots, y_T$ be a sample of T observations of Y_t which provides a variance and $T-1$ autocovariances:

$$\hat{\gamma}_j = \hat{\gamma}_{-j} = \frac{1}{T}\sum_{t=j+1}^{T}(y_t - \bar{y})(y_{t-j} - \bar{y}) \qquad \text{for } j = 0, 1, 2, \ldots, T-1 \tag{4.10}$$

and $\bar{y}$ is a sample mean

$$\bar{y} = T^{-1}\sum_{t=1}^{T} y_t.$$

So we can construct the *sample periodogram*

$$\hat{s}_y(\omega) = \frac{1}{2\pi}\sum_{j=-T+1}^{T-1}\hat{\gamma}_j e^{-i\omega j}, \tag{4.11}$$

which is natural estimator of the spectrum. The sample periodogram can be also alternatively rewritten as

$$\hat{s}_y(\omega) = \frac{1}{2\pi}\left\{\hat{\gamma}_0 + 2\sum_{j=1}^{T-1}\hat{\gamma}_j \cos(\omega j)\right\}. \tag{4.12}$$

Analogous to the relation between the population spectrum and total variance, the area under the periodogram is the sample variance of y.

$$\int_{-\pi}^{\pi}\hat{s}_y(\omega)d\omega = \hat{\gamma}_0.$$

To use the symmetry of sample periodogram, this equation can be rewritten as follows

$$2\int_{0}^{\pi}\hat{s}_y(\omega)d\omega = \hat{\gamma}_0.$$

4.5 Estimation of the Spectrum

The population spectrum $s_Y(\omega)$ defined in (4.5) can be estimated using one of two approaches: a non-parametric or a parametric approach.

The simplest way to estimate the population spectrum is to estimate spectrum $s_Y(\omega)$ by the sample periodogram $\hat{s}_y(\omega)$. This approach is based on the replacing the theoretical autocovariances in (4.5) by the sample autocovariances. Thus, an obvious estimator of the spectrum is the sample periodogram

$$\hat{s}_y(\omega) = \frac{1}{2\pi}\left\{ \sum_{j=-T+1}^{T-1} \hat{\gamma}_j e^{-i\omega j} \right\}$$

or alternatively

$$\hat{s}_y(\omega) = \frac{1}{2\pi}\left\{ \hat{\gamma}_0 + 2\sum_{j=1}^{T-1} \hat{\gamma}_j \cos(\omega j) \right\}.$$

However, this approach has some disadvantages:

- High variance of the estimation.
- The estimation is not more accurate as the sample size T increases. The more observations we have, the more autocovariances have to be estimated. Hence, if T increases, the number of estimated parameters increase as well.

4.5.1 Non-parametric Estimates of the Spectrum

Since a sample periodogram as an estimator of the population spectrum has some disadvantages, a number of methods have been suggested to improve the properties of this estimator.

One ways to resolve this issue is to use *non-parametric estimates*. Their main idea lies in the similarity of the population spectrum $s_Y(\omega)$ and $s_Y(\lambda)$ if the frequency ω is close to the frequency λ. The spectrum might be therefore estimated with weighted average of the values of sample periodogram $\hat{s}_y(\omega_j)$ for frequencies λ from neighborhood of the frequency ω, where the weights depend on the distance between λ and ω. Let $\hat{s}_Y(\omega)$ denote an estimation of population spectrum $s_Y(\omega)$. Then the non-parametric estimation is based on the following formula

$$\hat{s}_Y(\omega_j) = \sum_{m=-h}^{h} \kappa(\omega_{j+m}, \omega_j).\hat{s}_y(\omega_{j+m}), \tag{4.13}$$

where $\omega_j = 2\pi j/T$, h (bandwidth) is a smoothing parameter that represents how many frequencies are used and useful for estimation. The function $\kappa(\omega_{j+m}, \omega_j)$, called kernel, indicates weights assigned to used frequencies. The sum of weights has to be 1.

$$\sum_{m=-h}^{h} \kappa(\omega_{j+m}, \omega_j) = 1$$

Averaging method of sample periodogram $\hat{s}_y(\omega)$ over different frequencies can be also represented as multiplying the jth sample autocovariance $\hat{\gamma}_j$ for $j > 0$ in (4.11) by a weight κ_j^*

$$\hat{s}_Y(\omega) = \frac{1}{2\pi}\Big\{\hat{\gamma}_0 + \sum_{j=1}^{T-1} \kappa_j^* \hat{\gamma}_j \cos(\omega j)\Big\}, \tag{4.14}$$

where κ_j^* is also called *kernel*, because the specification of kernel function $\kappa(\omega_{j+m}, \omega_j)$ in (4.13) can be equivalently formulated in the terms of weights κ_j^*.

One of the simplest weighting scheme consists of truncating the sequence of autocovariances. This is tantamount to multiplying them with a rectangular function which is 1 inside some extend and 0 outside.

$$\kappa_j^\star = \begin{cases} 1 & \text{for } |j| \le h \\ 0 & \text{otherwise} \end{cases}$$

The function $\kappa_j^\star$ is called *truncated* or *rectangular* window.

One of the most popular choice for the weights in spectral analysis is *Bartlett kernel*, called also *Bartlett* or *triangular* window, which is defined as

$$\kappa_j^\star = \begin{cases} 1 - \frac{|j|}{h} & \text{for } |j| \le h \\ 0 & \text{otherwise} \end{cases}$$

Thus the Bartlett estimation of population spectrum is

$$\hat{s}_Y(\omega) = \frac{1}{2\pi}\Big\{ \sum_{j=-h}^{h} \Big(1 - \frac{|j|}{h}\Big)\hat{\gamma}_j e^{-i\omega j} \Big\} \tag{4.15}$$

and it can be also alternatively rewritten as

$$\hat{s}_Y(\omega) = \frac{1}{2\pi}\Big\{\hat{\gamma}_0 + 2\sum_{j=1}^{h} \Big(1 - \frac{|j|}{h}\Big)\hat{\gamma}_j \cos(\omega j)\Big\}. \tag{4.16}$$

There are some another possibilities for computing the weights:

- *Tukey* window: $\kappa_j^\star = 0.5 + 0.5\cos\left(\frac{\pi j}{h}\right) \qquad |j| \leq h$

  The window is also called the Tukey-Hanning or Blackman-Tukey window.
- *Welch* window: $\kappa_j^\star = 1 - \left(\frac{j}{h}\right)^2 \qquad |j| \leq h$
- *Hamming* window: $\kappa_j^\star = 0.54 + 0.46\cos\left(\frac{\pi j}{h}\right) \qquad |j| \leq h$
- *Parzen* (de la Valle-Poussin) window:

$$\kappa_j^\star = \begin{cases} 1 - 6\left(\frac{j}{h}\right)^2 + 6\left(\frac{|j|}{h}\right)^3 & \text{for } |j| \leq \frac{h}{2} \\ 2\left(1 - \frac{|j|}{h}\right)^3 & \text{for } \frac{h}{2} \leq |j| \leq h \\ 0 & \text{otherwise} \end{cases}$$

- *Blackman* window: $\kappa_j^\star = 0.54 + 0.5\cos\left(\frac{\pi j}{h}\right) + 0.08\cos(2\frac{\pi j}{h}) \qquad |j| \leq h$
- *Lanczos* window: $\kappa_j^\star = sin(\frac{\pi j}{h})/\frac{\pi j}{h} \qquad |j| \leq h$

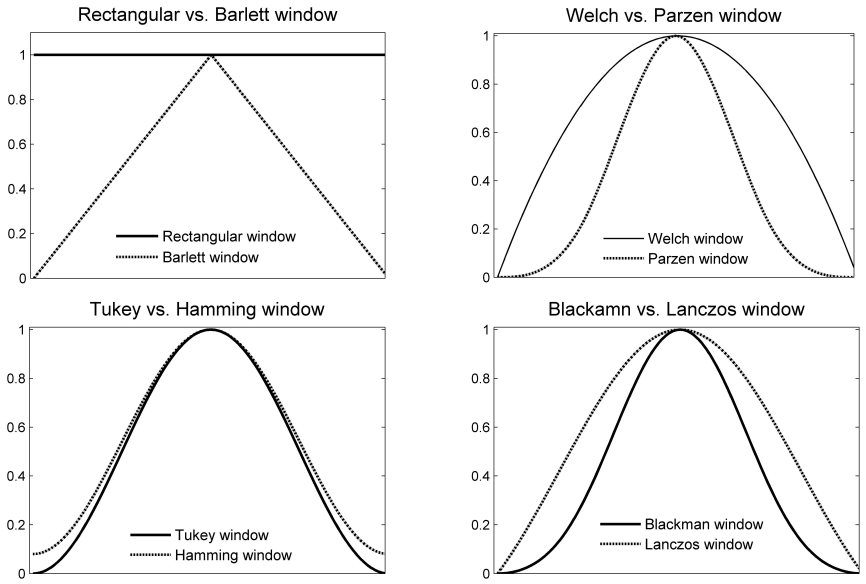

Figure 4.2: Graphical representation of the windows.

A bandwidth parameter h in the mentioned formulas denotes the size of the corresponding window.

The periodogram, contains only T observations, is asymptotically unbiased but it has a large variance. One way to resolve the large variance is to reduce the autocovariances by using the mentioned window. But this procedure introduces some bias. The

severity of bias depends on the size of bandwidth h. When h is small, the variance of the spectrum is relatively small but bias increase. On the other hand, large h acquires the large variance but the periodogram becomes asymptotically unbiased.

Thus one practical question arises: How should one choose the value for the bandwidth h? Diebold ([21], p.129) suggests to take h equal to the square root of the number of observations T. Chatfield ([14]) claims that h approximately equals to $2\sqrt{T}$ is large enough to provide the resolution. Hamilton ([35]) suggests that one "practical guide is to plot an estimate of the spectrum using several different bandwidths and rely on subjective judgment to choose the bandwidth that produces the most plausible estimate." Finally, Hannan ([36]) says, "the experience is the real teacher."

4.5.2 Parametric Estimates of the Spectrum

Another popular way to go about estimating the spectrum of a time series is to adopt a parametric approach. Therefore we introduce few of parametric methods for spectrum estimation in this section.

The Autoregressive Method

The evidence, that any linear process can be approximated by pth-order autoregressive process, $AR(p)$, expressed in the form

$$Y_t = \mu + \phi_1 Y_{t-1} + \ldots + \phi_p Y_{t-p} + \varepsilon_t,$$

where $E(\varepsilon_t^2) = \sigma^2$, has led Parzen ([72]) to suggest a technique known as *autoregressive spectral estimation*.

The first step of this procedure is to estimate the coefficients of an $AR(p)$ process by OLS. These estimates are then substituted for the parameters $\phi_1, \phi_2, \ldots, \phi_p$ in the population spectrum of an $AR(p)$ process

$$s_Y(\omega) = \frac{\sigma^2}{2\pi} \cdot \frac{1}{(1 - \sum_{j=1}^{p} \phi_j e^{-i\omega j})(1 - \sum_{j=1}^{p} \phi_j e^{i\omega j})}^2, \tag{4.17}$$

thereby yielding an estimator of the population spectrum. In other words, an $AR(p)$ process is fitted to the data and the estimator of the population spectrum is then taken as the theoretical spectrum of the fitted process.

[2]The derivation of population spectrum for autoregressive processes is described in section 7.3.

One difficulty of this method lies in decision on the order of the AR process. If the p is too small, the estimated spectrum may be badly biased but a large p increases a variance of the spectrum. According to Harvey ([38]), one solution to find an appropriate order of the model is to determine it on the goodness of fit criterion, given by or maximizing the adjusted R^2 or minimizing Akaike's information criterion (AIC)

$$\text{AIC} = -\frac{2l}{T} + \frac{2p}{T}, \tag{4.18}$$

where l is log likelihood function using p estimated parameters, T is number of observations.

Such methods have been used in autoregressive spectral estimation with some success, because in this case the estimator is a theoretical spectrum and it tends to be smoother than a spectrum produced by standard methods.

The Yule-Walker Method

Yule-Walker method, called also the *autocorrelation method*, is similar to the autoregressive method described above. It uses the same evidence that any linear process can be approximated by pth-order autoregressive process. The only difference between these two methods is the estimation of coefficients of autoregressive process.

Let $AR(p)$ process be defined as

$$Y_t = c + \phi_1 Y_{t-1} + \phi_2 Y_{t-2} + \ldots + \phi_p Y_{t-p} + \varepsilon_t,$$

where $E(\varepsilon_t) = 0$, $E(\varepsilon_t^2) = \sigma^2$ and its mean is calculated as

$$E(Y_t) = \mu = \frac{c}{1 - \phi_1 - \phi_2 - \ldots - \phi_p} \tag{4.19}$$

$$\mu = c + \phi_1\mu + \phi_2\mu + \ldots + \phi_p\mu \tag{4.20}$$

Using (4.20), the basic $AR(p)$ can be rewritten to

$$Y_t - \mu = \phi_1(Y_{t-1} - \mu) + \phi_2(Y_{t-2} - \mu) + \ldots + \phi_p(Y_{t-p} - \mu) + \varepsilon_t.$$

Multiplying the both sides of the equation by $(Y_{t-j} - \mu)$ and taking expectation we get

$$\gamma_j = \begin{cases} \phi_1\gamma_{j-1} + \phi_2\gamma_{j-2} + \ldots + \phi_p\gamma_{j-p} & \text{for } j = 1, 2, \ldots, p \\ \phi_1\gamma_1 + \phi_2\gamma_2 + \ldots + \phi_p\gamma_p + \sigma^2 & \text{for } j = 0. \end{cases} \tag{4.21}$$

Dividing (4.21) by γ_0 produces *Yule-Walker equation*

$$\varrho_j = \phi_1 \varrho_{j-1} + \phi_2 \varrho_{j-2} + \ldots + \phi_p \varrho_{j-p} \qquad \text{for } j = 1, 2, \ldots, p, \tag{4.22}$$

where ϱ_j is jth autocorrelation of $AR(p)$ process defined as jth autocovariance divided by the variance γ_0

$$\varrho_j = \frac{\gamma_j}{\gamma_0}.$$

Thus the first step of Yule-Walker procedure, parametric method of spectrum estimation, is to estimate the coefficients of an $AR(p)$ process defined by Yule-Walker equation (4.22). These estimates are then substituted for the parameters $\phi_1, \phi_2, \ldots, \phi_p$ in the population spectrum of an $AR(p)$ process

$$s_Y(\omega) = \frac{\sigma^2}{2\pi} \cdot \frac{1}{(1 - \sum_{j=1}^{p} \phi_j e^{-i\omega j})(1 - \sum_{j=1}^{p} \phi_j e^{i\omega j})}, \tag{4.23}$$

thereby yielding an estimator of the population spectrum. Again the difficulty of this method lies in deciding on the order of the AR process.

5

Cross-Spectral Analysis

Cross-spectral analysis is the extension of classical spectral analysis to the simultaneous analysis of two time series. While univariate spectral analysis allows a detection of movements inside each series, by cross-spectral analysis it is possible to describe pairs of time series in frequency domain by decomposing their covariance in frequency components.

The main purpose of cross-spectral analysis is to determine the relationship between two time series as a function of frequencies. One of the attractions of cross-spectral analysis is that it may be permit the characterizations of cyclical relationship which are difficult to model in the time domain.

5.1 The Population Spectrum for Vector Processes

The concept of population spectrum described for univariate time series may be extended for multivariate time series.

Let $\boldsymbol{Y}_t$ be a covariance-stationary $(n \times 1)$ vector process with mean $E(\boldsymbol{Y}_t) = \boldsymbol{\mu}$ and jth autocovariance matrix

$$E[(\boldsymbol{Y}_t - \boldsymbol{\mu})(\boldsymbol{Y}_{t-j} - \boldsymbol{\mu})'] = \boldsymbol{\Gamma}_j. \tag{5.1}$$

The symmetry of autocovariances known for scalar processes, $\gamma_j = \gamma_{-j}$, is not true for vector processes, $\boldsymbol{\Gamma}_j \neq \boldsymbol{\Gamma}_{-j}$. The correct relation between the autocovariance matrices

is

$$\mathbf{\Gamma}_j' = \mathbf{\Gamma}_{-j}. \tag{5.2}$$

If the sequence of autocovariance matrices $\{\mathbf{\Gamma}_j\}_{j=-\infty}^{\infty}$ is absolutely summable and if z is complex scalar, the *autocovariance-generating function* of $\boldsymbol{Y}_t$ is defined as

$$\mathbf{G}_{\mathbf{Y}}(z) = \sum_{j=-\infty}^{\infty} \mathbf{\Gamma}_j z^j. \tag{5.3}$$

If the autocovariance-generating function from (5.3) is evaluated for $z = e^{-i\omega}$ and divided by 2π, we obtain the *population spectrum* for vector $\boldsymbol{Y}$

$$\mathbf{s}_{\mathbf{Y}}(\omega) = \frac{1}{2\pi}\mathbf{G}_{\mathbf{Y}}(e^{-i\omega}) = \frac{1}{2\pi}\sum_{j=-\infty}^{\infty} \mathbf{\Gamma}_j e^{-i\omega j}. \tag{5.4}$$

Recall that the relation between the population spectrum $s_Y(\omega)$ for univariate process Y and jth autocovariance γ_j is couched in formula (4.6) or equivalently in (4.7). For covariance-stationary vector process $\boldsymbol{Y}_t$, the relation between its population spectrum $\mathbf{s}_{\mathbf{Y}}(\omega)$ and the jth autocovariance matrix can be expressed by analogy as

$$\mathbf{\Gamma}_j = \int_{-\pi}^{\pi} \mathbf{s}_{\mathbf{Y}}(\omega) e^{i\omega j} d\omega. \tag{5.5}$$

This means that the population spectrum and the sequence of autocovariance matrices $\{\mathbf{\Gamma}_j\}_{j=-\infty}^{\infty}$ contains the same information. If j in (5.5) is set to zero, the following result is obtained

$$\mathbf{\Gamma}_0 = \int_{-\pi}^{\pi} \mathbf{s}_{\mathbf{Y}}(\omega) d\omega. \tag{5.6}$$

It means that the area under the population spectrum between $[-\pi, \pi]$ gives $\mathbf{\Gamma_0}$, the unconditional variance-covariance matrix of $\boldsymbol{Y}$.

The population spectrum for multivariate vector processes are described in previous formulas. Now concentrate on a case of $n = 2$ variables to gain more deeply into understanding of multivariate spectrum. So let

$$\boldsymbol{Y}_t = \begin{bmatrix} X_t \\ Y_t \end{bmatrix}$$

where X_t is covariance-stationary process with mean equals μ_X and Y_t is also covariance-stationary process with mean μ_Y. The jth autocovariance matrix of such defined $\boldsymbol{Y}_t$ is

$$\boldsymbol{\Gamma}_j = E\begin{bmatrix}(X_t-\mu_X)(X_{t-j}-\mu_X) & (X_t-\mu_X)(Y_{t-j}-\mu_Y)\\ (Y_t-\mu_Y)(X_{t-j}-\mu_X) & (Y_t-\mu_Y)(Y_{t-j}-\mu_Y)\end{bmatrix} = \begin{bmatrix}\gamma_{XX}^{(j)} & \gamma_{XY}^{(j)}\\ \gamma_{YX}^{(j)} & \gamma_{YY}^{(j)}\end{bmatrix}. \tag{5.7}$$

Then the population spectrum for such defined vector process would be

$$\mathbf{s}_{\mathbf{Y}}(\omega) = \frac{1}{2\pi}\begin{bmatrix}\sum\limits_{j=-\infty}^{\infty}\gamma_{XX}^{(j)}e^{-i\omega j} & \sum\limits_{j=-\infty}^{\infty}\gamma_{XY}^{(j)}e^{-i\omega j}\\ \sum\limits_{j=-\infty}^{\infty}\gamma_{YX}^{(j)}e^{-i\omega j} & \sum\limits_{j=-\infty}^{\infty}\gamma_{YY}^{(j)}e^{-i\omega j}\end{bmatrix}. \tag{5.8}$$

Using DeMoivre theorem, relation (5.2) and the trigonometry facts that $\cos(-\omega) = \cos(\omega)$ and $\sin(-\omega) = -\sin(\omega)$, the population spectrum (5.8) can be simplified to

$$\mathbf{s}_{\mathbf{Y}}(\omega) = \frac{1}{2\pi}\begin{bmatrix}\sum\limits_{j=-\infty}^{\infty}\gamma_{XX}^{(j)}\cos(\omega j) & \sum\limits_{j=-\infty}^{\infty}\gamma_{XY}^{(j)}\{\cos(\omega j)-i.\sin(\omega j)\}\\ \sum\limits_{j=-\infty}^{\infty}\gamma_{YX}^{(j)}\{\cos(\omega j)-i.\sin(\omega j)\} & \sum\limits_{j=-\infty}^{\infty}\gamma_{YY}^{(j)}\cos(\omega j)\end{bmatrix}. \tag{5.9}$$

After simplification, it is clear that the diagonal elements have not imaginary part and off-diagonal elements are complex numbers.

5.1.1 Estimation of the Multivariate Spectrum

Non-parametric Estimates of the Multivariate Spectrum

Let $\boldsymbol{y}_1, \boldsymbol{y}_2, \ldots, \boldsymbol{y}_T$ denote samples of T observations of $\boldsymbol{Y}_t$. Then we can construct *sample multivariate periodogram*

$$\hat{\mathbf{s}}_y(\omega) = \frac{1}{2\pi}\sum_{j=-T+1}^{T-1}\hat{\boldsymbol{\Gamma}}_j e^{-i\omega j}, \tag{5.10}$$

where $\hat{\boldsymbol{\Gamma}}_j = T^{-1}\sum_{t=j+1}^{T}(\boldsymbol{y}_t-\bar{\boldsymbol{y}})(\boldsymbol{y}_{t-j}-\bar{\boldsymbol{y}})$ and $\bar{\boldsymbol{y}} = T^{-1}\sum_{t=1}^{T}\boldsymbol{y}_t$.

Non-parametric method for estimation of multivariate population spectrum applies weighting coefficients κ_j^* to sample autocovariances $\hat{\boldsymbol{\Gamma}}_j$ in the formula for sample multivariate periodogram. Thus an estimate of multivariate population spectrum would take the form

$$\hat{\mathbf{s}}_Y(\omega) = \frac{1}{2\pi}\sum_{j=-T+1}^{T-1}\kappa_j^*\hat{\boldsymbol{\Gamma}}_j e^{-i\omega j} \tag{5.11}$$

or alternatively

$$\hat{\mathbf{s}}_Y(\omega) = \frac{1}{2\pi}\Big\{\hat{\mathbf{\Gamma}}_0 + \sum_{j=1}^{T-1} \kappa_j^* \big(\hat{\mathbf{\Gamma}}_j e^{-i\omega j} + \hat{\mathbf{\Gamma}}_j^{'} e^{i\omega j}\big)\Big\}. \tag{5.12}$$

The *Bartlett* window defined in 4.5.1 is applicable also in the multivariate case. Thus the modified Bartlett estimation of multivariate population spectrum is

$$\hat{\mathbf{s}}_Y(\omega) = \frac{1}{2\pi}\Big\{ \sum_{j=-h}^{h} \Big(1 - \frac{|j|}{h}\Big)\hat{\mathbf{\Gamma}}_j e^{-i\omega j}\Big\} \tag{5.13}$$

and it can be also alternatively rewritten as

$$\hat{\mathbf{s}}_Y(\omega) = \frac{1}{2\pi}\Big\{\hat{\mathbf{\Gamma}}_0 + \sum_{j=1}^{h} \Big(1 - \frac{|j|}{h}\Big) \big(\hat{\mathbf{\Gamma}}_j e^{-i\omega j} + \hat{\mathbf{\Gamma}}_j^{'} e^{i\omega j}\big)\Big\}. \tag{5.14}$$

Parametric Estimation of the Multivariate Spectrum

By analogy with the estimation of the population spectrum for univariate process, the population spectrum for $\boldsymbol{Y}_t$ can be estimated also by *parametric approach* which is based on the evidence that multivariate time series can be reasonably described by pth-order vector autoregressive process VAR(p) defined in the form

$$\boldsymbol{Y}_t = \mathbf{C} + \mathbf{\Phi}_1 \boldsymbol{Y}_{t-1} + \mathbf{\Phi}_2 \boldsymbol{Y}_{t-2} + \ldots + \mathbf{\Phi}_p \boldsymbol{Y}_{t-p} + \boldsymbol{\varepsilon_t}, \tag{5.15}$$

where $\mathbf{C}$ is $(n \times 1)$ vector of constants, $\mathbf{\Phi}_j$ is $(n \times n)$ matrix of autoregressive coefficients for $j = 1, 2, \ldots, p$ and $\boldsymbol{\varepsilon}$ is vector generalization of white noise [1].

The first step of this procedure is to estimate the coefficients of a VAR(p) process by OLS. The optimal lag structure of VAR(p) process should be identified using the information criteria, especially Akaike's information criterion (AIC)[2]. These estimates are then substituted for the parameters $\mathbf{\Phi}_1, \mathbf{\Phi}_2, \ldots, \mathbf{\Phi}_p$ in the theoretical population spectrum of pth-order vector autoregressive process

$$\begin{aligned} \mathbf{s_Y}(\omega) =& \frac{1}{2\pi}[\mathbf{I_n} - \mathbf{\Phi}_1 e^{-i\omega} - \mathbf{\Phi}_2 e^{-i2\omega} - \ldots - \mathbf{\Phi}_p e^{-ip\omega}]\mathbf{\Omega} \\ & \times [\mathbf{I_n} - \mathbf{\Phi}_1^{'} e^{i\omega} - \mathbf{\Phi}_2^{'} e^{i2\omega} - \ldots - \mathbf{\Phi}_p^{'} e^{ip\omega}]^{'}, \end{aligned} \tag{5.16}$$

thereby yielding an estimator of the population spectrum.

[1] For vector generalization of white noise holds that $E(\boldsymbol{\varepsilon}_t) = \mathbf{0}$, $E(\boldsymbol{\varepsilon}_t \boldsymbol{\varepsilon}_\tau^{'}) = \mathbf{\Omega}$ for $t = \tau$, where $\mathbf{\Omega}$ is $(n \times n)$ symmetric positive definitive matrix and if $t \neq \tau$ $E(\boldsymbol{\varepsilon}_t \boldsymbol{\varepsilon}_\tau^{'}) = \mathbf{0}$.

[2] For definition of AIC criterion see (4.18).

5.2 The Cross Spectrum and Its Components

Let $\{X_t\}_{t=-\infty}^{\infty}$ be covariance-stationary process with mean equals μ_X and $\{Y_t\}_{t=-\infty}^{\infty}$ be also covariance-stationary process with mean μ_Y. The *population cross spectrum* from X_t to Y_t is defined as:

$$\begin{aligned} s_{YX}(\omega) &= \frac{1}{2\pi}\sum_{j=-\infty}^{\infty}\gamma_{YX}^{(j)}e^{-i\omega j} \\ &= \frac{1}{2\pi}\sum_{j=-\infty}^{\infty}\gamma_{YX}^{(j)}\{\cos(\omega j) - i.\sin(\omega j)\}, \end{aligned} \tag{5.17}$$

where $\gamma_{YX}^{(j)}$ is j-th autocovariance between X and Y equal to

$$\gamma_{YX}^{(j)} = E(Y_t - \mu_Y)(X_{t-j} - \mu_X).$$

Since the cross spectrum is a complex number it can be presented as a sum of real and imaginary part:

$$s_{YX}(\omega) = c_{YX}(\omega) + i.q_{YX}(\omega). \tag{5.18}$$

The real component of cross spectrum $c_{YX}(\omega)$ is called *cospectrum* between X and Y and it is calculated as

$$c_{YX}(\omega) = \frac{1}{2\pi}\sum_{j=-\infty}^{\infty}\gamma_{YX}^{(j)}\cos(\omega j). \tag{5.19}$$

It is characterized by the following properties:

- The cospectrum between X and Y is the same as the cospectrum between Y and X: $c_{YX}(\omega) = c_{XY}(\omega)$.
- The cospectrum is symmetric function: $c_{YX}(-\omega) = c_{YX}(\omega)$.

The imaginary component of the cross spectrum $q_{YX}(\omega)$ is called *quadrature spectrum* from X to Y:

$$q_{YX}(\omega) = -\frac{1}{2\pi}\sum_{j=-\infty}^{\infty}\gamma_{YX}^{(j)}\sin(\omega j). \tag{5.20}$$

The quadrature spectrum has the following properties:

- The quadrature spectrum from X to Y is the negative of quadrature spectrum from Y to X: $q_{YX}(\omega) = -q_{XY}(\omega)$.

- The quadrature spectrum is odd function: $q_{YX}(-\omega) = -q_{YX}(\omega)$.

By analogy with the relation (4.8), the area under the cross spectrum is equal to the covariance between X and Y:

$$\int_{-\pi}^{\pi} s_{YX}(\omega)d\omega = E(Y_t - \mu_Y)(X_t - \mu_X). \tag{5.21}$$

It further follows from (5.18) and from properties of quadrature spectrum that (5.21) can be rewritten as

$$\int_{-\pi}^{\pi} c_{YX}(\omega)d\omega = E(Y_t - \mu_Y)(X_t - \mu_X). \tag{5.22}$$

Thus, the covariance between X and Y is equal to the area under the cospectrum between X and Y. The cospectrum $c_{YX}(\omega)$ expressed by the portion of covariance between X and Y corresponds to cycles with frequency ω.

5.3 Coherence, Coherency, Phase and Gain

The relationship between two time series is normally characterized by the *gain* and the *phase*. These two quantities are derived from cross spectrum.

Let Y_t and X_t be jointly covariance-stationary processes with continuous spectrum $s_Y(\omega)$ and $s_X(\omega)$ respectively. The cross spectrum from X_t to Y_t is defined by

$$s_{YX}(\omega) = \frac{1}{2\pi} \sum_{j=-\infty}^{\infty} \gamma_{YX}^{(j)} e^{-i\omega j}.$$

It can be also alternatively represented in polar coordinate form

$$s_{YX}(\omega) = c_{YX}(\omega) + i.q_{YX}(\omega) = R_{YX}(\omega).e^{i\theta(\omega)}, \tag{5.23}$$

where the function $R_{YX}(\omega)$ is called the *gain* and it shows the amplitude of relationship between time series as a function of frequency. It is represented as

$$R_{YX}(\omega) = \{[c_{YX}(\omega)]^2 + [q_{YX}(\omega)]^2\}^{1/2}. \tag{5.24}$$

The *phase function* $\theta(\omega)$ represents the phase difference between the frequency components of two time series as a function of frequency and it satisfies

$$\theta(\omega) = \tan^{-1}\left[\frac{q_{YX}(\omega)}{c_{YX}(\omega)}\right]. \tag{5.25}$$

Although the gain and the phase characterize the relationship between time series, the relationship is not an exact one. This suggest the need for a third quantity, coherency or coherence respectively, which measures the strength of the relationship at different frequencies.

Coherency function can show at which frequencies two sets of time series are coherent and at which frequencies they are not. It is defined as

$$C_{YX}(\omega) = \frac{s_{YX}}{\sqrt{s_Y(\omega)s_X(\omega)}} = \frac{c_{YX}(\omega) + i.q_{YX}(\omega)}{\sqrt{s_Y(\omega)s_X(\omega)}}, \tag{5.26}$$

where $s_{YX}(\omega)$ is cross spectrum from X to Y, $c_{YX}(\omega)$ is a cospectrum between X and Y and $q_{YX}(\omega)$ is quadrature spectrum from X to Y. Hence, the coherency is complex in general and it is not a symmetric function. Priestley in [75] calls the function defined in (5.26) the *complex coherency* and its absolute value $|C_{YX}(\omega)|$ the *coherency*. He also claims that "$C_{YX}(\omega)$ represents a correlation coefficient in the frequency domain".

Coherency raised to the second power is called *population coherence* between X and Y or *squared coherency*. The coherence is numerically defined as

$$h_{YX}(\omega) = \frac{|s_{YX}(\omega)|^2}{s_Y(\omega)s_X(\omega)} = \frac{[c_{YX}(\omega)]^2 + [q_{YX}(\omega)]^2}{s_Y(\omega)s_X(\omega)}. \tag{5.27}$$

Therefore the coherence is real and symmetric function. However, it does not measure correlation of two processes at different frequencies, because it disregards the phase difference between variables. It indicates how well X corresponds to Y at each frequency. The values of the coherence satisfies $0 \leq h_{YX}(\omega) \leq 1$ for all ω.

To take the moduli on both sides of (5.23) we see that $|s_{YX}(\omega)|^2 = R_{YX}(\omega)^2$, so the information about the phase is lost in coherence $h_{YX}(\omega)$.

The gain factor combined with coherency function and phase function would give us fair clear picture about the relationship between two sets of time series. The analysis of these three quantities together with spectrum of each series give us an overall view of the frequency interactions of the time series.

5.4 Dynamic Correlation

The correlation analysis is the fundamental approach, which has been applied in the literature to study the degrees of synchronization between economic variables.

The most common measure of co-movement between time series is *classical correlation*, which is also used in the literature to measure the business cycle correlation.

The classical correlation, $\text{corr}(X_t, Y_t)$, between two random variables X_t and Y_t is defined as

$$\text{corr}(X_t, Y_t) = \frac{E(X_t Y_t) - E(X_t)E(Y_t)}{\sqrt{E(X_t^2) - E(X_t)^2}\sqrt{E(Y_t^2) - E(Y_t)^2}}$$

Unfortunately, the classical correlation is associated with two main drawbacks: Firstly, it does not allow for a separation of idiosyncratic components and common co-movements. Secondly, it is basic tool of static analysis that fails to capture any dynamics in the co-movement.

An alternative measure of synchronization in case of business cycles is the *dynamic correlation*. The spectral based dynamic correlation was proposed by Croux *et al.* in [15]. This indicator provides a formal measure of correlation, degree of comovement, between two time series at each individual frequency.

Let X_t and Y_t be two covariance-stationary processes and $s_X(\omega)$ and $s_Y(\omega)$ be the spectral density functions belong to them. The cospectrum between these time series is represented by the value $c_{YX}(\omega)$ which is defined by (5.19). Thus, the *dynamic correlation* between X_t and Y_t is defined as

$$\rho_{YX}(\omega) = \frac{c_{YX}(\omega)}{\sqrt{s_X(\omega)s_Y(\omega)}}. \tag{5.28}$$

It is clear from definition that the dynamic correlation, which lies between -1 and 1, is conceptually similar to the classical correlation between two series in the time domain. The higher dynamic correlation of time series is, the more similar the fluctuations at that frequency are. However, unlike the classical correlation, one obtains a correlation coefficient that can vary across different frequencies. Thus, the concept of dynamic correlation is more comprehensive because it looks at the correlation across entire frequency band.

An illustrative example of dynamic correlation between ε_t and ε_{t-1}, where ε_t is white noise process, is provided by the following figure 5.1. From the figure it is clear, that the dynamic correlation ranges from 1 at the frequency zero to -1 at the frequency π. The

lowest frequencies show highest correlation implying that the long-run fluctuations in the series are strongly related. The higher frequencies corresponds to perfect negative correlation.

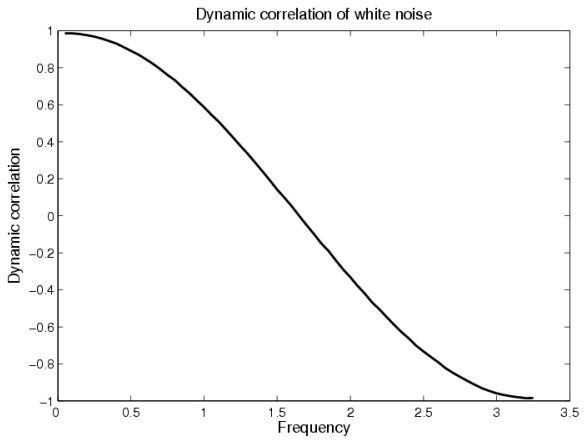

Figure 5.1: Dynamic correlation between ε_t and ε_{t-1}.

In this case, the classical correlation corr$(\varepsilon_t, \varepsilon_{t-1})$ is the simple mean of the dynamic correlation over the presented interval and it equals zero. This is due to fact that the white noise has a flat spectrum over the interval $[0, \pi]$[3]. But generally the relation between dynamic and static correlation is not so simple and obvious like in the case of white noise process.

Alternatively, we could aggregate the dynamic correlation defined in (5.28) across a frequency band $\Omega = [\omega_1, \omega_2]$ as

$$\rho_{YX}(\Omega) = \int_{\Omega} \rho_{YX}(\omega) d\omega = \frac{\int_{\Omega} c_{YX}(\omega) d\omega}{\sqrt{\int_{\Omega} s_X(\omega) d\omega \int_{\Omega} s_Y(\omega) d\omega}}, \tag{5.29}$$

where $0 \leq \omega_1 < \omega_2 \leq \pi$.

The *dynamic correlation within the frequency band*, as it is defined in (5.29), can be used also for measurement of the co-movement of seasonal components of two economic time series since we can select the frequency band of our interest (business cycle frequencies, or short-run and long-run frequencies) and then evaluate the dynamic correlation within this frequency band.

[3]The derivation of population spectrum for white noise process is described in 7.1.

In particular case, if $\omega_1 = 0$ and $\omega_2 = \pi$, the dynamic correlation within frequency band $\rho_{YX}(\Omega)$ is reduced to static correlation corr(X, Y), what is confirmed by the previous illustrative example. Hereby, we can extract the static correlation from the dynamic correlation.

5.5 Cohesion and Cross-Cohesion

Croux *et al.* in [15] used the notion of dynamic correlation to construct a multivariate index of co-movement, called *cohesion*. The cohesion provides a measure of the degrees of co-movement within a group of variables. An extension of cohesion which measure a co-movements between two groups of variables is called *cross-cohesion*.

The cohesion, defined in frequency domain, is a measure of dynamic co-movement between time series. In bivariate case, the measure is reduced to the dynamic correlation (5.28). The cohesion is useful for studying problems of business cycle synchronization and investigating short-run and long-run dynamic properties of multiple time series. It is an appropriate technique to obtain the facts on co-movements of macroeconomic variables at specified frequency band.

Let $\boldsymbol{Y}_t = (Y_{1t}, \ldots, Y_{nt})'$ be a vector of $n \geq 2$ variables and $w = (w_1, \ldots, w_n)'$ be a vector of the non-normalized positive weights of the variables in $\boldsymbol{Y}_t$. The *cohesion* of the variables in $\boldsymbol{Y}_t$ is defined as the weighted average of dynamic correlation between all possible pairs of series. Therefore, the cohesion is defined as

$$\text{coh}_Y(\omega) = \frac{\sum_{i \neq j} w_i w_j \rho_{Y_i Y_j}(\omega)}{\sum_{i \neq j} w_i w_j}. \tag{5.30}$$

Clearly $\text{coh}_Y(\omega) = 1$ if and only if all the variables in $\boldsymbol{Y}_t$ are perfectly co-moved at frequency ω. But the small cohesion index does not need to imply the small pairwise co-movements because it can be originated from large negative and positive covariances canceling out each other. Croux *et al.* in [15] excludes the diagonal terms in (5.30) for two reasons. First, it is reasonable to require that, if the entries in $\boldsymbol{Y}_t$ are pairwise uncorrelated at all leads and lags, cohesion is zero at all frequencies. And second, the inclusion of the diagonal terms would render cohesion dependent on n.

Alternatively, we could aggregate the cohesion defined in (5.30) across a frequency band $\Omega = [\omega_1, \omega_2]$ as

$$\text{coh}_Y(\Omega) = \frac{\sum_{i \neq j} w_i w_j \rho_{Y_i Y_j}(\Omega)}{\sum_{i \neq j} w_i w_j}, \tag{5.31}$$

where $0 \leq \omega_1 < \omega_2 \leq \pi$.

The cohesion index can be generalized to an index measuring the *cross-cohesion* between the $(n \times 1)$ vector $\boldsymbol{Y}_t$ and $(m \times 1)$ vector $\boldsymbol{X}_t$. Thus, the cross-cohesion between $\boldsymbol{Y}_t$ and $\boldsymbol{X}_t$ at frequency ω is given by

$$\text{coh}_{YX}(\omega) = \frac{\sum_{i=1}^{n}\sum_{j=1}^{m} w_{Y_i} w_{X_j} \rho_{Y_i X_j}(\omega)}{\sum_{i=1}^{n}\sum_{j=1}^{m} w_{Y_i} w_{X_j}}. \tag{5.32}$$

If the Y_t and X_t are scalars, then the cross-cohesion is reduced to the dynamic correlation (5.28).

6

Autocovariance-Generating Function

The concept of autocovariance-generating function for univariate processes was introduced in the section 4.2. Thus *autocovariance-generating function* for univariate time series Y_t is defined as

$$g_Y(z) = \sum_{j=-\infty}^{\infty} \gamma_j z^j,$$

where its argument (z) is a complex scalar and γ_j is jth autocovariance of Y_t. Then, in the section 5.1, we extend this concept for multivariate processes. The *autocovariance-generating function* of vector process $\boldsymbol{Y}_t$ is therefore defined as

$$\mathbf{G}_{\mathbf{Y}}(z) = \sum_{j=-\infty}^{\infty} \boldsymbol{\Gamma}_j z^j,$$

where $\boldsymbol{\Gamma}_j$ is autocovariance matrix related to $\boldsymbol{Y}_t$.

In this chapter we derive the autocovariance-generating function for various processes, for univariate ones (white noise, autoregressive process, moving average process and ARMA process) and also for vector processes (vector white noise, vector autoregression,...) in order to obtain the population spectrum for them.

6.1 White Noise

We start with the simplest process, the *white noise*.

Let $\{\varepsilon_t\}_{t=-\infty}^{\infty}$ be a white noise whose elements have mean zero and variance σ^2,

$$E(\varepsilon_t) = 0 \tag{6.1}$$

$$\gamma_0 = E(\varepsilon_t^2) = \sigma^2, \tag{6.2}$$

and for which the ε's are uncorrelated across time:

$$\gamma_j = E(\varepsilon_t \varepsilon_{t-j}) = 0 \qquad \text{for } j \neq 0. \tag{6.3}$$

The autocovariance-generating function for a vector white noise, $Y_t = \varepsilon_t$, could be therefore calculated from

$$g_Y(z) = \sigma^2 z^0 = \sigma^2. \tag{6.4}$$

6.2 Moving Average Processes

6.2.1 The First-Order Moving Average Process

Let $\{\varepsilon_t\}_{t=-\infty}^{\infty}$ be a white noise satisfied equations (6.2) and (6.3). Consider the process

$$Y_t = \mu + \varepsilon_t + \theta\varepsilon_{t-1}, \tag{6.5}$$

where μ and θ are any real constants. This time series is called *first-order moving average process*, denoted $MA(1)$.

The mean of the first-order moving average process is given by

$$E(Y_t) = E(\mu + \varepsilon_t + \theta\varepsilon_{t-1}) = \mu + E(\varepsilon_t) + \theta E(\varepsilon_{t-1}) = \mu. \tag{6.6}$$

The variance of Y_t is

$$\gamma_0 = E(Y_t - \mu)^2 = E(\varepsilon_t + \theta\varepsilon_{t-1})^2 = (1 + \theta^2)\sigma^2. \tag{6.7}$$

The first autocovariance of $MA(1)$ process is

$$\begin{aligned} \gamma_1 = E(Y_t - \mu)(Y_{t-1} - \mu) &= E(\varepsilon_t + \theta\varepsilon_{t-1})(\varepsilon_{t-1} + \theta\varepsilon_{t-2}) \\ &= E(\varepsilon_t\varepsilon_{t-1} + \theta\varepsilon_{t-1}^2 + \theta\varepsilon_t\varepsilon_{t-2} + \theta^2\varepsilon_{t-1}\varepsilon_{t-2}) \\ &= \theta\sigma^2 \end{aligned} \tag{6.8}$$

and higher autocovariances are all zero

$$\gamma_j = E(Y_t - \mu)(Y_{t-j} - \mu) = 0 \qquad \text{for } j > 1.$$

According to the previous equations of variance and autocovariances, the autocovariance-generating function for the first-order moving average process is calculates as

$$g_Y(z) = [\theta\sigma^2]z^{-1} + [(1+\theta^2)\sigma^2]z^0 + [\theta\sigma^2]z^1.$$

It can be rewritten as follows

$$g_Y(z) = \sigma^2(1+\theta z)(1+\theta z^{-1}). \tag{6.9}$$

6.2.2 The qth-Order and Infinite-Order Moving Average Process

The *qth-order moving average process*, denoted $MA(q)$, is expressed as

$$Y_t = \mu + \varepsilon_t + \theta_1\varepsilon_{t-1} + \theta_2\varepsilon_{t-2} + \ldots + \theta_q\varepsilon_{t-q}, \tag{6.10}$$

where ε_t is a white noise defined in previous section and μ and $(\theta_1, \theta_2, \ldots, \theta_q)$ could be any real numbers. With using the lag operator the process can be alternatively rewritten as

$$Y_t = \mu + (1 + \theta_1 L + \theta_2 L^2 + \ldots + \theta_q L^q)\varepsilon_t.$$

The qth-order moving average process has mean equals to

$$E(Y_t) = \mu + E(\varepsilon_t) + \theta_1 E(\varepsilon_{t-1}) + \theta_2 E(\varepsilon_{t-2}) + \ldots + \theta_q E(\varepsilon_{t-q}) = \mu. \tag{6.11}$$

And the variance of $MA(q)$ process is

$$\begin{aligned}\gamma_0 = E(Y_t - \mu)^2 &= E(\varepsilon_t + \theta_1\varepsilon_{t-1} + \theta_2\varepsilon_{t-2} + \ldots + \theta_q\varepsilon_{t-q})^2 \\ &= E(\varepsilon_t^2 + \theta_1^2\varepsilon_{t-1}^2 + \theta_2^2\varepsilon_{t-2}^2 + \ldots + \theta_q^2\varepsilon_{t-q}^2 + \ldots) \\ &= (1 + \theta_1^2 + \theta_2^2 + \ldots + \theta_q^2)\sigma^2. \end{aligned} \tag{6.12}$$

The autocovariances of $MA(q)$ process are given by

$$\gamma_j = \begin{cases} (\theta_j + \theta_{j+1}\theta_1 + \theta_{j+2}\theta_2 + \ldots + \theta_q\theta_{q-j})\sigma^2 & \text{for } j = 1, 2, \ldots, q \\ 0 & \text{for } j > q. \end{cases}$$

Consequently the autocovariance-generating function for $MA(q)$ process could be specified as

$$g_Y(z) = \sigma^2(1 + \theta_1 z + \theta_2 z^2 + \ldots + \theta_q z^q)(1 + \theta_1 z^{-1} + \theta_2 z^{-2} + \ldots + \theta_q z^{-q}). \quad (6.13)$$

By analogy, we can derive an autocovariance-generating function also for *infinity-order moving average process*, $MA(\infty)$, that is defined as

$$Y_t = \mu + \sum_{j=0}^{\infty} \psi_j \varepsilon_{t-j}.$$

If $MA(\infty)$ is rewritten as

$$Y_t = \mu + \psi(L)\varepsilon_t \quad (6.14)$$

with $\psi(L) = \psi_0 + \psi_1 L + \psi_2 L^2 + \ldots$, then its autocovariance-generating function is defined as

$$g_Y(z) = \sigma^2 \psi(z)\psi(z^{-1}). \quad (6.15)$$

6.3 Autoregressive Processes

If ε_t is a white noise satisfying (6.2) and (6.3), then a *first-order autoregression*, denoted $AR(1)$, is characterized by

$$Y_t = c + \phi Y_{t-1} + \varepsilon_t. \quad (6.16)$$

It can be also written as

$$Y_t = \mu + (1 - \phi L)^{-1}\varepsilon_t,$$

where μ is a mean of $AR(1)$ process, calculated as $\mu = c/(1 - \phi)$. This notation is very similar to $MA(\infty)$ definition in (6.14). $AR(1)$ process is a special form of $MA(\infty)$ where $\psi(L) = 1/(1 - \phi L)$. Therefore autocovariance-generating function of $AR(1)$ process could be calculated as

$$g_Y(z) = \frac{\sigma^2}{(1 - \phi z)(1 - \phi z^{-1})}. \quad (6.17)$$

The same method for the derivation of the autocovariance-generating function should be applied to for *pth-order autoregressive process*, $AR(p)$

$$Y_t = c + \phi_1 Y_{t-1} + \phi_2 Y_{t-2} + \ldots + \phi_p Y_{t-p} + \varepsilon_t. \quad (6.18)$$

Analogous to $AR(1)$ process, the process $AR(p)$ can be rewritten in lag operator form in the following way

$$Y_t = \mu + \psi(L)\varepsilon_t,$$

where μ is a mean of $AR(p)$ process, calculated as $\mu = c/(1 - \phi_1 - \phi_2 - \ldots - \phi_p)$, and $\psi(L) = 1/(1 - \phi_1 L - \phi_2 L^2 - \ldots - \phi_p L^p)$. So the $AR(p)$ process in this form is viewed as $MA(\infty)$ process. Therefore autocovariance-generating function of $AR(p)$ process could be calculated as

$$g_Y(z) = \frac{\sigma^2}{(1 - \phi_1 z - \phi_2 z^2 - \ldots - \phi_p z^p)(1 - \phi_1 z^{-1} - \phi_2 z^{-2} - \ldots - \phi_p z^{-p})}. \tag{6.19}$$

6.4 Mixed Autoregressive Moving Average Processes

A *mixed autoregressive moving average process*, $ARMA(p, q)$, consisting from both autoregressive and moving average term, is defined as

$$Y_t = c + \phi_1 Y_{t-1} + \phi_2 Y_{t-2} + \ldots + \phi_p Y_{t-p} + \varepsilon_t + \theta_1 \varepsilon_{t-1} + \theta_2 \varepsilon_{t-2} + \ldots + \theta_q \varepsilon_{t-q}, \tag{6.20}$$

It can be alternatively rewritten into lag operator form

$$(1 - \phi_1 L - \phi_2 L^2 - \ldots - \phi_p L^p) Y_t = c + (1 + \theta_1 L + \theta_2 L^2 + \ldots + \theta_q L^q)\varepsilon_t.$$

or

$$Y_t = \mu + \psi(L)\varepsilon_t,$$

where

$$\psi(L) = \frac{1 + \theta_1 L + \theta_2 L^2 + \ldots + \theta_q L^q}{1 - \phi_1 L - \phi_2 L^2 - \ldots - \phi_p L^p},$$

and

$$\mu = c/(1 - \phi_1 - \phi_2 - \ldots - \phi_p).$$

The autocovariance-generating function for a stationary $ARMA(p, q)$ process can be written as

$$\begin{aligned} g_Y(z) = \sigma^2 & \frac{(1 + \theta_1 z + \theta_2 z^2 + \ldots + \theta_q z^q)}{(1 - \phi_1 z - \phi_2 z^2 - \ldots - \phi_p z^p)} \\ & \times \frac{(1 + \theta_1 z^{-1} + \theta_2 z^{-2} + \ldots + \theta_q z^{-q})}{(1 - \phi_1 z^{-1} - \phi_2 z^{-2} - \ldots - \phi_p z^{-p})}. \end{aligned} \tag{6.21}$$

6.5 Vector Processes

6.5.1 Vector White Noise

Let $\boldsymbol{\varepsilon_t}$ be a *vector white noise process* which satisfies the following equations

$$E(\boldsymbol{\varepsilon_t}) = \mathbf{0} \tag{6.22}$$

$$E(\boldsymbol{\varepsilon_t}\boldsymbol{\varepsilon}_{\boldsymbol{\tau}}^{'}) = \begin{cases} \boldsymbol{\Omega} \text{ for } t = \tau \\ \mathbf{0} \text{ otherwise,} \end{cases} \tag{6.23}$$

where $\boldsymbol{\Omega}$ is $(n \times n)$ symmetric positive definitive matrix.

The autocovariance-generating function for a vector white noise, $\boldsymbol{Y}_t = \boldsymbol{\varepsilon_t}$, could be therefore calculated from

$$\mathbf{G}_{\mathbf{Y}}(z) = \boldsymbol{\Omega}. \tag{6.24}$$

6.5.2 Vector Moving Average Process

A *vector qth-order moving average process*, denoted $MA(q)$, is characterized by

$$\boldsymbol{Y}_t = \boldsymbol{\mu} + \boldsymbol{\varepsilon_t} + \boldsymbol{\Theta}_1\boldsymbol{\varepsilon_{t-1}} + \boldsymbol{\Theta}_2\boldsymbol{\varepsilon_{t-2}} + \ldots + \boldsymbol{\Theta}_q\boldsymbol{\varepsilon_{t-q}}, \tag{6.25}$$

where $\boldsymbol{\varepsilon_t}$ is a vector white noise defined in previous section and $\boldsymbol{\Theta}_j$ denotes $(n \times n)$ matrix of MA coefficients for $j = 1, 2, \ldots, q$.
The mean of vector qth-order moving average process is $\boldsymbol{\mu}$, variance of $\boldsymbol{Y}_t$ is

$$\begin{aligned} \boldsymbol{\Gamma}_0 &= E[(\boldsymbol{Y}_t - \boldsymbol{\mu})(\boldsymbol{Y}_t - \boldsymbol{\mu})'] \\ &= \boldsymbol{\Omega} + \boldsymbol{\Theta}_1\boldsymbol{\Omega}\boldsymbol{\Theta}_1^{'} + \boldsymbol{\Theta}_2\boldsymbol{\Omega}\boldsymbol{\Theta}_2^{'} + \ldots + \boldsymbol{\Theta}_q\boldsymbol{\Omega}\boldsymbol{\Theta}_q^{'} \end{aligned} \tag{6.26}$$

and jth autocovariance

$$\boldsymbol{\Gamma}_j = \begin{cases} \boldsymbol{\Theta}_j\boldsymbol{\Omega} + \boldsymbol{\Theta}_{j+1}\boldsymbol{\Omega}\boldsymbol{\Theta}_1^{'} + \ldots + \boldsymbol{\Theta}_q\boldsymbol{\Omega}\boldsymbol{\Theta}_{q-j}^{'} & \text{for } j = 1, 2, \ldots, q \\ \boldsymbol{\Omega}\boldsymbol{\Theta}_{-j}^{'} + \boldsymbol{\Theta}_1\boldsymbol{\Omega}\boldsymbol{\Theta}_{-j+1}^{'} + \ldots + \boldsymbol{\Theta}_{q+j}\boldsymbol{\Omega}\boldsymbol{\Theta}_q^{'} & \text{for } j = -1, -2, \ldots, -q \\ \mathbf{0} & \text{otherwise.} \end{cases}$$

Analogous to autocovariance-generating function for univariate $MA(q)$ process (6.13), the autocovariance-generating function for vector $MA(q)$ process has form

$$\begin{aligned} \mathbf{G}_{\mathbf{Y}}(z) = (\mathbf{I_n} &+ \boldsymbol{\Theta}_1 z + \boldsymbol{\Theta}_2 z^2 + \ldots + \boldsymbol{\Theta}_q z^q)\boldsymbol{\Omega} \\ &\times (\mathbf{I_n} + \boldsymbol{\Theta}_1^{'} z + \boldsymbol{\Theta}_2^{'} z^2 + \ldots + \boldsymbol{\Theta}_q^{'} z^{-q}). \end{aligned} \tag{6.27}$$

We can derive an autocovariance-generating function also for *vector infinity-order moving average process*, $MA(\infty)$, that is defined as

$$\boldsymbol{Y}_t = \boldsymbol{\mu} + \boldsymbol{\Psi}(\boldsymbol{L})\boldsymbol{\varepsilon_t} \tag{6.28}$$

with $\boldsymbol{\Psi}(\boldsymbol{L}) = \boldsymbol{\Psi_0} + \boldsymbol{\Psi_1 L} + \boldsymbol{\Psi_2 L^2} + \ldots$, as generalization of relation (6.27). Therefore autocovariance-generating function for vector $MA(\infty)$ process could be calculated as

$$\mathbf{G_Y}(z) = [\boldsymbol{\Psi}(\boldsymbol{z})]\boldsymbol{\Omega}[\boldsymbol{\Psi}(\boldsymbol{z^{-1}})]' \tag{6.29}$$

6.5.3 Vector Autoregression

A *pth-order vector autoregressive process*, denoted $VAR(p)$, is defined in the form

$$\boldsymbol{Y}_t = \mathbf{C} + \boldsymbol{\Phi}_1\boldsymbol{Y}_{t-1} + \boldsymbol{\Phi}_2\boldsymbol{Y}_{t-2} + \ldots + \boldsymbol{\Phi}_p\boldsymbol{Y}_{t-p} + \boldsymbol{\varepsilon_t}, \tag{6.30}$$

where $\mathbf{C}$ is $(n \times 1)$ vector of constants, $\boldsymbol{\Phi}_j$ is $(n \times n)$ matrix of autoregressive coefficients for $j = 1, 2, \ldots, p$ and $\boldsymbol{\varepsilon_t}$ is vector generalization of white noise satisfying equations (6.22) and (6.23).

Such defined $VAR(p)$ process can be rewritten in lag operator form as

$$\boldsymbol{Y}_t = \boldsymbol{\mu} + \boldsymbol{\Psi}(\boldsymbol{L})\boldsymbol{\varepsilon_t},$$

where mean $\boldsymbol{\mu}$ of $VAR(p)$ process is calculated as $\boldsymbol{\mu} = (\mathbf{I_n} - \boldsymbol{\Phi}_1 - \boldsymbol{\Phi}_2 - \ldots - \boldsymbol{\Phi}_p)^{-1}\mathbf{C}$ and $\boldsymbol{\Psi}(\boldsymbol{L}) = (\mathbf{I_n} - \boldsymbol{\Phi}_1 L - \boldsymbol{\Phi}_2 L^2 - \ldots - \boldsymbol{\Phi}_p L^p)^{-1}$ indicates an $(n \times n)$ matrix polynomial in lag operator. So $VAR(p)$ process in this form is viewed as vector $MA(\infty)$ process, (6.28).

Therefore autocovariance-generating function for $VAR(p)$ process could be calculated as

$$\begin{aligned}\mathbf{G_Y}(z) = (\mathbf{I_n} - \boldsymbol{\Phi}_1 z - \boldsymbol{\Phi}_2 z^2 - \ldots - \boldsymbol{\Phi}_p z^p)^{-1}\boldsymbol{\Omega} \\ \times (\mathbf{I_n} - \boldsymbol{\Phi}_1' z^{-1} - \boldsymbol{\Phi}_2' z^{-2} - \ldots - \boldsymbol{\Phi}_p' z^{-p})^{-1}.\end{aligned} \tag{6.31}$$

7

Population Spectrum

In previous chapter we derived the autocovariance-generating function for various univariate and multivariate processes. This chapter describes how to calculate the population spectrum from the autocovariance-generating function. The presentation of population spectrum is defined in the section 4.3 for univariate processes and in the section 5.1 for multivariate processes.

The population spectrum $s_Y(\omega)$ of univariate process Y_t is generally defined in (4.4). The multivariate extension of population spectrum $\mathbf{s_Y}(\omega)$ of vector process $\boldsymbol{Y}_t$ is generally defined by the relation (5.4).

7.1 White Noise

Let $Y_t = \varepsilon_t$ where $\{\varepsilon_t\}_{t=-\infty}^{\infty}$ be a white noise satisfying equations (6.2) and (6.3) with autocovariance-generating function defined in (6.4). Thus, the population spectrum for white noise

$$s_Y(\omega) = \frac{\sigma^2}{2\pi}, \tag{7.1}$$

where σ^2 is the variance of Y_t, is a constant for all ω. The flat spectrum of white noise process is also shown in figure 7.1. Looking at the figure, it might be obvious that the area under the spectrum over the range $[-\pi, \pi]$ is actually equal to the variance of the white noise process, σ^2.

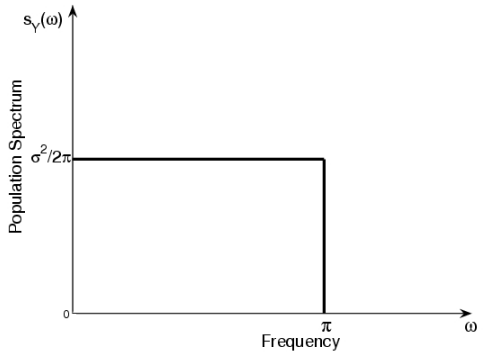

Figure 7.1: Population spectrum for white noise process.

In fact, figure 7.1 and the equation (7.1) provide a definition of white noise process in the frequency domain. Harvey in [38] claims that the spectrum of white noise may be regarded as consisting of an infinite number of cyclical components all of which have equal weight.

7.2 Moving Average Processes

7.2.1 The First-Order Moving Average Process

The first-order moving average process $MA(1)$ defined in (6.5) as

$$Y_t = \mu + \varepsilon_t + \theta\varepsilon_{t-1}$$

has $\gamma_0 = (1+\theta^2)\sigma^2$, $\gamma_1 = \theta\sigma^2$ and higher autocovariances of the $MA(1)$ process are all zero, $\gamma_j = 0$ for $j > 1$. Substituting the autocovariance-generating function of $MA(1)$ process derived from mentioned relations

$$g_Y(z) = \sigma^2(1+\theta z)(1+\theta z^{-1})$$

into (4.4) gives the definition of population spectrum for the first-order moving average process

$$s_Y(\omega) = \frac{\sigma^2}{2\pi}(1+\theta e^{-i\omega})(1+\theta e^{i\omega}). \tag{7.2}$$

According to the consequence of DeMoivre's theorem, (7.2) may be rewritten as

$$s_Y(\omega) = \frac{\sigma^2}{2\pi}(1 + \theta^2 + 2\theta \cos \omega). \tag{7.3}$$

If the process is defined with positive θ, the spectrum $s_Y(\omega)$ is monotonically decreasing function of ω from $[0, \pi]$. It means that the spectrum is greater at the lower frequencies. Whereas when the $MA(1)$ process is defined with negative θ, the spectrum is monotonically increasing and greater at the higher frequencies.

The example of decreasing ($\theta = 0.5$) and increasing ($\theta = -0.5$) population spectrum for $MA(1)$ process is illustrated in figure 7.2.

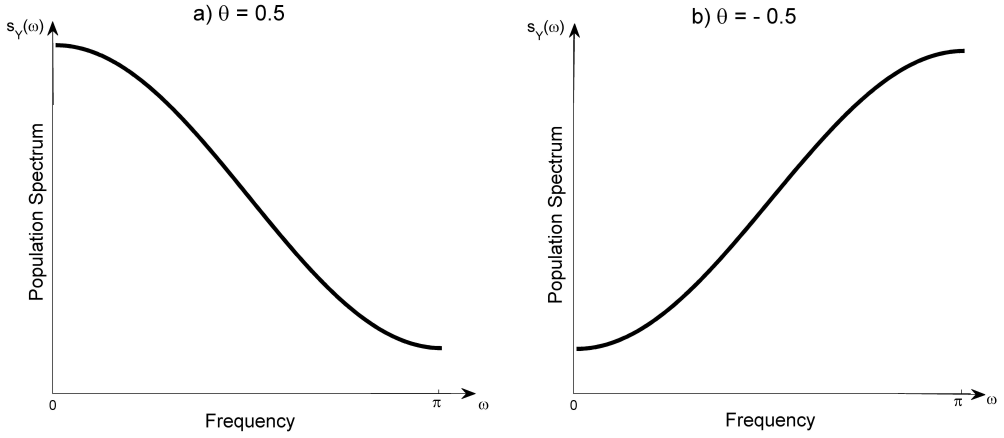

Figure 7.2: Example of population spectrum for $MA(1)$ process.

Because the Y_t is defined as weighted average of current and lagged disturbance terms, the series changes more slowly than the white noise. This is reflected by positive first-order autocovariance in time domain or by higher values of spectrum at the lower frequencies in frequency domain. This fact confirms the relation between the spectrum and the autocovariance function described in the section 4.3.2 that they are complementary rather than competitive.

7.2.2 The qth-Order and Infinity-Order Moving Average Process

Let $MA(q)$ process

$$Y_t = \mu + \varepsilon_t + \theta_1 \varepsilon_{t-1} + \theta_2 \varepsilon_{t-2} + \ldots + \theta_q \varepsilon_{t-q},$$

has an autocovariance-generating function defined in (6.13). The population spectrum of qth-order moving average process can be then defined as

$$\begin{aligned} s_Y(\omega) = \frac{\sigma^2}{2\pi}(1 + \theta_1 e^{-i\omega} + \theta_2 e^{-i2\omega} + \ldots + \theta_q e^{-iq\omega}) \\ \times (1 + \theta_1 e^{i\omega} + \theta_2 e^{i2\omega} + \ldots + \theta_q e^{iq\omega}). \end{aligned} \tag{7.4}$$

If the moving average polynomial is factored in the following form

$$1 + \theta_1 z + \theta_2 z^2 + \ldots + \theta_q z^q = (1 - \eta_1 z)(1 - \eta_2 z)\ldots(1 - \eta_q z),$$

then the population spectrum for $MA(q)$ process can be rewritten as

$$s_Y(\omega) = \frac{\sigma^2}{2\pi}\prod_{j=1}^{q}[1 + \eta_j^2 - 2\eta_j.cos(\omega)].$$

Let Y_t be the infinity-order moving average process, $MA(\infty)$

$$Y_t = \mu + \psi(L)\varepsilon_t,$$

where $\psi(L) = \psi_0 + \psi_1 L + \psi_2 L^2 + \ldots$ and let $g_Y(z)$ defined in (6.15) be an autocovariance-generating function of $MA(\infty)$. Hence, the population spectrum for an $MA(\infty)$ process is given by

$$s_Y(\omega) = \frac{\sigma^2}{2\pi}\psi(e^{-i\omega})\psi(e^{i\omega}). \tag{7.5}$$

7.3 Autoregressive Processes

7.3.1 The First-Order Autoregressive Process

Let $AR(1)$ process

$$Y_t = c + \phi Y_{t-1} + \varepsilon_t$$

has an autocovariance-generating function defined in (6.17). Thus, the population spectrum of the first-order autoregressive process is given by

$$\begin{aligned} s_Y(\omega) &= \frac{\sigma^2}{2\pi} \cdot \frac{1}{(1 - \phi e^{-i\omega})(1 - \phi e^{i\omega})} \\ &= \frac{\sigma^2}{2\pi} \cdot \frac{1}{(1 + \phi^2 - 2\phi.\cos(\omega))}. \end{aligned} \tag{7.6}$$

The spectrum of $AR(1)$ process is similar to the spectrum of an $MA(1)$ process characterized by (7.2). Thus, if the $AR(1)$ process is defined with positive ϕ (positive autocorrelation), the spectrum $s_Y(\omega)$ is monotonically decreasing function of ω over $[0, \pi]$ and it is dominated by low frequency components. Whereas when the $AR(1)$ process is defined with negative ϕ (negative autocorrelation), the spectrum is monotonically increasing function of ω.

The example of decreasing ($\phi = 0.5$) and increasing ($\phi = -0.5$) population spectrum for $AR(1)$ process is drawn in figure 7.3.

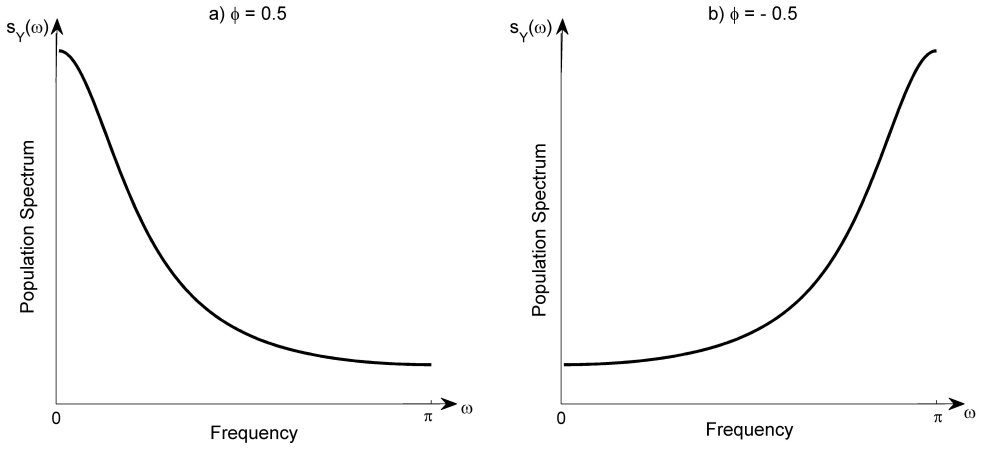

Figure 7.3: Example of population spectrum for $AR(1)$ process.

7.3.2 The pth-Order Autoregressive Process

Let $AR(p)$ process

$$Y_t = c + \phi_1 Y_{t-1} + \phi_2 Y_{t-2} + \ldots + \phi_p Y_{t-p} + \varepsilon_t$$

has an autocovariance-generating function defined in (6.19). Thus, the population spectrum of pth-order autoregressive process is given by

$$\begin{aligned} s_Y(\omega) = \frac{\sigma^2}{2\pi} \cdot \frac{1}{(1 - \phi_1 e^{-i\omega} - \phi_2 e^{-i2\omega} - \ldots - \phi_p e^{-ip\omega})} \\ \times \frac{1}{(1 - \phi_1 e^{i\omega} - \phi_2 e^{i2\omega} - \ldots - \phi_p e^{ip\omega})}. \end{aligned} \tag{7.7}$$

If the autoregressive polynomial is factored in the following form

$$1 - \phi_1 z - \phi_2 z^2 - \ldots - \phi_p z^p = (1 - \lambda_1 z)(1 - \lambda_2 z) \ldots (1 - \lambda_p z),$$

then the population spectrum for $AR(p)$ process can be formulated as

$$s_Y(\omega) = \frac{\sigma^2}{2\pi} \cdot \frac{1}{\prod_{j=1}^{p} [1 + \lambda_j^2 - 2\lambda_j . cos(\omega)]}.$$

The shape of the spectrum for $AR(p)$ process depends crucially on the values taken by the parameters $\phi_1, \phi_2, \ldots, \phi_p$. Monotonically decreasing or increasing population spectrum is typical only for $AR(1)$ processes as a special case of $AR(2)$ process, because it is similar to the spectrum of $MA(1)$ process.

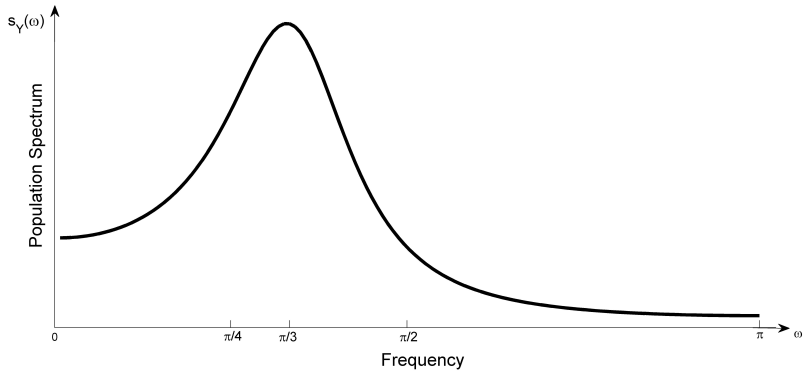

Figure 7.4: Example of population spectrum for $AR(2)$ process ($\phi_1 = 0.7$ and $\phi_2 = -0.5$).

Figure 7.4 represents the population spectrum for $AR(2)$ process with $\phi_1 = 0.7$ and $\phi_2 = -0.5$. The peak indicates a tendency towards a cycle what can be termed pseudo-cyclical behaviour, since the movements are not regular. The type of such pseudo-cyclical behaviour is attractive for economic modeling, because series generated by AR(2) processes can easily exhibit the kind of fluctuations often observed in practice.

7.4 Mixed Autoregressive Moving Average Processes

Let Y_t be the mixed autoregressive moving average process, $ARMA(p, q)$

$$Y_t = c + \phi_1 Y_{t-1} + \phi_2 Y_{t-2} + \ldots + \phi_p Y_{t-p} + \varepsilon_t + \theta_1 \varepsilon_{t-1} + \theta_2 \varepsilon_{t-2} + \ldots + \theta_q \varepsilon_{t-q}$$

with autocovariance-generating function defined in (6.21). Hence, the population spectrum for an $ARMA(p,q)$ process is given by

$$\begin{aligned} s_Y(\omega) = \frac{\sigma^2}{2\pi} \cdot \frac{(1+\theta_1 e^{-i\omega} + \theta_2 e^{-i2\omega} + \ldots + \theta_q e^{-iq\omega})}{(1-\phi_1 e^{-i\omega} - \phi_2 e^{-i2\omega} - \ldots - \phi_p e^{-ip\omega})} \\ \times \frac{(1+\theta_1 e^{i\omega} + \theta_2 e^{i2\omega} + \ldots + \theta_q e^{iq\omega})}{(1-\phi_1 e^{i\omega} - \phi_2 e^{i2\omega} - \ldots - \phi_p e^{ip\omega})}. \end{aligned} \tag{7.8}$$

Using the decomposition of moving average and autoregressive polynomials, the population spectrum for $ARMA(p,q)$ process can be written as

$$s_Y(\omega) = \frac{\sigma^2}{2\pi} \cdot \frac{\prod_{j=1}^{q}[1+\eta_j^2 - 2\eta_j.cos(\omega)]}{\prod_{j=1}^{p}[1+\lambda_j^2 - 2\lambda_j.cos(\omega)]}.$$

7.5 Vector Processes

7.5.1 Vector White Noise

Let $\boldsymbol{Y_t} = \boldsymbol{\varepsilon_t}$ where $\boldsymbol{\varepsilon_t}$ be a vector white noise satisfied equations (6.22) and (6.23) with autocovariance-generating function defined in (6.24). For that reason, the multivariate population spectrum for vector white noise process is calculated as

$$\mathbf{s_Y}(\omega) = \frac{1}{2\pi}\boldsymbol{\Omega}. \tag{7.9}$$

7.5.2 Vector Moving Average Process

Let vector $MA(q)$ process

$$\boldsymbol{Y_t} = \boldsymbol{\mu} + \boldsymbol{\varepsilon_t} + \boldsymbol{\Theta}_1\boldsymbol{\varepsilon_{t-1}} + \boldsymbol{\Theta}_2\boldsymbol{\varepsilon_{t-2}} + \ldots + \boldsymbol{\Theta}_q\boldsymbol{\varepsilon_{t-q}}$$

has an autocovariance-generating function defined in (6.27). The population spectrum of vector qth-order moving average process can be then defined as

$$\begin{aligned} \mathbf{s_Y}(\omega) = \frac{1}{2\pi} \cdot (\mathbf{I_n} + \boldsymbol{\Theta}_1 e^{-i\omega} + \boldsymbol{\Theta}_2 e^{-i2\omega} + \ldots + \boldsymbol{\Theta}_q e^{-iq\omega})\boldsymbol{\Omega} \\ \times (\mathbf{I_n} + \boldsymbol{\Theta}_1' e^{i\omega} + \boldsymbol{\Theta}_2' e^{i2\omega} + \ldots + \boldsymbol{\Theta}_q' e^{iq\omega}). \end{aligned} \tag{7.10}$$

Let $\boldsymbol{Y}_t$ be the infinity-order moving average process, $MA(\infty)$

$$\boldsymbol{Y}_t = \boldsymbol{\mu} + \boldsymbol{\Psi}(\boldsymbol{L})\boldsymbol{\varepsilon_t},$$

defined in (6.28) and let $\mathbf{G_Y}(z)$ defined in (6.29) be an autocovariance-generating function related to it. Hence, the population spectrum for vector $MA(\infty)$ process is given by

$$\mathbf{s_Y}(\omega) = \frac{1}{2\pi}[\boldsymbol{\Psi}(e^{-i\omega})]\boldsymbol{\Omega}[\boldsymbol{\Psi}(e^{i\omega})]'. \tag{7.11}$$

7.5.3 Vector Autoregression

Let vector $VAR(p)$ process

$$\boldsymbol{Y}_t = \mathbf{C} + \boldsymbol{\Phi}_1\boldsymbol{Y}_{t-1} + \boldsymbol{\Phi}_2\boldsymbol{Y}_{t-2} + \ldots + \boldsymbol{\Phi}_p\boldsymbol{Y}_{t-p} + \boldsymbol{\varepsilon_t}$$

has an autocovariance-generating defined in (6.31). Thus the population spectrum for pth-order vector autoregression is derived as

$$\begin{aligned}\mathbf{s_Y}(\omega) = \frac{1}{2\pi}(\mathbf{I_n} - \boldsymbol{\Phi}_1 e^{-i\omega} - \boldsymbol{\Phi}_2 e^{-i2\omega} - \ldots - \boldsymbol{\Phi}_p e^{-ip\omega})^{-1}\boldsymbol{\Omega} \\ \times (\mathbf{I_n} - \boldsymbol{\Phi}_1' e^{i\omega} - \boldsymbol{\Phi}_2' e^{i2\omega} - \ldots - \boldsymbol{\Phi}_p' e^{ip\omega})^{-1}.\end{aligned} \tag{7.12}$$

8

Monte Carlo Analysis of Spectrum Estimation

In this chapter we apply Monte Carlo simulations to analyse what method for spectrum estimation described in the section 4.5 is more precise. As the usual criterion of the method's quality and precision, we use the mean squared error (MSE) of the estimator, which should achieve lowest values for preferred method of estimation.

The application of spectral analysis means that a population spectrum of actual time series is estimated. In reality, those time series are characterized by different statistical properties as they can be generated by a large variety of random processes. Therefore, we would like to asses how precise the different method are for different data generating processes and how sensitive the estimates are to model misspecification. In other words we would like to know which estimation method described in the section 4.5 is more precise or accurate. In this case Monte Carlo method is an appropriate tool how to obtain the information about the quality of the applied methods.

The term *Monte Carlo* refers to the computer-based statistical method that over the years has been applied to a huge number of problems from different scientific areas like a statistical physics, molecular simulations, dynamic system analysis and statistical testing. This method was named after the city Monte Carlo because it is known for the number of casinos which are the symbol of a random number generator.

Monte Carlo method as a research tool was used at first in 1940s by von Neumann,

Ulam and Richtmyer ([68]) and first paper about this new method was written by Metropolis and Ulman ([65]) in 1949. Metropolis in his paper from 1980s ([66]) describes the beginning of the method in a more detail.

A Monte Carlo experiment attempts to replicate an actual data by generating the process using experiment. It means that simulated process is approximated by generating many random realizations of a stochastic process and averaging them in some way. In econometrics, the Monte Carlo method is used to explore the quantitative properties of the model with stochastic elements.

Monte Carlo experiments generally involve the following steps:

1. Specification of the model of our interest.
2. Generation a set of random variables of sample size T from the perspective distribution function of the error terms.
3. Evaluation the model with generated error terms.
4. Repeating the second and third step R times, i.e. R simulations.
5. Analysis of the results using summary statistics (e.g. mean squared error, variance, etc.).

8.1 Description of the Simulated Processes

We choose eleven different processes for Monte Carlo simulation. We try to comprehend in these processes different properties of time series. Nine of them are autoregressive processes with different order and two $ARMA$ processes.

Therefore, we apply the Monte Carlo analysis for eleven following processes and six number of simulations, $R = 50, 100, 200, 500, 1000$ and 2000.

- **Model 1:** $AR(5)$ $Y_t = 0.5Y_{t-1} - 0.6Y_{t-2} + 0.3Y_{t-3} - 0.4Y_{t-4} + 0.5Y_{t-5} + \varepsilon_t$
- **Model 2:** $AR(2)$ $Y_t = 0.7Y_{t-1} - 0.5Y_{t-2} + \varepsilon_t$
- **Model 3:** $AR(2)$ $Y_t = 0.6Y_{t-1} - 0.9Y_{t-2} + \varepsilon_t$
- **Model 4:** $AR(1)$ $Y_t = 0.9Y_{t-1} + \varepsilon_t$
- **Model 5:** $AR(1)$ $Y_t = -0.9Y_{t-1} + \varepsilon_t$
- **Model 6:** $AR(1)$ $Y_t = 0.5Y_{t-1} + \varepsilon_t$
- **Model 7:** $AR(1)$ $Y_t = -0.5Y_{t-1} + \varepsilon_t$

- **Model 8:** $AR(1)\ Y_t = 0.1Y_{t-1} + \varepsilon_t$
- **Model 9:** $AR(1)\ Y_t = -0.1Y_{t-1} + \varepsilon_t$
- **Model 10:** $ARMA(2,4)\ Y_t = 0.5Y_{t-1} - 0.6Y_{t-2} + \varepsilon_t + 0.3\varepsilon_{t-1} - 0.4\varepsilon_{t-2} + 0.5\varepsilon_{t-3} - 0.8\varepsilon_{t-4}$
- **Model 11:** $ARMA(2,1)\ Y_t = 0.75Y_{t-1} - 0.3Y_{t-2} + \varepsilon_t + 0.25\varepsilon_{t-1}$

where ε_t is a white noise defined in the section 6.1. These models are convenient because of their simplicity and the different spectra they represent.

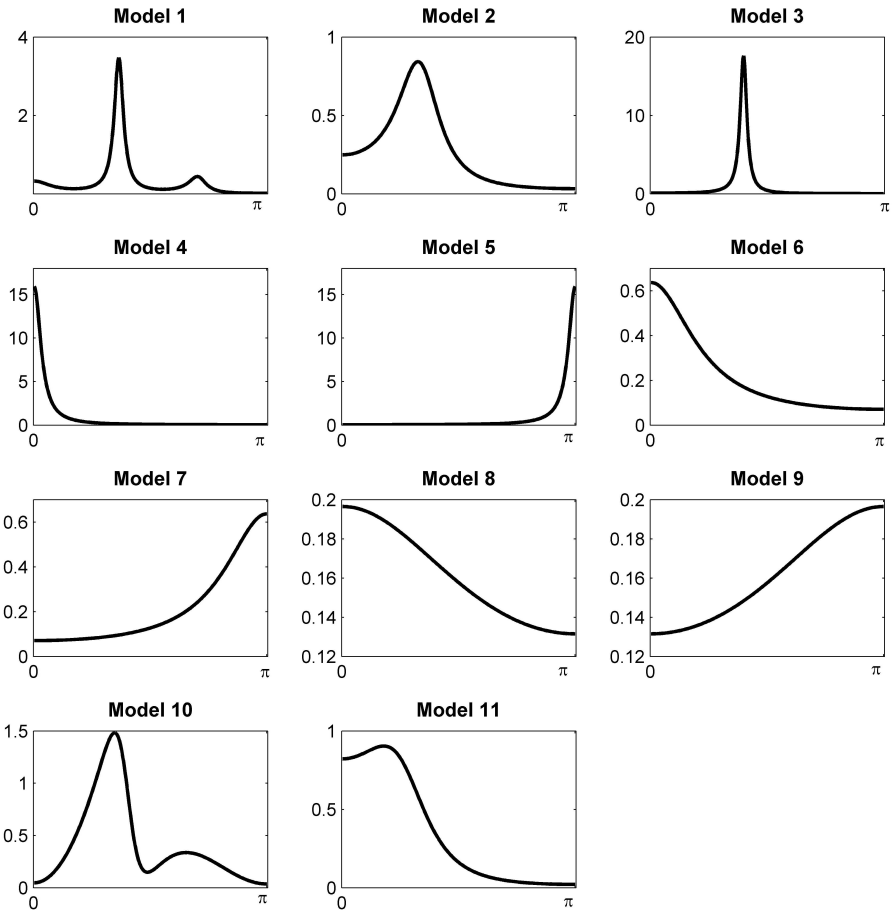

Figure 8.1: Graphical representation of theoretical population spectrum for simulated processes.

We do not normalize the time series to have equal variance or the same spectral density at the origin. Theoretical spectra of all simulated processes are illustrated in

figure 8.1. Those theoretical spectra are calculated according to the formulas derived in the chapter 7 where we focus on the AR, MA and $ARMA$ processes.

In general, we can see that relatively similar stochastic processes may have highly different spectrum. In figure 8.1, spectrum of model 1 shows multiple peaks, the higher one at frequency $\omega \approx \pi/3$ and the smaller one at frequency $\omega \approx 3\pi/4$. The spectrum of model 2 has local minimum at zero frequency and peak at frequency $\omega \approx 1$. Model 3 is flat at the origin but with a very sharp peak at frequency $\omega \approx 1.3$. The first-order autoregressive processes (model 4, 5, 6, 7, 8 ,9) have the typical spectral density. Spectrum is monotonically decreasing with a maximum at zero frequency if the process is defined with positive autocorrelation and the spectrum is monotonically increasing with maximum at $\omega = \pi$ if the process is defined with negative autocorrelation. In general, we can see that $AR(1)$ processes with higher autoregressive parameter ϕ show a flat spectrum for short-term frequencies and a sharp peak for long-run frequencies. The spectrum of model 10 show also several peaks. Finally the last plot represents the spectrum of model 11 which has peak in long-run frequencies and then it is decreasing function of frequency.

8.2 Monte Carlo Results

In order to derive implications for applied spectral analysis especially of business cycles, we perform several Monte Carlo simulations for individual models specified above and estimation methods introduced in the section 4.5.

We calculate the mean squared error and variance for all eleven models and six number of simulations and two sample size, T =100 or 1000 observations. We also present MSE and variance by frequencies. The long-run frequencies correspond to the low frequency band below $\pi/16$, the business cycles belong to the frequencies between $\omega = \pi/16$ and $\omega = \pi/3$ and short-run frequencies are higher than $\pi/3$. The detailed results of Monte Carlo simulations are presented in tables 8.1, 8.2, 8.3 and 8.4.

We employ the Monte Carlo analysis for parametric and also for non-parametric methods. From parametric methods described in the section 4.5.2 we choose the Yule-Walker method with different value of p. We perform the analysis for $p = 1, 2, \ldots, 6$ for all eleven models but in tables we present the results for p equals to real order of simulated process, for underestimate value of p, $(p-1)$, and also for overestimate

value of p, $(p+1)$. For first-order autoregressive processes we present the results for $p = 1, 2, 3$.

The estimation made by non-parametric methods was realized using three different windows Bartlett, Parzen and Blackman.[1] For comparison we present the results also for periodogram in spite of its known disadvantages.[2]

Tables 8.2 and 8.3 show the results for the *mean squared error* (MSE). The mean squared error of an estimator $\hat{\beta}$ with respect to the estimated parameter β is defined as

$$\mathbf{MSE}(\beta) = E(\hat{\beta} - \beta)^2.$$

Tables 8.2 and 8.3 confirm that the most accurate methods for the estimation of the spectrum for autoregressive processes are the parametric methods because they are based on the (true) AR process. By contrast, the non-parametric methods of spectrum estimation are most efficient for the $ARMA$ processes. This finding is supported by the following example. If we estimate the model 1 (5th-order autoregressive process) by Yule-Walker parametric method with $p = 5$, the MSE is equal to 0.00170 for 500 simulations and 100 observations across all frequencies. If we choose the non-parametric method with Bartlett window for the spectrum estimation, MSE is much higher (0.00349). But if we estimate the model 10 by Yule-Walker parametric method with $p = 6$, MSE = 0.06824 for the same conditions, 500 simulations, 100 observations and all frequencies. Moreover, the value of the mean squared error declines to 0.02561 if we choose the non-parametric method with Bartlett window.

For a final evaluation of robustness of different methods for empirical applications, we should keep in mind that we do not know the true data generating process in standard applications. In general, we try to approximate it by pth-order autoregressive process with lower value of p because empirical analysis may tend to underestimate the order of the autoregressive process. Actually, in this case the parametric methods for spectrum estimation are no longer the best performing methods. The non-parametric method are a better choice if the lag order of AR process is underestimated. For example, see the model 1 (5th-order autoregressive process) generated with 1000 observations and its MSE values for 1000 simulations across all frequencies (table 8.2). The mean squared error equals to 0.03749 for non-parametric method with Bartlett win-

[1] The definition of the window is described in the section 4.5.1.

[2] The section 4.5 reports more detailed information about the disadvantages of periodogram as the estimation method.

dow. If we estimate the correct p and use parametric Yule-Walker method with $p = 5$, the MSE = 0.00005. But if we underestimate the lag order and p set to 4 for Yule-Walker method, MSE rapidly increases to 0.20283. Therefore, we recommend to use of non-parametric methods with windows, because there is general tendency to underestimate the order of autoregressive process and non-parametric methods are most robust to models miss-specification. In turn, if the p is overestimated, we can see that MSE declines but not so rapidly. MSE for our example and Yule-Walker with $p = 6$ is equal to 0.000048. This findings deduced from numerical results is confirmed also by figure 8.2 which represents the estimated spectra obtained by Monte Carlo analysis with 50 simulations. For graphical representation we choose the lower number of simulations to see the spectra with underestimated order of autoregressive process much better.

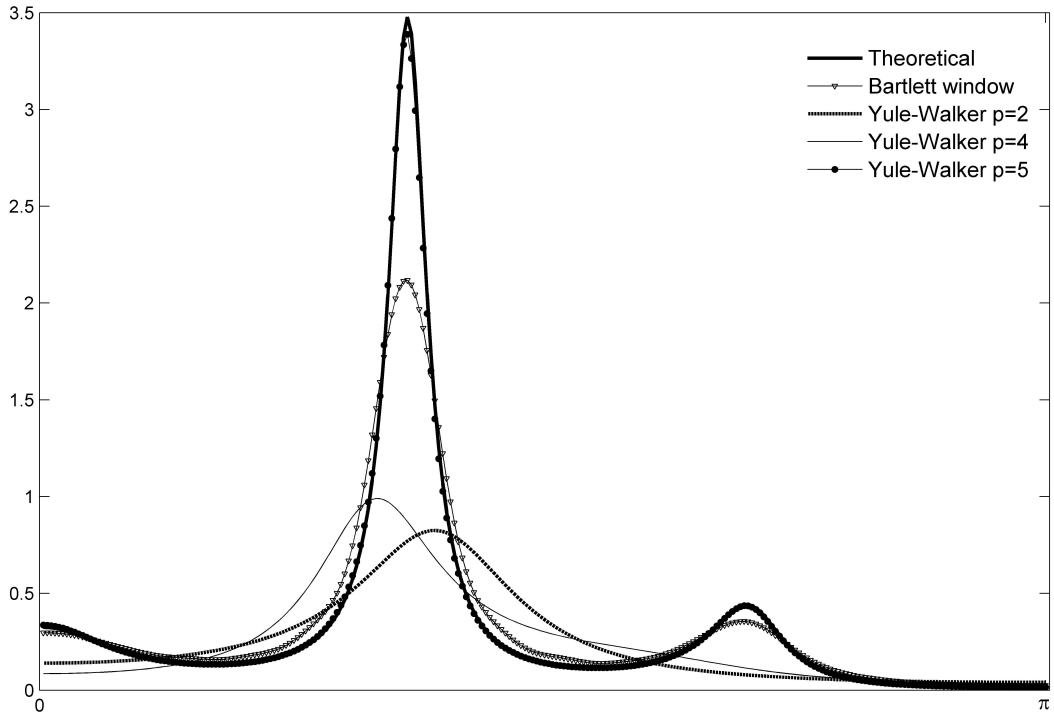

Figure 8.2: Theoretical population spectrum of $AR(5)$ process compared with spectrum estimated by Bartlett window and by Yule-Walker method with different value of p for 50 simulations and 1000 observations.

Tables 8.2 and 8.3 report also the sensitivity of the non-parametric methods to the window specifications, which affects the accuracy of these methods. The periodogram

represents the primitive non-parametric method without using the window. The quality of the periodogram estimate can be improved with windows. The Bartlett and Blackman windows seem to be the best solutions. For higher number of simulations, the mean squared error of non-autoregressive process for Blackman and Bartlett window is better than for periodogram. If we estimate model 11 with periodogram, the means squared error for 1000 simulations equals to 0.02080. If we choose the Blackman window for the estimation , the mean squared error is lower (0.00353).

Furthermore, the smoothness and clarity of estimated spectra may be regarded also as an important factor of quality of different estimation methods. Therefore, we analyze variance of estimated spectrum (overall variance and variance in specified intervals of the long-run, business cycle and short-run frequencies).

In table 8.4 we report the results for the variance of simulated processes. This table is not so comprehensive like the tables for the mean squared error (see tables 8.2 and 8.3). For simplicity, we do not present the variance results for models 8 and 9 because the results for them are very similar to the results for model 6 or 7 respectively. Moreover, we present the results only for selected methods and for selected number of simulations (50, 500 and 1000 simulations).

Table 8.4 strengthens our previous finding that one main disadvantage of the periodogram estimation is its high variance. In average, the variance for periodogram is the highest across all frequencies (or frequency band) and across all simulated processes. For example see the variance for 50 iterations, the variance for model 1 across all frequencies is equal to 0.37296 but the variance for Blackman window is several times lower (0.06503). This evidence is also obvious from figure 8.3 which represents the spectrum of model 10 estimated by periodogram for 50 and 1000 Monte Carlo simulations.

In turn, the estimations with Blackman and Bartlett window have the lowest variance. The variance results are not influenced by the selected process as much as the results for MSE. It means, that Blackman and Bartlett window reach the lower variance independently of process type, for autoregressive processes and also for other types of processes.

Tables 8.2 and 8.3 present also the results for two different number of observations. The results in table 8.3 corresponds to time series with 100 observations therefore they are relevant for short time series, like GDP data for European countries. Results in table 8.2 corresponds to time series with 1000 observations therefore these results are

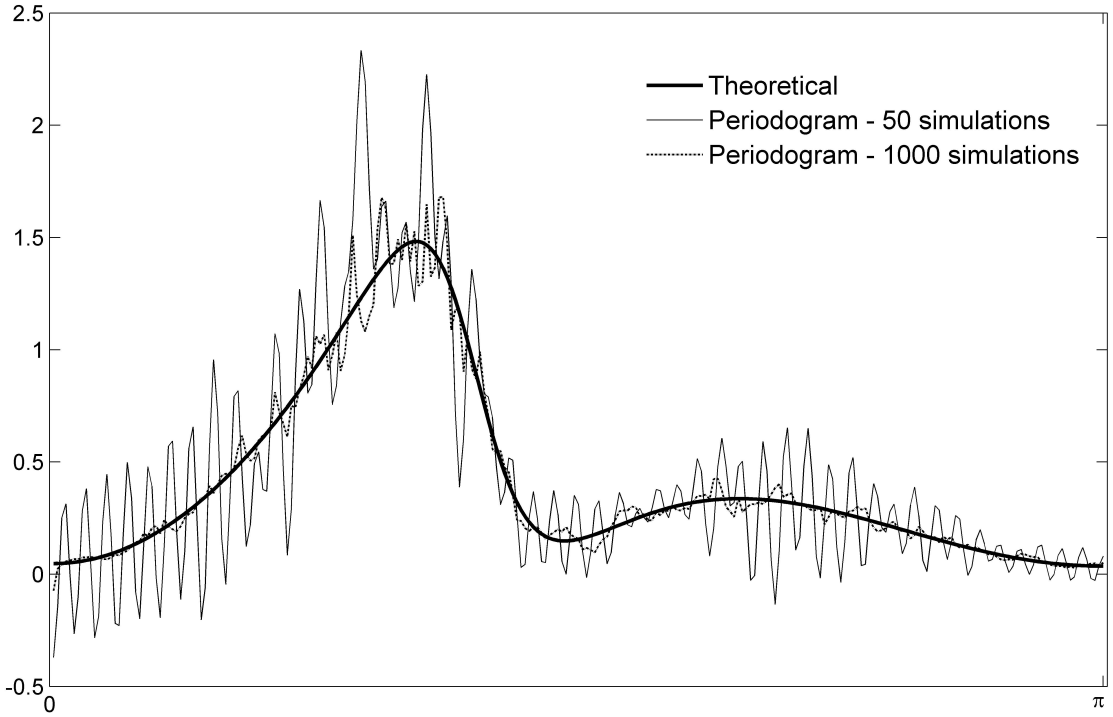

Figure 8.3: Theoretical population spectrum of model 10 compared with spectrum estimated by periodogram for 50 and 1000 simulations.

relevant if the source data have higher frequency like stock prices. By comparing these tables, it is clear that non-parametric methods are more precise for higher number of observations. This property reflects that the value of spectra is calculated using the bandwidth expressed by the expression

$$m = \sqrt{T}.$$

Figure 8.4 illustrates how the estimated value of spectrum converge to the theoretical value with increasing number of simulations and with increasing number of observations through all frequencies. We try to join all three aspects (number of observations, number of simulations and frequency) in one figure. Figure 8.4 illustrates the comparison between the theoretical spectrum of $AR(5)$ process, shown also in figure 8.1, and estimated spectrum. In this case, we estimate the spectrum by the non-parametric method with Blackman window in Monte Carlo simulations where the number of simulation is equal to number of observations. The figure confirms our previous

statement that the non-parametric method is more precise with increasing number of observations. If the number of simulations is 100, the mean squared error for all frequencies is equal to 0.21167 and it decreases with increasing number of observations. For $R = T = 1000$, the mean squared error for all frequencies is equal to 0.04942. Since both peaks of $AR(5)$ process lie in the short-run frequencies, so this part has the biggest share on MSE. Mean squared error of the short-run frequencies is equal to 0.29057 if the number of simulations is 100 and it declines to 0.06734 for 1000 simulations.

In turn, for $AR(1)$ processes with positive autocorrelation, where MSE is mainly attributed by the long-run frequencies because the spectrum gains the highest value for low frequencies close to zero. The graphical comparison of theoretical spectrum of $AR(1)$ process with $\phi = 0.9$ and estimated spectrum by non-parametric method with Bartlett window is illustrated in figure 8.5 which documents that the most problematic part is the peak area in the long-run frequency interval. As in the previous example, the estimate is more precise with an increasing number of observations because also in this case the number of simulations is equal to number of observations.

AR(5): $Y_t = 0.5Y_{t-1} - 0.6Y_{t-2} + 0.3Y_{t-3} - 0.4Y_{t-4} + 0.5Y_{t-5} + \varepsilon_t$

Number of simulations	**50**	**100**	**200**	**500**	**1000**	**2000**
Bandwidth $h = \sqrt{T}$						
All frequencies	0.05107	0.04915	0.05059	0.04966	0.04942	0.04964
Long-run frequencies	0.00035	0.00049	0.00051	0.00041	0.00037	0.00038
Bus. cycle frequencies	0.01873	0.01717	0.01572	0.01774	0.01708	0.01704
Short-run frequencies	0.06916	0.06689	0.06965	0.06744	0.06734	0.06769
Bandwidth $h = 2\sqrt{T}$						
All frequencies	0.01033	0.01124	0.01011	0.00948	0.00954	0.00936
Long-run frequencies	0.00018	0.00010	0.00018	0.00010	0.00010	0.00012
Bus. cycle frequencies	0.00253	0.00249	0.00234	0.00256	0.00253	0.00276
Short-run frequencies	0.01449	0.01588	0.01423	0.01321	0.01331	0.01294

Table 8.1: Mean squared error of estimated spectrum of $AR(5)$ process estimated by Blackman window for different value of bandwidth.

The influence of bandwidth value on the estimated spectrum should receive a special attention. Diebold ([21], p.129) suggests to set h equal to the squared root of the number of observations T. Chatfield ([14]) claims that h approximately equals to $2\sqrt{T}$ is large enough to provide the resolution. Our Monte Carlo simulations confirm

the Chatfield's suggestion, the h equals to $2\sqrt{T}$ is more suitable because the estimated spectrum with this value of bandwidth is more precise. This results is also obvious from table 8.1 which represent the numeric comparison of spectrum for model 1 estimated by non-parametric method with Blackman window for different values of bandwidth. The spectrum is estimated with bandwidth equal to the squared root of T and also with bandwidth equal to $2\sqrt{T}$ for 1000 observations. If $h = \sqrt{T}$ and number of simulations is 1000, the mean squared error of estimated spectrum for all frequencies is equal to 0.04942. If we use bandwidth $h = 2\sqrt{T}$, the mean squared error declines to 0.00954.

	50 simulations				500 simulations				1000 simulations			
	MSE: All frequencies	MSE: Long-run frequencies	MSE: Bus. cycle frequencies	MSE: Short-run frequencies	MSE: All frequencies	MSE: Long-run frequencies	MSE: Bus. cycle frequencies	MSE: Short-run frequencies	MSE: All frequencies	MSE: Long-run frequencies	MSE: Bus. cycle frequencies	MSE: Short-run frequencies
Model 1												
Periodogram	0.08350	0.04698	0.02875	0.10921	0.01030	0.03043	0.00906	0.00880	0.00574	0.02531	0.00258	0.00508
Bartlett window	0.03953	0.00028	0.00763	0.05631	0.03784	0.00027	0.00705	0.05400	0.03749	0.00025	0.00663	0.05365
Parzen window	0.06254	0.00046	0.02198	0.08508	0.06101	0.00055	0.02118	0.08309	0.06084	0.00050	0.02054	0.08309
Blackman window	0.05107	0.00035	0.01873	0.06916	0.04966	0.00041	0.01774	0.06744	0.04942	0.00037	0.01708	0.06734
Yule-Walker (p=4)	0.20702	0.04008	0.03579	0.29271	0.20197	0.04128	0.03418	0.28565	0.20283	0.04103	0.03402	0.28703
Yule-Walker (p=5)	0.00051	0.00007	0.00012	0.00070	0.00004	0	0	0.00006	0.00005	0	0	0.00007
Yule-Walker (p=6)	0.00056	0.00011	0.00013	0.00078	0.00003	0	0	0.00005	0.00005	0	0	0.00007
Model 2												
Periodogram	0.03147	0.02051	0.07581	0.01467	0.00511	0.01844	0.00693	0.00305	0.00330	0.01682	0.00513	0.00121
Bartlett window	0.00071	0.00007	0.00138	0.00051	0.00039	0.00005	0.00078	0.00027	0.00038	0.00010	0.00076	0.00025
Parzen window	0.00045	0.00005	0.00091	0.00031	0.00021	0.00001	0.00046	0.00014	0.00021	0.00001	0.00045	0.00013
Blackman window	0.00035	0.00008	0.00072	0.00023	0.00013	0.00001	0.00028	0.00008	0.00012	0	0.00028	0.00007
Yule-Walker (p=1)	0.05931	0.08335	0.10787	0.03732	0.05973	0.08807	0.10824	0.03734	0.05973	0.08802	0.10824	0.03734
Yule-Walker (p=2)	0.00001	0	0.00005	0	0	0	0	0	0	0	0	0
Yule-Walker (p=3)	0.00002	0	0.00005	0.00001	0	0	0.00001	0	0	0	0.00001	0
Model 3												
Periodogram	1.53702	0.01827	0.09371	2.27040	0.09653	0.00793	0.02563	0.13395	0.04625	0.00254	0.00675	0.06654
Bartlett window	1.21715	0.00195	0.03217	1.81611	1.22237	0.00182	0.03356	1.82341	1.19968	0.00195	0.03335	1.78937
Parzen window	1.87384	0.00001	0.08020	2.78387	1.87812	0	0.08380	2.78885	1.86305	0.00001	0.08212	2.76689
Blackman window	1.59698	0	0.04330	2.38266	1.60162	0	0.04618	2.38848	1.58550	0	0.04490	2.36477
Yule-Walker (p=1)	7.92833	0.05775	0.07966	11.87779	7.92837	0.05815	0.07974	11.87778	7.92835	0.05792	0.07969	11.87779
Yule-Walker (p=2)	0.01157	0	0	0.01739	0.00785	0	0	0.01180	0.00501	0	0	0.00753
Yule-Walker (p=3)	0.01104	0	0	0.01660	0.00699	0	0	0.01050	0.00397	0	0	0.00597
Model 4												
Periodogram	4.77922	68.04026	0.89933	0.05569	4.61459	69.64944	0.02700	0.00027	3.91819	59.19012	0.01039	0.00015
Bartlett window	0.47835	6.97138	0.06272	0.00055	0.38310	5.58335	0.05001	0.00053	0.41142	5.99943	0.05295	0.00054
Parzen window	0.63578	9.02762	0.14383	0.00001	0.55084	7.78993	0.13242	0	0.57711	8.17921	0.13436	0
Blackman window	0.51465	7.38711	0.09685	0	0.43199	6.19038	0.08383	0	0.45695	6.55595	0.08673	0
Yule-Walker (p=1)	0.00965	0.14519	0.00016	0	0.00094	0.01410	0.00003	0	0.00059	0.00874	0.00005	0
Yule-Walker (p=2)	0.01240	0.18717	0.00007	0	0.00165	0.02489	0.00003	0	0.00066	0.00979	0.00003	0
Yule-Walker (p=3)	0.01195	0.18025	0.00009	0	0.00202	0.03048	0.00002	0	0.00080	0.01200	0.00002	0
Model 5												
Periodogram	1.21151	0.00194	0.00264	1.81955	0.19556	0.00058	0.00076	0.29355	0.07349	0.00157	0.00053	0.11008
Bartlett window	0.33744	0.00016	0.00021	0.50704	0.32998	0.00015	0.00021	0.49583	0.31610	0.00016	0.00022	0.47496
Parzen window	0.52058	0	0	0.78238	0.51276	0	0	0.77064	0.50069	0	0	0.75250
Blackman window	0.40270	0	0	0.60523	0.39454	0	0	0.59297	0.38154	0	0	0.57343
Yule-Walker (p=1)	0.00389	0	0	0.00584	0.00096	0	0	0.00144	0.00062	0	0	0.00093
Yule-Walker (p=2)	0.00265	0	0	0.00398	0.00086	0	0	0.00130	0.00072	0	0	0.00108
Yule-Walker (p=3)	0.00098	0	0	0.00148	0.00125	0	0	0.00188	0.00103	0	0	0.00154
Model 6												
Periodogram	0.02087	0.16724	0.02538	0.00449	0.00869	0.09973	0.00656	0.00050	0.00668	0.09143	0.00167	0.00028
Bartlett window	0.00003	0.00025	0.00004	0.00001	0.00011	0.00110	0.00011	0.00001	0.00009	0.00100	0.00004	0.00001
Parzen window	0.00001	0.00001	0.00003	0	0.00004	0.00041	0.00003	0	0.00002	0.00032	0.00001	0
Blackman window	0.00001	0	0.00003	0.00001	0.00003	0.00031	0.00002	0	0.00002	0.00025	0	0

	50 simulations				500 simulations				1000 simulations			
	MSE: All frequencies	MSE: Long-run frequencies	MSE: Bus. cycle frequencies	MSE: Short-run frequencies	MSE: All frequencies	MSE: Long-run frequencies	MSE: Bus. cycle frequencies	MSE: Short-run frequencies	MSE: All frequencies	MSE: Long-run frequencies	MSE: Bus. cycle frequencies	MSE: Short-run frequencies
Model 6												
Yule-Walker (p=1)	0.00007	0.00071	0.00009	0	0	0	0	0	0	0.00001	0	0
Yule-Walker (p=2)	0.00006	0.00051	0.00008	0	0	0	0	0	0	0.00004	0	0
Yule-Walker (p=3)	0.00006	0.00060	0.00008	0	0	0	0	0	0	0.00004	0	0
Model 7												
Periodogram	0.02620	0.01131	0.00414	0.03658	0.00256	0.00111	0.00018	0.00366	0.00099	0.00124	0.00010	0.00133
Bartlett window	0.00006	0.00001	0.00002	0.00008	0.00011	0	0.00001	0.00016	0.00009	0.00001	0.00001	0.00013
Parzen window	0.00001	0	0.00001	0.00001	0.00003	0	0	0.00005	0.00002	0	0	0.00003
Blackman window	0.00001	0	0.00001	0.00001	0.00003	0	0	0.00004	0.00001	0	0	0.00002
Yule-Walker (p=1)	0	0	0	0	0	0	0	0.00001	0	0	0	0
Yule-Walker (p=2)	0.00001	0	0	0.00002	0	0	0	0.00001	0	0	0	0
Yule-Walker (p=3)	0.00001	0.00001	0	0.00001	0	0	0	0.00001	0	0	0	0
Model 8												
Periodogram	0.00666	0.00994	0.00833	0.00566	0.00128	0.00950	0.00120	0.00049	0.00096	0.00927	0.00053	0.00031
Bartlett window	0.00002	0.00010	0.00002	0.00001	0	0.00003	0	0	0	0.00002	0	0
Parzen window	0.00001	0.00008	0.00002	0.00001	0	0.00002	0	0	0	0.00001	0	0
Blackman window	0.00001	0.00008	0.00002	0.00001	0	0.00002	0	0	0	0.00001	0	0
Yule-Walker (p=1)	0	0	0	0	0	0	0	0	0	0	0	0
Yule-Walker (p=2)	0	0.00002	0	0	0	0	0	0	0	0	0	0
Yule-Walker (p=3)	0.00001	0.00002	0.00001	0	0	0	0	0	0	0	0	0
Model 9												
Periodogram	0.00897	0.00497	0.00627	0.01045	0.00102	0.00339	0.00078	0.00089	0.00066	0.00457	0.00036	0.00039
Bartlett window	0.00001	0.00002	0.00001	0.00001	0	0	0	0	0	0.00001	0	0
Parzen window	0.00001	0.00002	0.00001	0.00001	0	0	0	0	0	0.00001	0	0
Blackman window	0.00001	0.00003	0.00001	0.00001	0	0	0	0	0	0.00001	0	0
Yule-Walker (p=1)	0	0	0	0	0	0	0	0	0	0	0	0
Yule-Walker (p=2)	0	0	0	0	0	0	0	0	0	0	0	0
Yule-Walker (p=3)	0	0	0	0	0	0	0	0	0	0	0	0
Model 10												
Periodogram	0.05834	0.00622	0.09791	0.04755	0.00715	0.00126	0.01190	0.00581	0.00469	0.00103	0.00843	0.00354
Bartlett window	0.00244	0.00113	0.00217	0.00268	0.00220	0.00130	0.00173	0.00248	0.00251	0.00133	0.00233	0.00270
Parzen window	0.00202	0.00016	0.00073	0.00272	0.00190	0.00022	0.00055	0.00261	0.00217	0.00023	0.00094	0.00286
Blackman window	0.00128	0.00006	0.00035	0.00177	0.00118	0.00010	0.00024	0.00167	0.00140	0.00011	0.00054	0.00187
Yule-Walker (p=4)	0.07847	0.00024	0.08107	0.08520	0.07744	0.00025	0.07970	0.08419	0.07823	0.00025	0.08120	0.08479
Yule-Walker (p=5)	0.06982	0.00059	0.08719	0.06969	0.06903	0.00060	0.08590	0.06903	0.06996	0.00060	0.08723	0.06988
Yule-Walker (p=6)	0.06909	0.00026	0.08740	0.06854	0.06825	0.00027	0.08566	0.06799	0.06938	0.00026	0.08751	0.06894
Model 11												
Periodogram	0.08749	0.78633	0.11059	0.00870	0.02022	0.21358	0.01993	0.00111	0.01246	0.15385	0.00709	0.00057
Bartlett window	0.00044	0.00138	0.00098	0.00012	0.00031	0.00021	0.00088	0.00009	0.00024	0.00054	0.00049	0.00011
Parzen window	0.00019	0.00060	0.00050	0.00002	0.00009	0.00001	0.00032	0.00001	0.00006	0.00014	0.00014	0.00003
Blackman window	0.00018	0.00075	0.00044	0.00002	0.00007	0.00003	0.00024	0	0.00005	0.00019	0.00010	0.00002
Yule-Walker (p=2)	0.00318	0.01500	0.00672	0.00058	0.00326	0.01487	0.00703	0.00059	0.00370	0.01628	0.00841	0.00054
Yule-Walker (p=3)	0.00037	0.00152	0.00094	0.00003	0.00035	0.00159	0.00084	0.00003	0.00029	0.00124	0.00066	0.00005
Yule-Walker (p=4)	0.00008	0.00005	0.00022	0.00002	0.00004	0.00001	0.00011	0.00001	0.00001	0	0.00004	0

Table 8.2: Monte Carlo results for 50, 500, 1000 simulations and 1000 observations - Mean Squared Error

	50 simulations				500 simulations				1000 simulations			
	MSE: All frequencies	MSE: Long-run frequencies	MSE: Bus. cycle frequencies	MSE: Short-run frequencies	MSE: All frequencies	MSE: Long-run frequencies	MSE: Bus. cycle frequencies	MSE: Short-run frequencies	MSE: All frequencies	MSE: Long-run frequencies	MSE: Bus. cycle frequencies	MSE: Short-run frequencies
Model 1												
Periodogram	0.07680	0.05077	0.03570	0.09597	0.00708	0.03988	0.00202	0.00586	0.00611	0.03866	0.00258	0.00431
Bartlett window	0.18166	0.00637	0.03269	0.25920	0.17049	0.00349	0.04483	0.23779	0.17190	0.00320	0.04268	0.24082
Parzen window	0.23057	0.01221	0.05258	0.32409	0.22284	0.00895	0.06715	0.30693	0.22386	0.00837	0.06511	0.30933
Blackman window	0.21447	0.01217	0.04916	0.30128	0.20601	0.00865	0.06393	0.28296	0.20704	0.00803	0.06159	0.28552
Yule-Walker (p=4)	0.19061	0.03596	0.02654	0.27219	0.17063	0.03574	0.02945	0.24101	0.17833	0.03586	0.02678	0.25365
Yule-Walker (p=5)	0.01206	0.00047	0.00036	0.01793	0.00170	0.00005	0.00061	0.00231	0.00385	0.00005	0.00025	0.00569
Yule-Walker (p=6)	0.01028	0.00032	0.00030	0.01530	0.00156	0.00008	0.00064	0.00207	0.00367	0.00007	0.00030	0.00538
Model 2												
Periodogram	0.02689	0.03155	0.04073	0.02085	0.00364	0.02940	0.00295	0.00135	0.00353	0.03440	0.00300	0.00068
Bartlett window	0.00468	0.00064	0.00845	0.00356	0.00438	0.00029	0.00869	0.00304	0.00423	0.00024	0.00808	0.00307
Parzen window	0.00737	0.00165	0.01448	0.00507	0.00712	0.00117	0.01425	0.00483	0.00685	0.00126	0.01351	0.00472
Blackman window	0.00565	0.00077	0.01108	0.00394	0.00539	0.00046	0.01086	0.00367	0.00520	0.00046	0.01030	0.00361
Yule-Walker (p=1)	0.05948	0.08331	0.10834	0.03739	0.05955	0.08449	0.10834	0.03738	0.06006	0.08980	0.10887	0.03742
Yule-Walker (p=2)	0.00068	0.00008	0.00171	0.00033	0.00015	0.00008	0.00045	0.00004	0.00008	0.00013	0.00023	0.00001
Yule-Walker (p=3)	0.00039	0.00020	0.00051	0.00036	0.00006	0.00017	0.00009	0.00004	0.00004	0.00025	0.00004	0.00002
Model 3												
Periodogram	0.13326	0.03758	0.08216	0.16339	0.03842	0.00834	0.00346	0.05552	0.01763	0.00701	0.00898	0.02217
Bartlett window	4.32891	0.01185	0.47422	6.31350	4.14834	0.01172	0.65643	5.96860	4.19225	0.01137	0.60690	6.05461
Parzen window	5.09816	0.00106	0.73727	7.36455	4.96895	0.00040	0.97186	7.07576	4.99989	0.00050	0.90908	7.14759
Blackman window	4.83196	0.00054	0.70902	6.97592	4.69410	0.00010	0.94568	6.67327	4.72699	0.00015	0.88227	6.74829
Yule-Walker (p=1)	7.92840	0.05657	0.07943	11.87811	7.92843	0.05705	0.07952	11.87807	7.92844	0.05702	0.07952	11.87808
Yule-Walker (p=2)	0.89473	0.00002	0.00010	1.34467	0.35815	0.00001	0.00004	0.53825	0.43179	0.00001	0.00003	0.64893
Yule-Walker (p=3)	0.84859	0.00007	0.00022	1.27527	0.29268	0	0.00004	0.43985	0.37888	0.00001	0.00004	0.56941
Model 4												
Periodogram	5.62807	84.05082	0.20739	0.01894	4.96097	74.86641	0.02869	0.00153	4.92395	74.20600	0.05500	0.00093
Bartlett window	2.63809	38.39422	0.35625	0.00412	2.70032	39.45288	0.32724	0.00412	2.67420	38.92272	0.36026	0.00424
Parzen window	3.21719	45.54613	0.76028	0.00044	3.26580	46.48394	0.71013	0.00050	3.23834	45.88031	0.75651	0.00052
Blackman window	2.97147	42.05257	0.70647	0.00017	3.02309	43.03350	0.65691	0.00022	2.99602	42.43527	0.70345	0.00023
Yule-Walker (p=1)	0.10726	1.59167	0.00733	0.00001	0.05310	0.78451	0.00448	0	0.04589	0.67705	0.00412	0
Yule-Walker (p=2)	0.10404	1.53530	0.00923	0.00001	0.05132	0.76218	0.00335	0.00001	0.04884	0.73109	0.00178	0.00001
Yule-Walker (p=3)	0.09924	1.48681	0.00331	0.00001	0.04814	0.71954	0.00199	0.00001	0.04824	0.72263	0.00161	0.00001
Model 5												
Periodogram	0.55980	0.00284	0.00440	0.83929	0.03161	0.00131	0.00011	0.04734	0.00867	0.00370	0.00067	0.01239
Bartlett window	1.96617	0.00110	0.00261	2.95384	2.04422	0.00108	0.00281	3.07107	2.04645	0.00109	0.00276	3.07443
Parzen window	2.71299	0	0	4.07741	2.78620	0	0.00002	4.18744	2.78580	0	0.00001	4.18684
Blackman window	2.44001	0.00002	0	3.66715	2.50910	0	0.00001	3.77098	2.51014	0	0	3.77255
Yule-Walker (p=1)	0.03431	0	0	0.05156	0.06584	0	0	0.09895	0.06367	0	0	0.09569
Yule-Walker (p=2)	0.01630	0	0	0.02449	0.06415	0.00001	0	0.09641	0.06705	0	0	0.10077
Yule-Walker (p=3)	0.02232	0.00001	0	0.03354	0.06140	0.00001	0	0.09228	0.06853	0.00001	0	0.10299
Model 6												
Periodogram	0.01565	0.15812	0.01477	0.00184	0.01112	0.15798	0.00174	0.00031	0.01058	0.15178	0.00164	0.00016
Bartlett window	0.00230	0.02425	0.00233	0.00011	0.00160	0.01690	0.00144	0.00015	0.00149	0.01578	0.00121	0.00018
Parzen window	0.00204	0.02053	0.00231	0.00010	0.00142	0.01475	0.00149	0.00008	0.00133	0.01339	0.00138	0.00011
Blackman window	0.00180	0.01855	0.00199	0.00006	0.00116	0.01246	0.00113	0.00004	0.00107	0.01126	0.00105	0.00007

	50 simulations				500 simulations				1000 simulations			
	MSE: All frequencies	MSE: Long-run frequencies	MSE: Bus. cycle frequencies	MSE: Short-run frequencies	MSE: All frequencies	MSE: Long-run frequencies	MSE: Bus. cycle frequencies	MSE: Short-run frequencies	MSE: All frequencies	MSE: Long-run frequencies	MSE: Bus. cycle frequencies	MSE: Short-run frequencies
Model 6												
Yule-Walker (p=1)	0.00009	0.00121	0.00004	0	0.00002	0.00009	0.00004	0	0.00003	0.00033	0.00003	0
Yule-Walker (p=2)	0.00007	0.00044	0.00008	0.00002	0.00004	0.00036	0.00003	0.00001	0.00005	0.00052	0.00004	0.00001
Yule-Walker (p=3)	0.00015	0.00035	0.00040	0.00002	0.00009	0.00109	0.00003	0.00001	0.00013	0.00157	0.00006	0.00002
Model 7												
Periodogram	0.01069	0.00449	0.00330	0.01429	0.00278	0.00383	0.00061	0.00356	0.00066	0.00207	0.00008	0.00076
Bartlett window	0.00101	0.00005	0.00024	0.00142	0.00049	0.00004	0.00012	0.00069	0.00063	0.00001	0.00012	0.00090
Parzen window	0.00105	0	0.00006	0.00155	0.00053	0	0.00001	0.00080	0.00066	0.00001	0.00001	0.00099
Blackman window	0.00083	0	0.00005	0.00122	0.00033	0	0	0.00050	0.00045	0.00002	0.00001	0.00067
Yule-Walker (p=1)	0.00006	0.00001	0.00001	0.00009	0.00002	0	0	0.00003	0.00003	0.00001	0.00001	0.00004
Yule-Walker (p=2)	0.00015	0	0	0.00023	0.00005	0.00002	0.00001	0.00008	0.00004	0.00001	0	0.00006
Yule-Walker (p=3)	0.00018	0.00003	0.00001	0.00027	0.00010	0.00007	0.00001	0.00013	0.00010	0.00002	0	0.00015
Model 8												
Periodogram	0.00506	0.02225	0.00554	0.00316	0.00185	0.01965	0.00123	0.00033	0.00140	0.01820	0.00038	0.00014
Bartlett window	0.00009	0.00040	0.00002	0.00008	0.00006	0.00053	0.00004	0.00002	0.00003	0.00027	0.00002	0
Parzen window	0.00006	0.00018	0.00004	0.00006	0.00004	0.00028	0.00004	0.00002	0.00001	0.00013	0.00002	0
Blackman window	0.00007	0.00021	0.00004	0.00006	0.00004	0.00033	0.00004	0.00002	0.00001	0.00015	0.00001	0
Yule-Walker (p=1)	0.00001	0	0	0.00002	0.00001	0.00003	0.00001	0.00001	0.00001	0.00008	0.00002	0
Yule-Walker (p=2)	0.00003	0	0.00001	0.00004	0.00002	0.00001	0	0.00003	0.00002	0.00014	0.00002	0.00001
Yule-Walker (p=3)	0.00005	0	0.00003	0.00007	0.00004	0.00008	0.00002	0.00005	0.00005	0.00029	0.00003	0.00003
Model 9												
Periodogram	0.00782	0.01472	0.01385	0.00471	0.00101	0.00768	0.00024	0.00066	0.00077	0.00761	0.00020	0.00032
Bartlett window	0.00003	0.00002	0.00006	0.00003	0.00001	0.00009	0	0.00001	0.00001	0.00006	0.00001	0
Parzen window	0.00003	0	0.00002	0.00003	0.00001	0.00006	0.00001	0	0.00001	0.00005	0.00001	0
Blackman window	0.00003	0.00001	0.00002	0.00003	0.00001	0.00009	0.00001	0	0.00001	0.00007	0.00001	0
Yule-Walker (p=1)	0.00001	0.00002	0.00001	0	0.00001	0.00001	0.00001	0.00001	0.00001	0.00002	0.00001	0.00001
Yule-Walker (p=2)	0.00003	0.00010	0.00002	0.00002	0.00002	0.00004	0.00001	0.00002	0.00001	0.00003	0.00001	0.00002
Yule-Walker (p=3)	0.00004	0.00017	0.00003	0.00003	0.00004	0.00007	0.00001	0.00005	0.00003	0.00007	0.00001	0.00004
Model 10												
Periodogram	0.06113	0.06863	0.13005	0.03257	0.01132	0.02233	0.01678	0.00803	0.00198	0.00590	0.00228	0.00148
Bartlett window	0.01861	0.01389	0.01306	0.02133	0.02561	0.01427	0.02610	0.02654	0.02409	0.01349	0.02351	0.02538
Parzen window	0.03727	0.01916	0.03629	0.03947	0.04323	0.02258	0.04923	0.04287	0.04225	0.02043	0.04679	0.04258
Blackman window	0.02907	0.01106	0.02481	0.03258	0.03493	0.01400	0.03656	0.03636	0.03384	0.01247	0.03406	0.03588
Yule-Walker (p=4)	0.06673	0.00027	0.06338	0.07469	0.07770	0.00034	0.08424	0.08276	0.07474	0.00031	0.08161	0.07937
Yule-Walker (p=5)	0.05820	0.00064	0.06580	0.06085	0.06882	0.00096	0.08872	0.06754	0.06603	0.00082	0.08688	0.06411
Yule-Walker (p=6)	0.05575	0.00028	0.06267	0.05848	0.06824	0.00041	0.08890	0.06664	0.06483	0.00037	0.08604	0.06268
Model 11												
Periodogram	0.05091	0.44330	0.06518	0.00615	0.02038	0.26818	0.00819	0.00066	0.02080	0.29008	0.00515	0.00034
Bartlett window	0.00419	0.01135	0.01074	0.00084	0.00209	0.00638	0.00336	0.00115	0.00353	0.01152	0.00757	0.00111
Parzen window	0.00353	0.00345	0.01031	0.00080	0.00181	0.00018	0.00389	0.00113	0.00298	0.00216	0.00776	0.00112
Blackman window	0.00269	0.00381	0.00783	0.00051	0.00113	0.00037	0.00221	0.00077	0.00218	0.00267	0.00549	0.00079
Yule-Walker (p=2)	0.00238	0.01482	0.00420	0.00041	0.00224	0.01075	0.00457	0.00046	0.00278	0.01660	0.00540	0.00034
Yule-Walker (p=3)	0.00095	0.00108	0.00315	0.00004	0.00054	0.00342	0.00108	0.00003	0.00078	0.00092	0.00247	0.00009
Yule-Walker (p=4)	0.00086	0.00088	0.00290	0.00003	0.00021	0.00043	0.00061	0.00002	0.00018	0.00017	0.00055	0.00003

Table 8.3: Monte Carlo results for 50, 500, 1000 simulations and 100 observations - Mean Squared Error

	50 simulations				500 simulations				1000 simulations			
	All frequencies	Long-run frequencies	Bus. cycle frequencies	Short-run frequencies	All frequencies	Long-run frequencies	Bus. cycle frequencies	Short-run frequencies	All frequencies	Long-run frequencies	Bus. cycle frequencies	Short-run frequencies
Model 1												
Periodogram	0.37296	0.04058	0.07410	0.52333	0.39184	0.03252	0.05344	0.55915	0.37411	0.03286	0.06398	0.52894
Bartlett window	0.07271	0.00001	0.05897	0.08273	0.09023	0.00000	0.07344	0.10274	0.08717	0.00000	0.07020	0.09975
Blackman window	0.06503	0.00000	0.05001	0.07193	0.08037	0.00000	0.06135	0.08913	0.07749	0.00001	0.05882	0.08634
Yule-Walker (p=5)	0.24658	0.00117	0.05542	0.34685	0.31883	0.00134	0.06078	0.45251	0.29390	0.00145	0.05657	0.41676
Model 2												
Periodogram	0.08800	0.03405	0.07661	0.07111	0.06620	0.02986	0.04503	0.04772	0.06706	0.03480	0.04278	0.04824
Bartlett window	0.03865	0.00002	0.01535	0.02834	0.03884	0.00003	0.01499	0.02977	0.04027	0.00004	0.01558	0.03031
Blackman window	0.04139	0.00006	0.01191	0.03151	0.04149	0.00006	0.01225	0.03243	0.04312	0.00007	0.01274	0.03332
Yule-Walker (p=2)	0.05268	0.00002	0.02788	0.04067	0.05784	0.00002	0.03357	0.04452	0.05983	0.00002	0.03463	0.04590
Model 3												
Periodogram	6.98579	0.03926	0.12916	10.15619	8.10979	0.00828	0.07204	11.79885	7.73488	0.00737	0.06752	11.25746
Bartlett window	1.31536	0.00172	0.52502	1.70873	1.60986	0.00219	0.68161	2.07587	1.52926	0.00209	0.63794	1.97592
Blackman window	1.19347	0.00001	0.65220	1.47390	1.45526	0.00001	0.82584	1.78346	1.38396	0.00002	0.77840	1.69921
Yule-Walker (p=2)	3.42627	0.00000	0.05884	4.95795	4.69302	0.00000	0.06056	6.80502	4.47931	0.00000	0.06082	6.49204
Model 4												
Periodogram	6.57046	60.97182	0.81268	0.01984	5.65215	50.00607	0.68428	0.00259	5.49921	45.92256	0.63403	0.00211
Bartlett window	1.53666	0.09603	1.05349	0.00317	1.46830	0.09019	1.00318	0.00337	1.51134	0.09035	1.04129	0.00358
Blackman window	1.54996	0.03751	1.24373	0.00170	1.48331	0.03546	1.18245	0.00189	1.52949	0.03601	1.22113	0.00200
Yule-Walker (p=1)	5.25140	19.09528	0.43225	0.00115	5.52877	18.79541	0.45419	0.00113	5.70357	19.85095	0.45749	0.00113
Model 5												
Periodogram	6.99133	0.00266	0.00445	9.97311	6.55748	0.00130	0.00012	9.36609	6.45135	0.00376	0.00070	9.19945
Bartlett window	2.63884	0.00005	0.00023	3.50052	2.37858	0.00006	0.00024	3.15447	2.39432	0.00006	0.00024	3.17120
Blackman window	2.60988	0.00000	0.00003	3.39889	2.34366	0.00000	0.00003	3.04927	2.36452	0.00000	0.00003	3.07284
Yule-Walker (p=1)	6.56743	0.00000	0.00002	9.40232	5.40881	0.00000	0.00002	7.71776	5.46039	0.00000	0.00002	7.79311
Model 6												
Periodogram	0.03752	0.14515	0.02025	0.00311	0.03447	0.14774	0.01603	0.00176	0.03484	0.14099	0.01634	0.00171
Bartlett window	0.01905	0.00000	0.00527	0.00170	0.01967	0.00001	0.00717	0.00149	0.02037	0.00001	0.00733	0.00161
Blackman window	0.02161	0.00001	0.00547	0.00200	0.02226	0.00003	0.00720	0.00169	0.02305	0.00002	0.00732	0.00183
Yule-Walker (p=1)	0.03256	0.00046	0.01430	0.00139	0.03012	0.00033	0.01315	0.00136	0.03092	0.00037	0.01356	0.00137
Model 7												
Periodogram	0.04159	0.00459	0.00337	0.04500	0.03520	0.00384	0.00063	0.03771	0.03194	0.00200	0.00012	0.03296
Bartlett window	0.02335	0.00000	0.00008	0.02196	0.02414	0.00000	0.00004	0.02388	0.02363	0.00000	0.00006	0.02293
Blackman window	0.02643	0.00000	0.00008	0.02476	0.02718	0.00000	0.00004	0.02677	0.02666	0.00000	0.00006	0.02578
Yule-Walker (p=1)	0.02808	0.00000	0.00003	0.02944	0.03052	0.00000	0.00003	0.03226	0.03051	0.00000	0.00003	0.03229
Model 10												
Periodogram	0.26575	0.07000	0.38481	0.17463	0.17537	0.02371	0.18341	0.13994	0.17323	0.00683	0.18998	0.13713
Bartlett window	0.09772	0.00015	0.10766	0.06703	0.07862	0.00027	0.07692	0.05657	0.08068	0.00024	0.08146	0.05888
Blackman window	0.09480	0.00035	0.08504	0.06990	0.07729	0.00034	0.06421	0.05858	0.07898	0.00032	0.06764	0.06055
Yule-Walker (p=6)	0.07092	0.00001	0.13279	0.03106	0.05238	0.00001	0.08983	0.02547	0.05551	0.00001	0.09630	0.02781
Model 11												
Periodogram	0.15804	0.45839	0.07223	0.02523	0.14301	0.25786	0.02185	0.01946	0.13270	0.27564	0.01369	0.01948
Bartlett window	0.08628	0.00002	0.00420	0.01695	0.09722	0.00015	0.00760	0.01782	0.08967	0.00012	0.00574	0.01812
Blackman window	0.09727	0.00001	0.00494	0.02046	0.10949	0.00004	0.00739	0.02157	0.10109	0.00003	0.00580	0.02162
Yule-Walker (p=3)	0.11098	0.00004	0.00633	0.01609	0.12191	0.00014	0.00641	0.01866	0.11611	0.00009	0.00463	0.01958

Table 8.4: Monte Carlo results for 50, 500, 1000 simulations and 100 observations - Variance

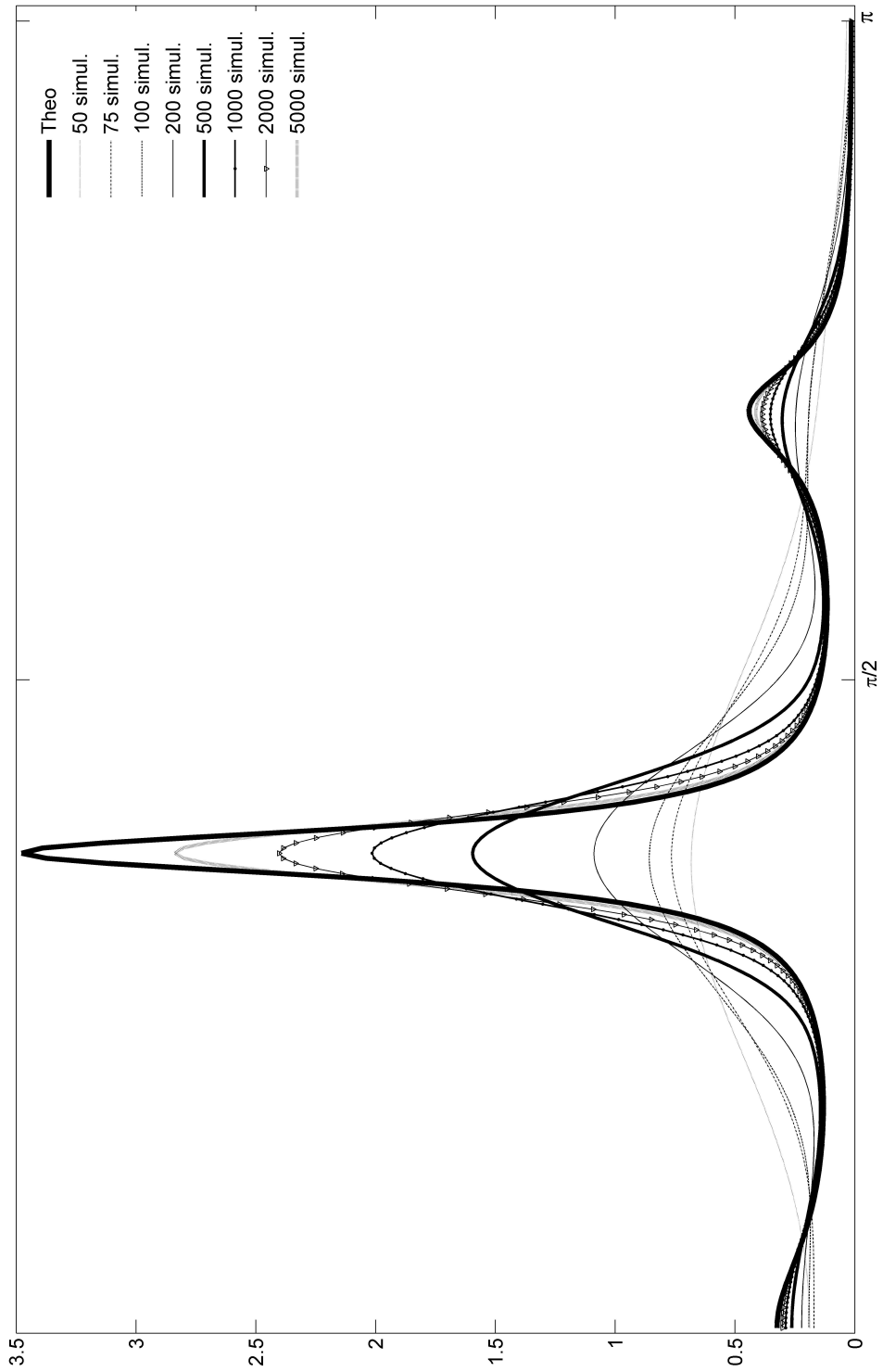

Figure 8.4: Theoretical population spectrum of $AR(5)$ process compared with spectrum estimated by Blackman window for different number of simulations.

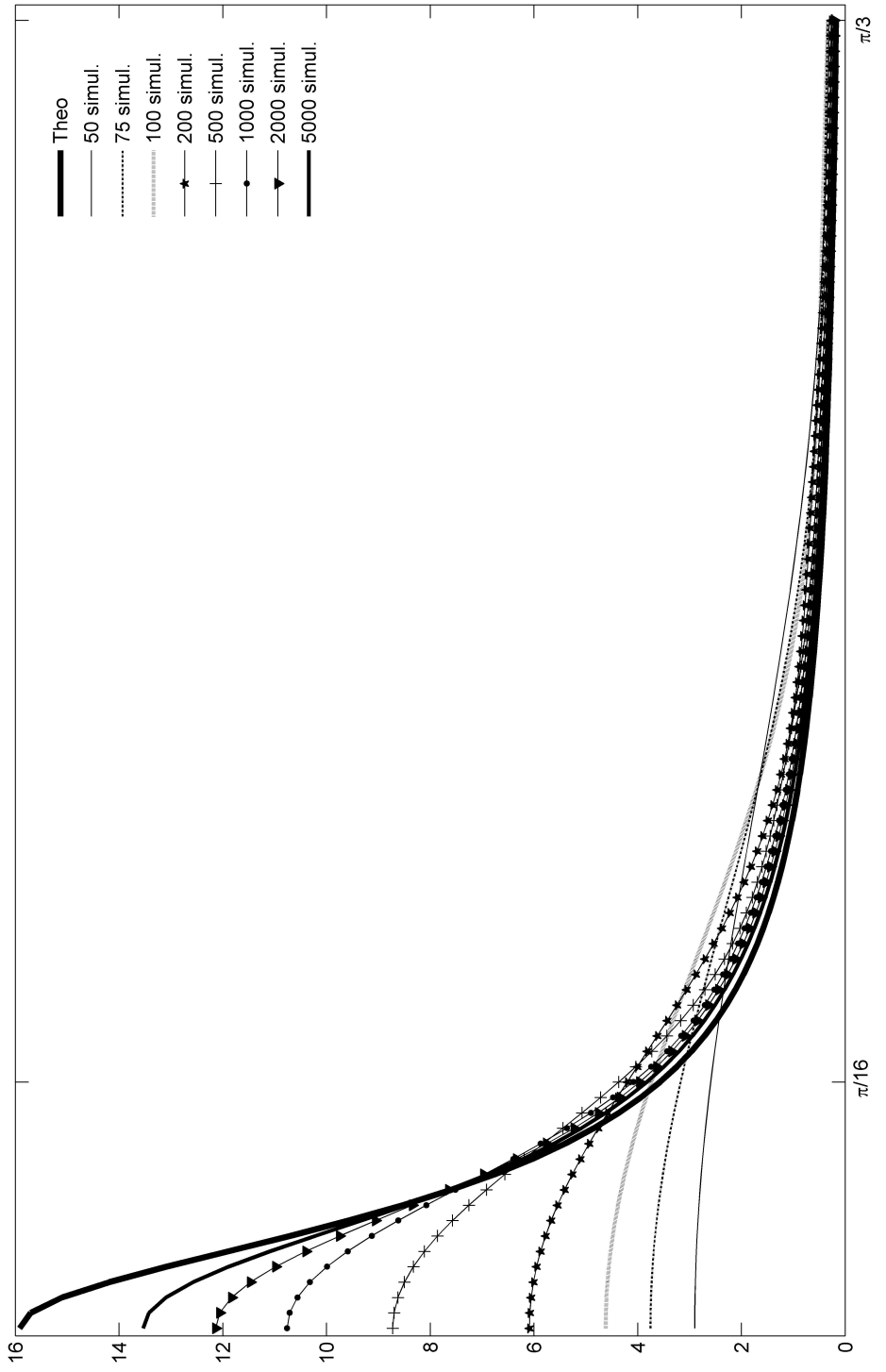

Figure 8.5: Theoretical population spectrum of $AR(1)$ process ($\phi = 0.9$) compared with spectrum estimated by Bartlett window for different number of simulations [a].

[a] Comparison is presented only for long-run and business cycle frequencies.

8.3 Monte Carlo Implications

Overall, we find that the all methods are more precise with an increasing number of observations. A higher the number of observations is associated with lower values of mean squared error. This characteristic we use in the [12] where we apply the spectral analysis for stock prices.

The parametric methods, in our case Yule-Walker method, is the best estimator for autoregressive processes. But for other processes, the non-parametric methods with windows are more precise. The sharp peaks in spectrum for different examined processes cause the problem during the estimation for both types of method.

The estimations with Bartlett or Blackman window have a lower variance and MSE in comparing with the results estimated with Parzen window or the periodogram. The periodogram achieves the higher variance among the examined method. Therefore the quality of the periodogram estimate can be improved by an appropriate selection of the windows.

However, usually we do not know the true data generating process. Mostly, the real time series are approximated by autoregressive processes. In general, there is the tendency to underestimate the order of the autoregressive process. Real time series have more complex structure, therefore we recommend to use the non-parametric methods smoothed by the Blackman or Bartlett window because they are better estimator of spectrum for autoregressive processes with underestimate value of order.

We also apply the Monte Carlo analysis to detect how the bandwidth of window affects the precision of the estimation. Monte Carlo simulations with different bandwidths confirmed the statement of Chatfield that h approximately equals to $2\sqrt{T}$ is high enough to provide a sufficient graphical resolution (see [14]).

9

China in the World Economy: Dynamic Correlation Analysis *

In the last decade the structure of the world economy has become more complex. Before 1990, the economic development was clearly dominated by the USA, Japan and several European economies. There was also significant effort to achieve some degree of policy coordination through the Organisation for Economic Co-operation and Development (OECD), International Monetary Fund (IMF), and especially the European Union (EU). In general, the emerging countries were highly dependent on economic development in the OECD countries and followed to some extent also their policies.

Few events in the world economy match the emergence of China in recent decades. Predominantly agrarian before 1980, China today boasts an extensive modern industrial economy with booming urban regions. The country's high trade growth is supported by large foreign direct investment (FDI) flows (Eichengreen and Tong, [22]). Not surprisingly, growth in the world's most populous country has changed the distribution of economic activities across the world. Between 1980 and 2006, the share of Chinese GDP in the world economy valued at market exchange rates increased from 1.7% to 5.5% (this share is even higher if purchasing-power-adjusted prices are used).

*This chapter is based on the papers *China in the world economy: Dynamic correlation analysis of business cycles* ([10]) and *New global players and disharmonies in the world orchestra: Cohesion analysis of business cycles of China* ([11]) elaborated in cooperation with Jarko Fidrmuc and Iikka Korhonen.

The international redistribution of economic activities holds important implications for business cycles. Emerging countries, and particularly China, contribute significantly to global growth. Thus, global economic prospects are less dependent than earlier on the performance of large developed economies such as the US and Germany. This situation may make countries in a particular region less vulnerable to demand shocks (IMF, [49]).

The literature on business cycle synchronization stresses the importance of foreign trade and capital flows. Thus, the emergence of China as a large trading nation and a target for international investment may have a significant impact on the business cycles of its partner countries.

Even as China has opened up to the world economy, recent business cycle trends suggest differences among countries in their intensity of trade and financial relations with China. This seems especially important in the case of European countries. We observe a joint EU cycle up to the 1980s (Artis and Zhang in [5], Fatás in [24]) that essentially vanishes in the 1990s (Artis, [4]). Moreover, the intensity of the trading and financial links with China has diverged among individual EU countries. For example, the UK, Germany, Finland, and the Netherlands have extensive links with China, while many other EU countries have quite modest economic ties with China.

Foreign trade and foreign direct investment (FDI) are generally seen as important factors of business cycles. However, their effects on correlation of international business cycles are ambiguous. Frankel and Rose in [27] find a robust positive relationship between trade intensity and correlation of business cycles between OECD countries. This is reflected in high shares of intra-industry trade between these countries. Yet China's specific position in the international division of labor should result in increased specialization. Krugman in [56], for example, argues that this should cause business cycle divergence between countries. Moreover, FDI can be either a substitute or a complement to exports between a pair of countries.

In addition to the rich literature on trade between China and the developed countries (Bussière *et al.*, [13]), there are also a range of authors (e.g. de Grauwe and Zhang, [20]) dealing with the determinants of the business cycles in Southeast Asia. Few papers deal specifically with the synchronization of business cycles in developed countries and China, so this study aims to help fill this gap in the literature.

Our study shows three findings. First, the business cycle in China is quite different from OECD countries (with the exception of Korea). Second, trade flows between

OECD countries and China have so far had rather limited effects on the comovements in China and OECD countries, although they have increased the comovement at the short-run frequencies. This stands in sharp contradiction to the positive relationship between trade and business cycle similarities between OECD countries extensively documented in the earlier literature (and confirmed here for OECD countries). Finally, trade and financial flows with China have lowered the degree of business cycle synchronization between OECD countries. To our knowledge, this result is novel to the literature.

9.1 Determinants of Business Cycle Synchronization

Economic development is determined by domestic factors (e.g. aggregate demand shocks and budgetary policy) and international factors (e.g. external demand and international prices for traded goods), as well as their interaction. In open economies, international factors play an important role, often driving the formulation of domestic policies designed to insulate the economy from adverse external economic shocks. Frankel and Rose in [27] argue that trade, and more generally economic integration among countries, results in increased synchronization of individual business cycles. They contend trade links provide a channel for transmission of shocks across countries. In line with approach, Kenen ([52]) shows that the correlation between two countries' output changes increases with the intensity of trade links. Kose and Yi ([55]) subsequently analyze this issue in an international real business cycle model. Although their model suggests a positive relation between trade and output comovement, only small qualitative effects are obtained.

The hypothesis of a positive relationship between trade and business cycles is not universally accepted, however. Krugman in [56], for example, argues that countries should be expected to increasingly specialize as they become more integrated. Thus, the importance of asymmetric or sectorspecific shocks should increase with the process of economic integration — a pattern perhaps more appropriate here to explaining Chinese business cycles.

The role of trade links has been studied extensively in the empirical literature. Despite the theoretical ambiguities, authors generally find that countries trading more intensively exhibit a higher degree of output comovement (e.g. Frankel and Rose, [27], Otto *et al.*, [69], Baxter and Kouparitsas, [8]). It is not trade relations per se, however,

that induce business cycle synchronization. Indeed, Frankel and Rose's hypothesis underscores the fact that bilateral trade is mainly intra-industry trade (although this indicator does not directly enter their analysis). Instead, they argue that specialization increases the exposure to sector-specific shocks transmitted via intra-industry trade. Fontagné ([26]) discusses the relation between intraindustry trade and the symmetry of shocks in a monetary union. Fidrmuc ([25]) demonstrates that intra-industry trade is a better indicator for business cycle symmetry than simple trade intensity.

Given China's tendency to specialize vertically, this channel may not be particularly relevant for the Chinese business cycle. Instead, the specialization forces discussed by Krugman ([56]) appear to dominate and drive the differences in business cycles of China and its various trading partners.

Financial integration between countries could also play an important role in synchronization of business cycles, but again, the impact of financial integration on business cycles is ambiguous. On the one hand, financial markets work similarly to trade links. Thus, business cycles in one country are likely to affect investment decisions and asset prices in other countries via financial flows. Conversely, FDI allows countries to specialize (Kalemli-Ozcan *et al.*, [50], Hoffmann, [42], Imbs, [48]) such that a high degree of financial integration may reduce the extent of co-fluctuations. Empirical analysis here seems to indicate a less robust impact of financial integration on business cycle synchronization (see Artis *et al.*, [4]).

In any case, the literature on business cycle correlation is concentrated on developed economies. Among the studies that look at business cycle correlation in Eastern Asia, we note the most relevant papers. Sato and Zhang ([76]) find common business cycles for the East Asian region. Shin and Sohn ([80]) show trade integration (and financial integration to a considerably lesser extent) enhances comovements of output in East Asia. Kumakura in [57] reports that the share of electronic products in foreign trade increases business cycle correlation for the countries around the Pacific. Finally, Shin and Wang ([79]) observe that trade is a significant determinant of business cycle correlation for East Asian countries. Few, if any, papers directly examine the correlation of business cycles between China and other emerging Asian economies and those of the OECD countries.

9.2 Stylized Facts for the Business Cycle in China and Selected Countries

We use quarterly GDP data taken from IMF International Financial Statistics. For developed countries, the time series start in the 1970s or 1980s. Where seasonal adjustment is required, we perform the US Census Bureau's X12 ARIMA procedure for the entire available period.

For China, we use national quarterly data in current prices deflated by the CPI. It is important to note here that these time series have undergone major revision recently. So far, only annual data are available according to the new methodology[1]. We adjusted the time series using the same procedure as for other countries. In China's case, the time series start from 1992. This restricts our analysis to the period between 1992 and 2006.

All time series were tested on unit root by Dickey-Fuller GLS test proposed by Elliott *et al.* ([23]), which improves the power of the ADF test by detrending. The test rejects clearly the null of unit root in output of all analyzed countries. Similarly, Kwiatkowski *et al.* ([58]) tests fail to reject the null of stationarity for all countries. Panel version of both tests (according to Im *et al.*, [47] and Hadri, [34]) confirms these results.

We calculate dynamic correlation defined in (5.28) between China and selected developed economies. Figure 9.1 presents these dynamic correlations of business cycles in China and selected developed economies between 1992 and 2006. As in most cited studies, we distinguish among three components of the aggregate correlation. First, the long-run movements (over 8 years) correspond to the low frequency band below $\pi/16$. Second, the traditional business cycles (i.e. cycles with a period between 1.5 and 8 years) belong to the medium part of the figure (marked as a shadow area) between $\pi/16$ and $\pi/3$. Finally, the short-run movements are defined by frequencies over $\pi/3$. Although it is usual to neglect these developments in literature, we look at them here as the short-run dependences of economic development could potentially be important in China's case.

We can see that business cycles in China and selected economies vary significantly over the frequencies. Some of countries show comparably high positive correlation with

[1]The impact of the revision on correlations should be moderate as long as the dynamic properties of the time series remain the same.

the long-run cycles of China. These countries include mainly the non-European OECD countries (the US, Korea, Australia, Japan and New Zealand). To a lesser degree, we also see positive correlations of the long-run development in Denmark, Italy, Norway and Turkey. In general, the non-European OECD countries trade more intensively with China than the remaining countries of our sample, which may help explain the extent of business cycle correlation. For European countries, however, this explanation is less credible.

We find a more homogenous picture for the traditional business cycle frequencies (between $\pi/16 \approx 0.2$ and $\pi/3 \approx 1$). In general, negative correlations of business cycles in China and OECD countries dominate. Basically, only Korea and Denmark show a positive correlation over the whole interval of business cycle frequencies. This confirms the earlier findings of Shin and Sohn ([80]) and Sato and Zhang ([76]). As before, the non-European OECD countries show a positive correlation at the lower range of the interval (close to eight years). Only Belgium and Spain show positive correlation at frequencies close to 1.5 years.

Finally, we see large differences in short-run frequencies. In general, the dynamic correlations tend to increase at the right end of the spectrum (see figure 9.1). This would correspond to strong business linkages between suppliers from China and final producers in developed countries. Among the European countries, short-term correlation appears to be high for Finland, the Netherlands, and Sweden. Short-run correlations are also high also for the US and Korea, but only marginally positive for Japan. All these countries can be characterized as having highly intensive relationships with China over a longer period.

Figure 9.2 compares average dynamic correlations at the business cycle and the short-run frequencies with the static correlations for the sample. We can see that the negative correlations dominate for nearly all countries especially for the business cycle frequencies. Only Korea, Denmark, Norway and Italy show a positive correlation of business cycles with China. At the same time, several countries show positive dynamic correlations for the short-run frequencies. This is especially strong for Korea, Netherlands, Sweden, Spain, and the USA. Thus, there could be also some signs of increasing similarities of business cycles. Cui and Syed ([18]) find that China is moving away from traditional assembly operations in its processing activities and its exports have started to rely more on domestically sourced components.

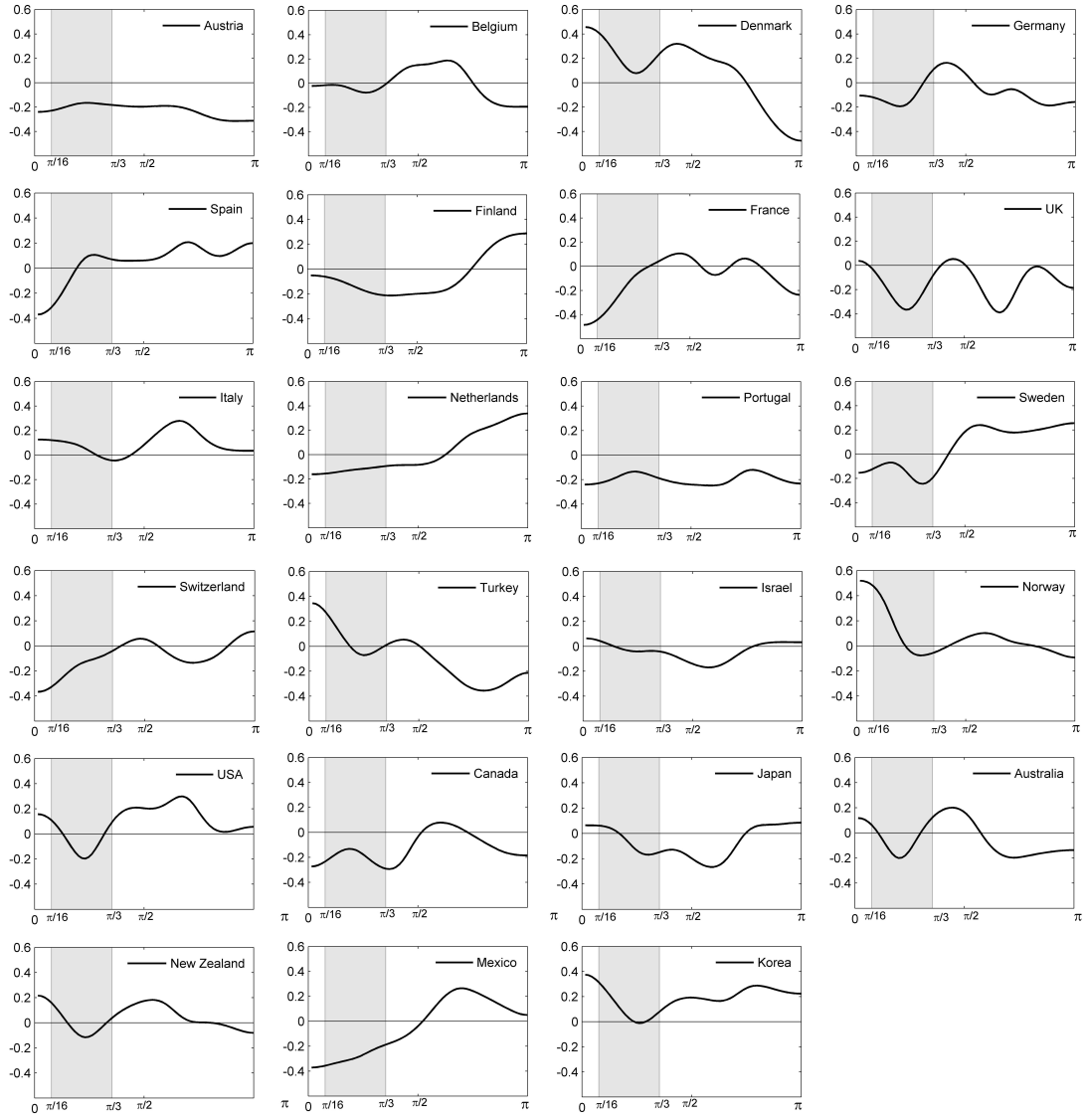

Figure 9.1: Dynamic correlations between China and selected countries, 1992-2006 [a].

[a] Business cycle frequencies are marked by the shadow area.

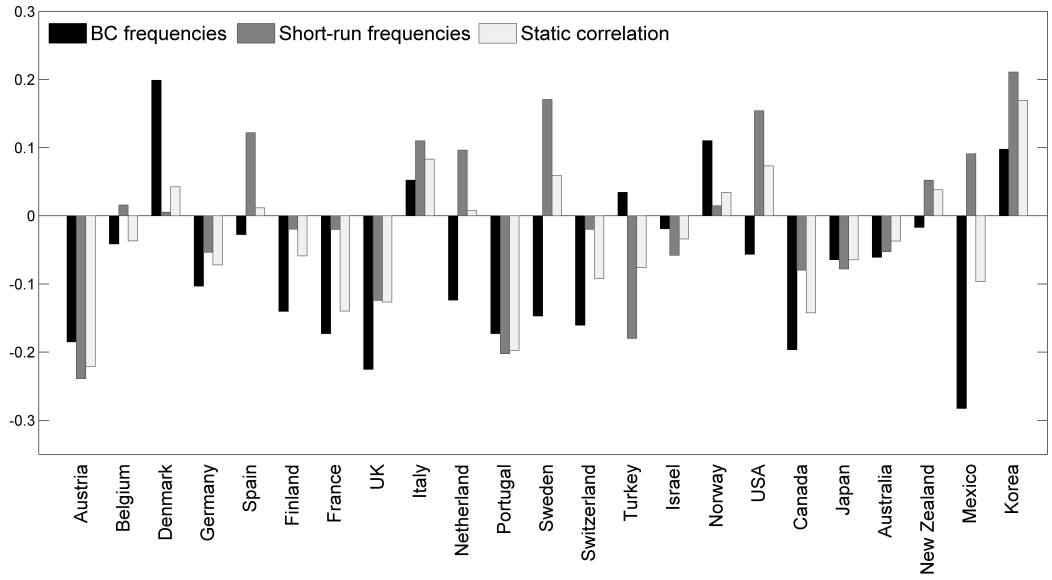

Figure 9.2: Aggregate correlations of business cycles in China and selected countries, 1992-2006.

9.3 Cohesion Analysis and Chinese Effect on World Business Cycles

As we know from the section 5.5, the cohesion, an extension of dynamic correlation, defined in (5.30) is a measure of dynamic co-movement within a group of variables. Hence, it is an appropriate technique for study of problems of business cycle synchronization.

Therefore, in order to illustrate the synchronization across the surveyed countries, it is possible to compute the cohesion, which provides a better measure of the dynamic co-movements between time series than alternative methods.

Figure 9.3 illustrates a graphical representation of cohesion for selected regions of the world economy at all frequencies. The figure provides a comparison of the cohesion among OECD countries (except Japan and Korea that are involved in Asia group), Asian countries and members of European Union.

We can see that OECD countries show a high level of cohesion for all frequencies. In general, we confirm a high degree of synchronization of business cycles in OECD

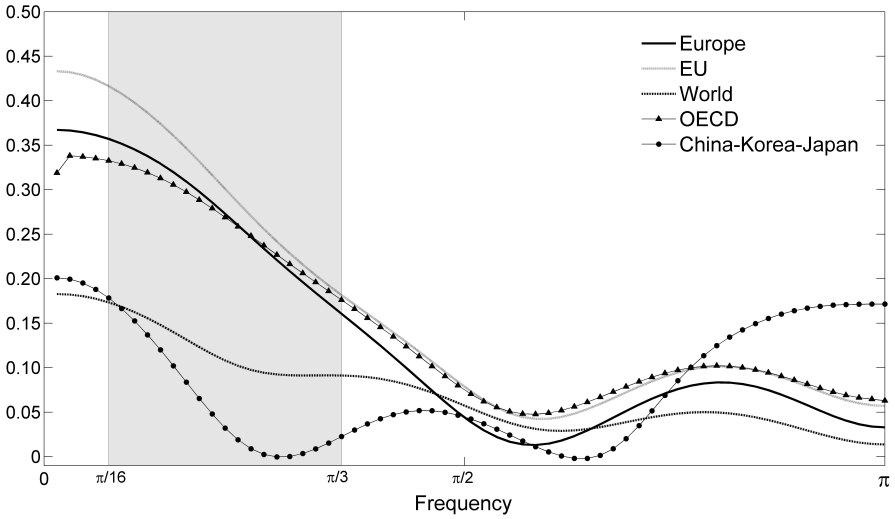

Figure 9.3: Cohesion of business cycles in selected regions, 1992-2006 [a].

[a] Business cycle frequencies are marked by the shadow area.

countries. Not surprising, the highest values of cohesion are found for the European Union (defined as 15 member states before 2004). Nevertheless, the addition of the non-European OECD countries does not change the picture significantly.

By contrast, the level of cohesion between China, Korea and Japan is close to zero at the business cycle frequencies. In turn, the Asian cohesion is higher for the very short-term frequencies than in other regions. The inclusion of the Asian countries to the worldwide level of cohesion makes a difference, although we reflect the different size of the countries by using the GDP weights. For business cycle frequencies, we can see that the degree of cohesion drops approximately by one half and it stays at relatively low levels also for the short-run movements. Actually, future developments can result even in further declines of the worldwide level of cohesion as the weights of emerging countries increase. The evidence on business cycle decoupling indicates that this process can be counteracted only slowly with the convergence of business cycles in emerging countries with those in OECD countries (see Kose *et al.*, [54]).

9.4 Exposure to a Globalization Shock and Business Cycles of OECD Countries

The stylized facts of the previous sections show that the business cycles in China and in the OECD countries are largely not synchronized. Furthermore, the intensity of economic links with China differs largely between the OECD countries. This can influence the business cycles of the individual OECD countries as shown partially in the previous section. In addition to increased synchronization of movements at particular frequencies, the synchronization between OECD countries may decline as a result of different exposure to the 'globalization' or 'China' shock. Alternatively, different specialization patterns achieved during the globalization period may lead also to increasing dissimilarities in business cycles of the OECD countries despite similar exposure to trade and financial integration with China and other emerging markets.

Therefore, we extend our analysis to the business cycles between the OECD countries (excluding Korea and Mexico from the previous sample because they are possibly more similar to emerging economies and due to data reasons). We start with the estimation of the traditional OCA endogeneity equation which follows Frankel and Rose ([27]) for individual frequencies,

$$\rho_{YX}(\omega) = \beta_1(\omega) + \beta_2(\omega) b_{YX} + \epsilon_{YX}(\omega). \tag{9.1}$$

where ρ_{YX} is the dynamic correlation between X and Y at frequency ω and b_{YX} stands for trade to GDP ratio of countries Y and X. Because estimating (9.1) by OLS may be inappropriate (see Imbs, [48]), we use two stage OLS. This reflects that bilateral trade flows might be influenced by exchange rate policies. Therefore, trade and FDI intensities have to be instrumented by exogenous determinants of bilateral trade and financial flows. Such instruments are provided by the so-called 'gravity model' (Bussière *et al.*, [13]) including the log of GDP and GDP per capita, log of distance between trading partners, a dummy for geographic adjacency, countries with a common language, and a dummy for the 15 earlier member states of the EU and the NAFTA.

Usually, equations similar to (9.1) are estimated for static correlation between OECD countries, which represents also the starting point of our analysis. The results are presented in the first column of table 9.1. Similarly, other authors sometimes use the band-pass filter (BPF), which is also presented in the third column in table 9.1. In

addition, table 9.1 presents results for all intervals of dynamic correlations for selected frequency intervals. As expected, we can see that the trade coefficient estimated for the average dynamic correlations over all frequencies is nearly equal to the results for the static correlation. The same is true for the average of dynamic correlations over the business cycle frequencies, while the results for the band-pass filter are much higher. We can see also that trade coefficient is nonsignificant for the average dynamic correlation over the short-run frequencies. This means that trade has mainly an effect on business cycle and long-run frequencies. This is an interesting extension of Frankel and Rose ([27]) result.

The detailed results for individual frequencies are reported in figure 9.4. We can see that the positive relationship between business cycle similarities and the degree of trade integration is fully confirmed for the business cycle frequencies as well as for the long-run frequencies in OECD countries. Somewhat surprisingly, the relationship is positive but no longer significant for the short-run frequencies.

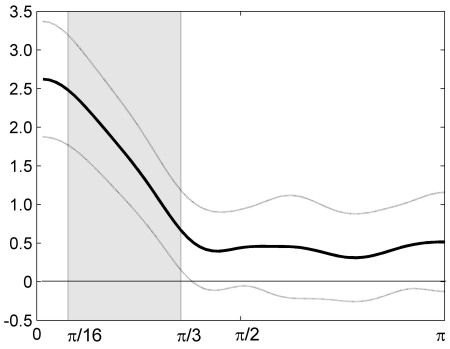

Figure 9.4: Estimation results by frequencies: Bilateral OECD trade/GDP [a].

[a] Confidence bands are constructed as 1.96 standard errors and business cycle frequencies are marked by the shadow area.

In the next step, we extend equation (9.1) to

$$\rho_{YX}(\omega) = \beta_1(\omega) + \beta_2(\omega) b_{YX} + \delta(\omega) x_Y + \delta(\omega) x_X + \epsilon_{YX}(\omega). \tag{9.2}$$

where x represents the measures of economic and financial integration with China, which enters for both countries Y and X. In particular, we take the ratio of bilateral trade, FDI stock, and flows (between 2001 and 2005) recorded between OECD coun-

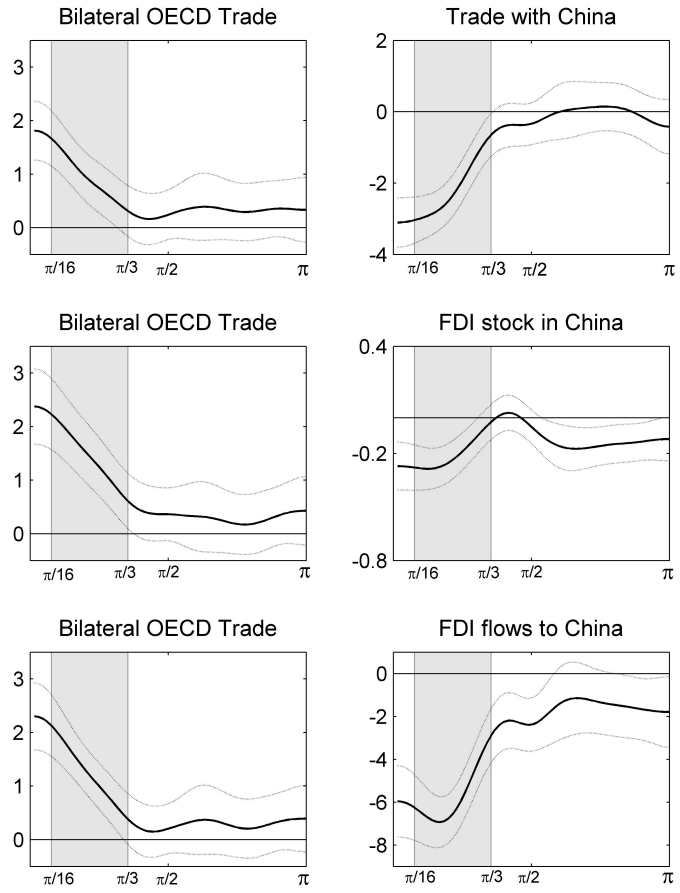

Figure 9.5: Estimation results by frequencies, determinants of business cycle of OECD countries [a].

[a] Each block of the table corresponds to a regression set, which includes the bilateral OECD trade and a proxy for countries' links to China. Confidence bands are constructed as 1.96 standard errors. Business cycle frequencies are marked by the shadow area. For better comparison, explanatory variables have been rescaled to yield coefficients of the same size.

tries and China to GDP of the analyzed OECD countries. This shows the importance of economic and financial links from the perspective of the OECD countries. We restrict the coefficient for economic and financial integration with China, δ, to be the same for both countries, as the differences between them are caused by different ordering of the countries in the data matrix. This reflects also that we use only one half of the all possible combinations of N countries, because the indicators are the same (except for possible errors in trade statistics) for the country pair Y and X as well as for the pair

X and Y.

The previous results for bilateral trade intensities of OECD countries remain unchanged (see table 9.1) if we include data for trade and financial links of OECD countries with China. Furthermore, we can see that the adjusted coefficients of determination improve as well. Actually, trade flows between OECD countries explain only 4 per cent of variance of our measure of similarity of comovements at the business cycle frequencies. The inclusion of trade intensity with China explains additional 15% of variance of business cycle similarities for the average of dynamic correlations for business cycle frequencies. The share of explained variance is even higher for static correlations, correlations using the band-pass filter and average dynamic correlations for the long-run frequencies.

In contradiction to trade integration between OECD countries, figure 9.5 and table 9.1 show that x has negative sign and is highly significant especially at the longer-term business cycles frequencies. This pattern is the same for all indicators of economic and financial links between OECD countries and China. This confirms our hypothesis that high intensity of trade and financial links to China has a negative effect on country's synchronization with business cycles of other OECD countries. For the short-run frequencies, the estimated coefficients are insignificant and in few cases they have positive signs.

In all estimations, the effects of bilateral OECD trade intensity remains positive and significant for the business cycle frequencies (especially those at the right-hand spectrum). However, the size of the coefficients is slightly lower in all estimations when economic ties with China are included. This finding can be visible also for the individual frequencies in figure 9.5.

	Static correlation	Average dynamic correlation	Static correlation for BPF	ADC: Bus. cycle frequencies	ADC: Short-run frequencies	ADC: Long-run frequencies
Basic equation (Only OECD bilateral data)						
OECD Trade	0.709^{***}	0.613^{***}	1.264^{***}	0.684^{***}	0.311	1.602^{***}
	(0.188)	(0.187)	(0.370)	(0.244)	(0.205)	(0.304)
Intercept	0.136^{***}	0.130^{***}	0.304^{***}	0.226^{***}	0.058^{***}	0.295^{***}
	(0.017)	(0.017)	(0.034)	(0.022)	(0.019)	(0.028)
n	171	171	171	171	171	171
Adjusted R^2	0.087	0.059	0.004	0.037	0.023	0.049
Augmented equation 1 (Including OECD countries' trade with China)						
OECD Trade	0.669^{***}	0.581^{***}	1.149^{***}	0.629^{***}	0.307	1.498^{***}
	(0.175)	(0.179)	(0.311)	(0.226)	(0.206)	(0.244)
Trade with China	-1.135^{***}	-0.893^{***}	-3.274^{***}	-1.568^{***}	-0.130	-2.944^{***}
	(0.221)	(0.225)	(0.392)	(0.284)	(0.259)	(0.307)
Intercept	0.336^{***}	0.288^{***}	0.881^{***}	0.502^{***}	0.081	0.814^{***}
	(0.042)	(0.043)	(0.075)	(0.054)	(0.049)	(0.059)
n	171	171	171	171	171	171
Adjusted R^2	0.208	0.135	0.297	0.181	0.019	0.388
Augmented equation 2 (Including OECD countries' FDI stock in China)						
OECD Trade	0.930^{***}	0.773^{***}	1.932^{***}	1.075^{***}	0.324	2.070^{***}
	(0.195)	(0.192)	(0.407)	(0.259)	(0.215)	(0.317)
FDI stocks in China	-0.134^{***}	-0.147^{***}	-0.122^{***}	-0.144^{***}	-0.110^{***}	-0.278^{***}
	(0.037)	(0.037)	(0.078)	(0.049)	(0.041)	(0.060)
Intercept	0.161^{***}	0.163^{***}	0.298^{***}	0.244^{***}	0.089^{***}	0.346^{***}
	(0.021)	(0.020)	(0.043)	(0.028)	(0.023)	(0.034)
n	171	171	171	171	171	171
Adjusted R^2	0.134	0.126	-0.060	0.047	0.059	0.090
Augmented equation 3 (Including OECD countries' FDI flows to China)						
OECD Trade	0.843^{***}	0.680^{***}	1.730^{***}	0.836^{***}	0.280	1.936^{***}
	(0.176)	(0.172)	(0.357)	(0.211)	(0.208)	(0.264)
FDI flows to China	-3.045^{***}	-3.151^{***}	-5.793^{***}	-4.962^{***}	-1.730^{***}	-6.465^{***}
	(0.468)	(0.458)	(0.951)	(0.563)	(0.554)	(0.703)
Intercept	0.269^{***}	0.273^{***}	0.545^{***}	0.447^{***}	0.141^{***}	0.575^{***}
	(0.027)	(0.026)	(0.054)	(0.032)	(0.031)	(0.040)
n	171	171	171	171	171	171
Adjusted R^2	0.262	0.259	0.143	0.333	0.070	0.334

Note: BPF - band pass filter, ADC - average dynamic correlation over selected frequencies. Standard errors are in parentheses. ***, ** and * denote significance at 1%, 5% and 10 %, respectively.

Table 9.1: Estimation results for static correlation, Band-Pass filter, and average dynamic correlation over selected frequency intervals.

9.5 Policy Implications

The emergence of China as an important trading nation has been one of the major events in the world economy in the past two decades. During this gradual process, China gained in economic weights and influenced economic developments around the world. Thus, China has become an important factor of growth of the global economy. However, we are interested how much influence China has on business cycles in the developed OECD countries.

We show that the interdependence between the economic development in China and in developed economies is generally relatively small. However, many countries show a high correlation of the short-run fluctuations. Many transnational companies use China as a part of their production chain (see Dean *et al.*, [19]), and this is especially true for the other Asian countries. In turn, most countries show a negative correlation with China for the traditional business cycles (cycles with periods between 1.5 and 8 years). It seems that countries, which have more intensive economic and financial relationships with China, have also higher dynamic correlation with Chinese economy. This seems to be especially true for the long-term developments.

In sum, our results confirm a special position of China in the world economy, although the countries having already intensive trading relationships with China (e.g. Korea, Japan, and the USA) have also more similar cycles with China over all frequencies. Despite the increased trade links between the countries, Chinese business cycle remains in general rather different from the rest of the world.

Finally, we show that countries engaged intensively in trade and investment in China tend to have a lesser degree of synchronization of business cycles with the other OECD countries. At the same time, trade and financial integration between the OECD countries strengthen the similarity of business cycles in the OECD countries. Both effects are less important for the short-run comovements. Although these findings may be subject to data problems, our results confirm the dissynchronization effects of trade specialization between China and OECD countries on their business cycles as described by Krugman in [56], while synchronization effects prevail between the OECD countries (Frankel and Rose, [27]).

10 Conclusions

In presented thesis we performed extensive analysis of methods of spectrum estimation. The main question of this thesis was to evaluate which method of spectrum estimation is more precise and to use the theoretical findings in practical evaluation.

First of all, using Monte Carlo simulations we find that the all methods are more precise with an increasing number of observations. A higher the number of observations is associated with lower values of mean squared error. This characteristic we use in the [12] where we apply the spectral analysis for stock prices.

The parametric methods, in our case Yule-Walker method, is the best estimator for autoregressive processes. But for other processes, the non-parametric methods with windows are more precise. The sharp peaks in spectrum for different examined processes cause the problem during the estimation for both types of method.

The estimations with Bartlett or Blackman window have a lower variance and MSE in comparing with the results estimated with Parzen window or the periodogram. The periodogram achieves the higher variance among the examined method. Therefore the quality of the periodogram estimate can be improved by an appropriate selection of the windows.

However, usually we do not know the true data generating process. Mostly, the real time series are approximated by autoregressive processes. In general, there is the tendency to underestimate the order of the autoregressive process. Real time series have more complex structure, therefore we recommend to use the non-parametric methods

smoothed by the Blackman or Bartlett window because they are better estimator of spectrum for autoregressive processes with underestimate value of order.

Then we use the knowledge of dynamic correlation and cohesion and we apply our finding from Monte Carlo analysis to illustrate the impact of China and globalizations on business cycles in the developed OECD countries. The spectrum for dynamic correlation is calculated using non-parametric method smoothed by the Bartlett window.

We also show that the interdependence between the economic development in China and in developed economies is generally relatively small. However, many countries show a high correlation of the short-run fluctuations. Many transnational companies use China as a part of their production chain, and this is especially true for the other Asian countries. In turn, most countries show a negative correlation with China for the traditional business cycles (cycles with periods between 1.5 and 8 years). It seems that countries, which have more intensive economic and financial relationships with China, have also higher dynamic correlation with Chinese economy. This seems to be especially true for the long-term developments

In sum, our results confirm a special position of China in the world economy, although the countries having already intensive trading relationships with China (e.g. Korea, Japan, and the USA) have also more similar cycles with China over all frequencies. Despite the increased trade links between the countries, Chinese business cycle remains in general rather different from the rest of the world.

Mathematical Symbols Used in the Text

- ω or λ - frequency
- Ω - frequency band, $\Omega = [\omega_1, \omega_2]$
- $\mathbf{T}$ - period, $\mathbf{T} = 2\pi/\omega$
- γ_0 - variance
- γ_j - jth autocovariance
- ϱ_j - jth autocorrelation
- $\boldsymbol{\Gamma_j}$ - jth autocovariance matrix
- $\boldsymbol{\Gamma}_0$ - variance-covariance matrix
- $\gamma_{XY}^{(j)}$ - jth autocovariance between X and Y
- $g_Y(z)$ - autocovariance-generating function
- $\mathbf{G_Y}(z)$ - autocovariance-generating function of vector process
- $s_Y(\omega)$ - population spectrum, spectral density function
- $\boldsymbol{s_Y}(\omega)$ - population spectrum for vector process
- $\bar{y}$ - sample mean
- $\hat{s}_y(\omega)$ - sample periodogram
- $\kappa(\omega_{j+m}, \omega_j)$ - kernel
- h - bandwidth
- $s_{YX}(\omega)$ - population cross spectrum from X to Y
- $c_{YX}(\omega)$ - cospectrum between X and Y
- $q_{YX}(\omega)$ - quadrature spectrum from X to Y
- $R_{YX}(\omega)$ - gain
- $\theta(\omega)$ - phase
- $C_{YX}(\omega)$ - coherency
- $h_{YX}(\omega)$ - population coherence between X and Y, squared coherency

- $corr(X, Y)$ - classical correlation between X and Y
- $\rho_{YX}(\omega)$ - dynamic correlation between X and Y at frequency ω
- $\rho_{YX}(\Omega)$ - dynamic correlation between X and Y within frequency band Ω
- $coh_{Y}(\omega)$ - cohesion of Y at frequency ω
- $coh_{Y}(\Omega)$ - cohesion of Y within frequency band $\Omega = [\omega_1, \omega_2]$
- $coh_{YX}(\omega)$ - cross-cohesion between X and Y at frequency ω
- b_{YX} - trade to GDP ratio of countries Y and X
- x_i - coefficient for economic and financial integration country i with China

Resumé

Ústrednou témou predloženej dizertačnej práce je spektrálna analýza. Spektrálna analýza bola metóda primárne vyvinutá a aplikovaná vo vedách ako geofyzika, astronómia, meteorológia, ale svoju úlohu zohrala aj pri digitálnom spracovaní signálu. Až neskôr sa použila aj pri analyzovaní časových radov, teda našla svoje uplatnenie aj v ekonometrii.

Vlastnosti časových radov sa v ekonometrii popisujú prevažne pomocou metód založených na časovej štruktúre dát. Spektrálna analýza poskytuje iný pohľad na vlastnosti časových radov a pomáha analyzovať a riešiť také otázky aplikovanej ekonómie ako identifikácia trendu a sezónnosti ekonomických časových radov, štúdium medzinárodného hospodárskeho cyklu a analýza vzájomnej interakcie časových radov.

Nerlove v [67], ako prvý, používa frekvenčný prístup pri riešení problému sezónneho očistenia, teda prvá aplikácia spektrálnej analýzy v ekonometrii sa datuje do polovice 60-tych rokoch minulého storočia. Detailnejší prehľad literatúry o aplikáciách spektrálnych metód v ekonometrii ponúka kapitola 3.

Kapitola 4 popisuje klasickú 1-rozmernú spektrálnu analýzu. V tejto kapitole definujeme, čo je spektrum a aké sú jeho vlastnosti a ako sa vypočíta. Spoznávame pojem periodogram a metódy používané na odhad spektra.

Existujú dva typy metód odhadu spektra – parametrické a neparametrické metódy. Podstata parametrických metód je založená na fakte, že každý lineárny process je možné aproximovať pomocou autoregresného procesu. Medzi parametrické metódy odhadu patria *autoregresívna* a *Yule-Walker* metóda. Rozdiel medzi týmito dvomi metódami spočíva len v odhade parametrov autoregresného procesu, ktorý aproximuje analyzovaný časový rad.

Spektrum je možné odhadnúť aj pomocou periodogramu, kde sa teoretické hodnoty autokovariancií nahradia reálnymi hodnotami vypočítanými z odhadovaných dát. Periodogram ako metóda pre odhad spektra má však určité nevýhody, preto sa ako neparametrická metóda odhadu používa vylepšená verzia. Spektrum sa teda odhaduje ako vážený priemer hodnoty periodogramu.

Piata kapitola popisuje krížovú spektrálnu analýzu, rozšírenie jednorozmernej spektrálnej metódy na analýzu vzájomnej interakcie dvoch časových radov. Zatiaľ čo kla-

sická spektrálna analýza umožňuje detekovať pohyb v rámci jednej časovej rady, krížová spektrálna analýza dokáže určiť vzťah medzi dvomi časovými radmi. Táto kapitola taktiež definuje pojem spektra pre vektorové procesy, popisuje ako sa takéto spektrum vypočíta a ako sa odhaduje. V kapitole sa zoznamujeme s pojmom *dynamickej korelácie* dvoch časových radov, a s pojmom *kohézie* a *krížovej kohézie*.

V šiestej a siedmej kapitole sme všeobecne odvodili spektrum pre procesy kĺzavých priemerov prvého a q-teho rádu, pre autoregresné procesy prvého a p-teho rádu a pre $ARMA$ procesy. Všeobecné výsledky sme názorne ilustrovali na niekoľkých príkladoch.

Ôsma kapitola práce je venovaná Monte Carlo simuláciám, pomocou ktorých sme sa snažili odpovedať na otázku, ktorá vyššie popísaná metóda odhadu populačného spektra je najvhodnejšia. Ako všeobecné kritérium pre posúdenie presnosti metódy sme použili minimalizáciu MSE. Výsledky simulácií sú prezentované v tabuľkách a názorných grafoch.

V deviatej kapitole sme prakticky využili poznatky o krížovej spektrálnej analýze teoreticky popísané v piatej kapitole. Naším cieľom bolo pomocou krížovej spektrálnej analýzy zistiť, aký veľký vplyv má Čína na hospodárske cykly v rozvinutých krajinách OECD. Naše výsledky získané pomocou aplikácie dynamickej korelácie a kohézie potvrdzujú špeciálne postavenie Číny vo svetovej ekonomike. Zdá sa, že krajiny, ktoré majú intenzívnejšie ekonomické a finančné vzťahy s Čínou (napr. Japonsko, Kórea a USA), majú tiež vyššiu dynamickú koreláciu s čínskou ekonomikou, predovšetkým v dlhodobom časovom horizonte. Vzájomná závislosť medzi hospodárskym rozvojom ostatných vyspelých krajinách OECD a Čínou je však vo všeobecnosti pomerne malá. Výnimkou je krátkodobý časový horizont, pre ktorý mnohé krajiny vykazujú vysokú koreláciu.

Záverečná desiata kapitola je zhrnutím základných výsledkov a záverov z nich plynúcich.

Bibliography

[1] A'HEARN, Brian and WOITEK, Ulrich (2001). *More international evidence on the historical properties of business cycles.* Journal of Monetary Economics 47, 321-346.

[2] ALLEN, Myles R., DETTINGER, Michael D., GHIL, Michael, IDE, Kayo, KONDRASHOV, Dmitri, MANN, Mike, ROBERTSON, Andrew W., SAUNDERS, Amira, TIAN, Yudong, VARADI, Ferenc and YIOU, Pascal (2002). *Advanced spectral methods for climatic time series.* Reviews of Geophysics 40 (1), 1-41.

[3] ARTIS, Michael J. (2003). *Is there a European business cycle?* Working Paper No. 1053, CESifo, Munich.

[4] ARTIS, Michael J., FIDRMUC, Jarko and SCHARLER, Johann (2008). *The transmission of business cycles: Implications for EMU enlargement.* Economics of Transition 16, 559–582.

[5] ARTIS, Michael J. and ZHANG, Wenda (1997). *International business cycles and the ERM: Is there a European business cycle?* International Journal of Finance and Economics 2, 1099-1158.

[6] ATESOGLU, H. Sonmez and VILASUSO, Jon R. (1999). *A band spectral analysis of exports and economic growth in the United States.* Review of International Economics 7 (1), 140-152.

[7] BAXTER, Marianne and KING, Robert G. (1999). *Measuring business cycles: Approximate band-pass filters for economic time series.* Review of Economics and Statistics 81, 575-593.

[8] BAXTER, Marianne and KOUPARITSAS, Michael A. (2005). *Determinants of business cycle comovement: A robust analysis.* Journal of Monetary Economics 52, 113-57.

[9] BÁTOROVÁ, Ivana (2007). *Application of factor models in business cycle analysis in the enlarged EU.* Unpublished master thesis, Bratislava.

[10] BÁTOROVÁ, Ivana, FIDRMUC, Jarko and KORHONEN, Iikka (2008). *China in the world economy: Dynamic correlation analysis of business cycles.* BOFIT Discussion Paper 7/2008, Bank of Finland, Helsinki.

[11] BÁTOROVÁ, Ivana, FIDRMUC, Jarko and KORHONEN, Iikka (2009). *New global players and disharmonies in the world orchestra: Cohesion analysis of business cycles of China.* The Economic Performance of the European Union, London: Palgrave Macmillan.

[12] BÁTOROVÁ, Ivana, FIDRMUC, Jarko and KORHONEN, Iikka (2011). *From decoupling of Asian stock markets to re-coupling during the Great recession.* Steven Rosefielde, Masaaki Kuboniwa and Satoshi Mizobata, eds., Two Asias: The Emerging Postcrisis Divide, Singapore: World Scientific.

[13] BUSSIÈRE, Matthieu, FIDRMUC, Jarko and SCHNATZ, Bernd (2008). *EU enlargement and trade integration: Lessons from a gravity model.* Review of Development Economics 12 (3), 562–576.

[14] CHATFIELD, Chris (1996). *The analysis of time series: An introduction,* 5th edition. Chapman and Hall, London, UK.

[15] CROUX, Christophe, FORNI, Mario and REICHLIN, Lucrezia (1999). *A measure of comovement for economic variables: Theory and empirics.* CEPR Discussion paper No. 2339.

[16] CROUX, Christophe, DEKIMPE, Marnik G. and LEMMENS, Aurélie (2005). *The European consumer: United in diversity?* ERIM Report Series Reference No. ERS-2005-022-MKT.

[17] CROUX, Christophe, DEKIMPE, Marnik G. and LEMMENS, Aurélie (2008). *Measuring and testing granger causality over the spectrum: An application to European production expectation surveys.* International Journal of Forecasting 24 (3), 414-431.

[18] CUI, Li and SYED, Murtaza H. (2007). *The shifting structure of China's trade and production.* IMF Working Paper No. 07/214, Washington.

[19] DEAN, Judith M., FUNG, K. C. and WANG, Zhi (2008). *How vertically specialized is Chinese trade?* Bank of Finland Institute for Economies in Transition Discussion Paper 31/2009, Bank of Finland, Helsinki.

[20] DE GRAUWE, Paul and ZHANG, Zhaoyong (2006). *Introduction: Monetary and economic integration in the East Asian region.* World Economy 29 (12), 1643-1647.

[21] DIEBOLD, Francis X. (2007). *Elements of forecasting*, 4th edition. South-Western College Publishing, Cincinnati.

[22] EICHENGREEN, Barry and TONG, Hui (2005). *Is China's FDI coming at the expense of other countries?* NBER Working paper No. 11335.

[23] ELLIOTT, Graham, ROTHENBERG, Thomas J. and STOCK, James H. (1996). *Efficient tests for an autoregressive unit root.* Econometrica 64, 813–836.

[24] FATÁS, Antonio (1997). *EMU: Countries or regions?* European Economic Review 41, 753-60.

[25] FIDRMUC, Jarko (2004). *The endogeneity of the optimum currency area criteria, intra-industry trade, and EMU enlargement.* Contemporary Economic Policy 22, 1-12.

[26] FONTAGNÉ, Lionel and FREUDENBERG, Michael (1999). *Endogenous symmetry of shocks in a monetary union.* Open Economies Review 10, 263-87.

[27] FRANKEL, Jeffrey A. and ROSE, Andrew K. (1998). *The endogeneity of the optimum currency area criteria.* Economic Journal 108, 1009-25.

[28] FULLER, Wayne A. (1976). *Introduction to statistical time series.* Wiley, New York.

[29] GHIL, Michael, HALLEGATTE, Stéphane, SELLA, Lisa and VIVALDO, Gianna (2008). *Economic cycles and their synchronization: Spectral analysis of GDP time series from Italy, the Netherlands, and the UK.* Econophysics Colloquium 2008, Germany.

[30] GRANGER, Clive W. J. and HATANAKA, Michio (1964). *Spectral analysis of economic time series*. Princeton University Press, Princeton, New Jersey.

[31] GRANGER, Clive W. J. (1966). *The typical spectral shape of an economic variable*. Econometrica 34 (1), 150-161.

[32] GRANGER, Clive W. J. (1969). *Investigating casual relations by econometric models and cross-spectral methods*. Econometrica 37 (3), 424-438.

[33] GREEN, William H. (2003). *Econometric analysis*, 5th edition. Prentice Hall, New York.

[34] HADRI, Kaddour (2000). *Testing for stationarity in heterogenous panel data.* Econometrics Journal 3 (2), 148-161.

[35] HAMILTON, James D. (1994). *Time series analysis.* Princeton University Press, Princeton, New Jersey.

[36] HANNAN, James E. (1970). *Multiple time series.* Wiley, New York.

[37] HARRIS, Fredric J. (1978). *On the use of windows for harmonic analysis with discrete Fourier transform*. Proceedings of the IEEE 66, No. 1.

[38] HARVEY, Andrew C. (1993). *Time series models*, 2nd edition. The MIT Press, Cambridge.

[39] HARVEY, Andrew C. and JAEGER, Albert (1993). *Detrending, stylized facts and the business cycle.* Journal of Applied Econometrics 8, 231-247.

[40] HATANAKA, Michio (1996). *Time-series-based econometrics.* Oxford University Press, New York.

[41] HIGO, Masahiro and NAKADA, Sachiko Kuroda (1998). *How can we extract a fundamental trend from an economic time series?* Monetary and Economic Studies 2, 61-111.

[42] HOFFMANN, Mathias (2003). *Financial integration, specialization and trade: More or less business cycle symmetry?* Department of Economics, University of Dortmund.

[43] HOSSEIN, Hassani (2007). *Singular spectrum analysis: Methodology and comparison.* MPRA paper No. 4991.

[44] HUGHES-HALLETT, Andrew J. and RICHTER, Christian (2004). *A time-frequency analysis of the coherences of the US business cycle and the European business cycle.* Center for Economic Policy Research Discussion Paper No. 4751.

[45] HUGHES-HALLETT, Andrew J. and RICHTER, Christian (2007). *Are the new member states converging on the Eurozone? A business cycle analysis for economies in transition.* Paper prepared for the INFER Conference, 28th – 29th June 2007, Coimbra.

[46] IACOBUCCI, Alessandra (2003). *Spectral analysis for economic time series.* OFCE Working papers No. 2003-07.

[47] IM, Kyung So, PESARAN, M. Hashem and SHIN Yongcheol (2003). *Testing for unit roots in heterogenous panels.* Journal of Econometrics 115 (1), 53-74.

[48] IMBS, Jean M. (2004). *Trade, finance, specialization, and synchronization.* Review of Economics and Statistics 86, 723-34.

[49] IMF (2007). *The changing dynamics of the global business cycle.* World Economic Outlook, Chapter 5, Washington, IMF, 67-94.

[50] KALEMLI-OZCAN, Sebnem, SØRENSEN, Bent E. and YOSHA, Oved (2001). *Economic integration, industrial specialization, and the asymmetry of macroeconomic fluctuations.* Journal of International Economics 55, 107-37.

[51] KAPOUNEK, Svatopluk and POMĚNKOVÁ, Jitka (2010). *Business cycle development in Czech and Slovak economies*. Bulletin of the Transilvania University of Braşov, Volume 3 (52) - 2010, Series V: Economic Sciences.

[52] KENEN, Peter B. (2000). *Currency areas, policy domains, and the institutionalization of fixed exchange rates.* Discussion Paper No. 467, London School of Economics, Centre for Economic Performance, London.

[53] KOČENDA, Evžen and HANOUSEK, Jan (1998). *Integration of emerging equity markets: Major Asian players.* Korean Economic Review 14 (1), 99-114.

[54] KOSE, M. Ayhan, OTROK, Christopher and PRASAD, Eswar S. (2008). *Global business cycles: Convergence or decoupling?* IMF Working Paper No. 08/143.

[55] KOSE, M. Ayhan and YI, Kei-Mu (2006). *Can the standard international business cycle model explain the relation between trade and comovement?* Journal of International Economics 68 (2), 267-295.

[56] KRUGMAN, Paul R. (1993). *Lessons of Massachusetts for EMU.* Cambridge University Press and CEPR, 241-261.

[57] KUMAKURA, Masanaga (2005). *Trade and business cycle correlations in Asia-Pacific.* Institute of Developing Economies Discussion Paper No. 44.

[58] KWIATKOWSKI, Denis, PHILLIPS, Peter C. B., SCHMIDT, Peter and SCHIN Yongcheol (1992). *Testing the null hypothesis of stationarity against the alternative of a unit root: How sure are we that economic time series have a unit root?* Journal of Econometrics 54, 159-178.

[59] LIU, Jun S. (2001). *Monte Carlo strategies in scientific computing.* Springer, New York.

[60] MARIO, Dell'Era (2008a). *Pricing of double barrier options by spectral theory.* MPRA paper No. 17502.

[61] MARIO, Dell'Era (2008b). *Pricing of the European options by spectral theory.* MPRA paper No. 17429.

[62] MARŠÁLEK, Roman and POMĚNKOVÁ, Jitka (2011). *Time and frequency domain in the business cycle structure.* MENDELU Working Papers in Business and Economics 7/2011.

[63] MARŠÁLEK, Roman and POMĚNKOVÁ, Jitka (2010a). *Spectral analysis of the cyclical behaving of the Czech republic industrial production.* Forum Statisticum Slovacum 2/2010, 123-128.

[64] MARŠÁLEK, Roman and POMĚNKOVÁ, Jitka (2010b). *Industrial production periodicity testing using R.A.Fisher test.* Acta universitatis agriculturae et silviculturae Mendeleianae Brunensis, LVIII, No. 3, 189-196.

[65] METROPOLIS, Nicholas and ULAM, Stanisław (1949). *The Monte Carlo method.* Journal of the American Statistical Association 44, 335-341.

[66] METROPOLIS, Nicholas (1987). *The beginning of the Monte Carlo method.* Los Alamos Science: 129. Special Issue dedicated to Stanisław Ulam.

[67] NERLOVE, Marc (1964). *Spectral analysis of seasonal adjustment procedures.* Econometrica 32 (3), 241–286.

[68] VON NEUMANN, John, RICHTMYER, Robert D. and ULAM, Stanisław (1947). *Statistical methods in neutron diffusion.* Los Alamos Scientific Laboratory report LAMS–551.

[69] OTTO, Glenn, VOSS, Graham and WILLARD, Luke (2001). *Understanding OECD output correlations.* Research Paper No. 2001-05, Reserve Bank of Australia, Sydney.

[70] OWENS, Raymond E. and SARTE, Pierre-Daniel G. (2005). *How well do diffusion indexes capture business cycles? A spectral analysis.* Federal Reserve Bank of Richmond Economic Quarterly, Volume 91/4.

[71] PACZYŃSKI, Wojciech and WOZNIAK, Przemysław (2007). *Business Cycle Coherence between euro area and the EU new member state: A time-frequency analysis.* Center for Economic Research and Graduate Education and the Economics Institute (CERGE-EI), Prague.

[72] PARZEN, Emanuel (1969). *Multiple time series modeling.* In Multivariate Analysis-II (P. Krishnaiah, ed.) 389-409. Academic Press, New York.

[73] PERCIVAL, Donald B. and WALDEN, Andrew T. (1993). *Spectral analysis for physical applications.* Cambridge University Press.

[74] POLLOCK, David S.G. (2008). *The frequency analysis of the business cycle.* Working paper No. 08/12, University of Leicester, UK.

[75] PRIESTLEY, Maurice B. (1981). *Spectral analysis and time series.* Academic Press Inc., London.

[76] SATO, Kiyotaka and ZHANG, Zhaoyong (2006). *Real output co-movements in East Asia: Any evidence for a monetary union?* World Economy 29 (12), 1671-1689.

[77] SELLA, Lisa (2008a). *Old and new spectral techniques for economic time series.* University of Turin, Department of Economics, Working paper No. 9/2008.

[78] SELLA, Lisa (2008b). *Economic fluctuations analysis: Alternative approaches.* Unpublished PhD. thesis, Turin.

[79] SHIN, Kwanho and WANG, Yunjong (2004). *Trade integration and business cycle comovements: The case of Korea with other Asian countries.* Japan and the World Economy 16, 213-230.

[80] SHIN, Kwanho and SOHN, Chan-Hyun (2006). *Local cross validation for spectrum bandwidth choice.* World Economy 29 (12), 1649-1669.

[81] VELASCO, Carlos (1998). *Spectral analysis of economic time series behaviour.* Universidad Carlos III de Madrid.

[82] WANG, Peijie (1999). *Spectral analysis of economic time series behaviour.* Manchester School of Management Working Paper No. 9914.